INSTITUTO SUPERIOR TÉCNICO
Universidade Técnica de Lisboa

DYNAMIC ANALYSIS OF OFFSHORE FLOATING WIND TURBINES

Hasan Bagbanci

Dissertation for the Degree of Master of

Naval Architecture and Marine Engineering

Jury

President:	Prof. Yordan Garbatov
Supervisor:	Prof. Carlos António Pancada Guedes Soares
Co-supervisor:	Dr. Debabrata Karmakar
Member:	Prof. Serge Sutulo

December 2011

DEDICATION

Dedicated to Teresa Leonor Lopes Miranda

ACKNOWLEDGMENTS

I express my sincere thanks and appreciation to my supervisor Professor Carlos Guedes Soares for his guidance, support and help during the tenure of the present research work. I am highly indebted to Professor Carlos Guedes Soares who has taken keen interest and offered valuable suggestions on the research work. I feel proud and honored to be a student of such a personality.

I sincerely appreciate and thank Dr Debabrata Karmakar for his co-operation and help right from the inception of the problem to the final preparation of the manuscript.

Thanks are also to the all the faculty members of the CENTEC for their technical suggestions at various times. My thanks are also to my colleagues and other labmates for their active cooperation with whom I shared so many nice moments together.

Lastly, I extend my sincerest gratitude to my parents and brothers for always standing by me and supporting me at this endeavor.

Hasan Bagbanci

ABSTRACT

A detailed study on offshore floating wind turbines and the working principle of various floater concepts and the conceptual designs for floating platforms used for floating wind turbines are presented. In the case of fixed wind turbine, the influence of the environmental conditions on wind turbine design loads for a monopole foundation is studied by analyzing the bending moment at the tower base and tower root for various values of water depth, tower height, pile diameter and turbulence model. The analysis is done using FAST code for 5MW wind turbine with a monopile foundation.

In the study of offshore floating wind turbine, a numerical time-domain model is used for the fully coupled dynamic analysis of deep water offshore floating wind turbines such as spar-type, barge-type and semi-submersible-type floating wind turbine. The hydrodynamic behaviour of the floaters is analysed using panel method. Hydrodynamic added mass, damping and exiting force are obtained in frequency domain and are validated with the available results. The hydrodynamic study of the floater is combined with and aerodynamic model to obtain a coupled aero-servo-hydro-elastic model. The performance of spar-type and barge-type floating wind turbine designed by the National Renewable Energy Laboratory (NREL) and semi-submersible type floating wind turbine designed by Principle Power are analyzed in detail. The mooring system attached to WindFloat semi-submersible floating wind turbine is also examined for six and eight mooring lines and the platform rotations along with motions results obtained are also compared.

Keywords: Renewable energy; Monopile wind turbine; Offshore floating wind turbine; Added mass; Damping coefficient; Mooring system.

RESUMO

Um estudo detalhado sobre mar turbinas eólicas flutuantes e o princípio de funcionamento de conceitos diversos floater e os projetos conceitual para plataformas flutuantes utilizadas para turbinas eólicas flutuantes são apresentados. No caso da turbina de vento fixo, a influência das condições ambientais em cargas de turbinas eólicas de design para uma fundação monopolo é estudada através da análise dos momentos de flexão na base da torre e torre de raiz para vários valores de profundidade de água, altura da torre, diâmetro pilha e modelo de turbulência. A análise é feita usando o código FAST para 5 MW de turbinas eólicas com uma fundação monopile.

No estudo da turbina eólica offshore flutuante, um modelo de domínio de tempo numérico é utilizado para a análise totalmente acoplado dinâmica de águas profundas ao largo de turbinas eólicas flutuantes, como longarina tipo, barcaça tipo e semi-submersível do tipo turbina eólica flutuante. O comportamento hidrodinâmico das moscas volantes é analisado utilizando o método de painel. Hidrodinâmica acrescentou massa, amortecimento e sair de força são obtidos no domínio da freqüência e são validados com os resultados disponíveis. O estudo hidrodinâmico do floater é combinado com e modelo aerodinâmico para obter um modelo combinado de aero-servo-hidro-elástica. O sistema de amarração anexado ao WindFloat semi-submersível turbina eólica flutuante também é examinado para seis e oito linhas de amarração e as rotações plataforma e os resultados obtidos movimentos também são comparados.

Palavras-chave: Energia renovável; Turbina eólica Monopile; Turbina eólica offshore flutuante; Adicionado em massa; Coeficiente de amortecimento, Sistema de amarração.

TABLE OF CONTENTS

LIST OF FIGURES

LIST OF TABLES

CHAPTER 1

INTRODUCTION

1.1 Offshore wind energy

The offshore wind energy is one of the most important renewable energy resources which can cover worldwide energy demands. This form of energy can practically substitute to replace the fossil fuels. The wind energy is observed as an essential and powerful energy resource for the socio-economic development and economic growth which helps in reducing the dependency on fossil fuels and provides clean energy. It has been estimated that about 10 million MW of energy are continuously available in the earth's wind and it provides security at a time when decreasing global reserves of fossil fuels threatens the long-term sustainability of global economy. Thus, wind energy emerged as a promising technology for the utilization of offshore wind resources for the large scale generation of electricity.

The generation of power from wind can be obtained from wind turbines which convert wind energy to electrical energy. The wind turbines can produce large quantities of electricity as compared to other energy sources which are generally placed onshore and offshore. It has been observed that relatively low surface roughness of the ocean results in higher wind speeds. So the offshore windmills are the best possible options for generating electricity.

In the year 1885, wind energy was first used for the production of electrical energy by Poul la Cour in Askov, Denmark. He converted an old wooden wind mill into the first wind turbine, which covered the energy demands of Askov high school. Thus, from 1885,

the use of wind energy for the production of electricity progressed with the increase in energy demands.

The concept of locating wind turbines in offshore region came after 1930 and it was suggested that the wind turbines to be placed on pylons, but the suggestion was never used. It was approximately 42 years after the original idea, the concept for large scale floating wind turbines for the production of electricity was introduced by Dr. William E Heronemus, professor at University of Massachusetts in 1972. It was in the year 1990, a company called "World Wind" first constructed and installed the offshore wind turbine at sea. Afterwards, many countries took part in the construction of offshore floating wind turbine but among them Denmark, Netherlands, Germany, Spain and United States are currently the world leaders in wind energy technology. These countries have a mega wind farm which comprises a few hundred wind turbines that are spread over hundreds of square kilometers.

1.1.1 Classification of offshore wind turbines

Offshore wind turbines are classified into three major types depending upon the water depths such as

- Shallow water foundation
- Transitional water foundation
- Deep water wind turbine structure

The shallow water wind turbines are generally placed in between 5m - 30m water depth and are in general classified as (i) Monopile structure (ii) Gravity base structure and (iii) Suction bucket structure.

The transitional offshore wind turbine are placed between 30m – 60m water depth and are classified as (i) Tripod tower, (ii) Guyed monopole, (iii) Full-height jacket, (iv) Submerged jacket with transition to tube tower and (v) Enhanced suction bucked or gravity base.

The deep water offshore wind turbines are generally floating structures and are placed in more than 60m water depth. The floating wind turbines in deep water falls into four main categories such as (i) Spar-type, (ii) Tension Leg Platform (TLP) type, (iii) Semi-submersible type and (iv) Pontoon type. In order to improve the wind energy production

and to get large scale generation of electricity, wind turbine technology needs offshore wind energy resources. So far, most projects of offshore wind farms are located in relatively shallow water and use bottom-fixed type wind turbines. Recently, most of the offshore wind power projects are proposed in deep water where the winds are of higher velocities. Thus the wind turbines on the floating support are the best solution to utilize the wind resources in areas with deep water depths. To extend wind turbine systems to deeper water, practical research of offshore floating wind turbine systems is required. Also, developing offshore floating wind farms is important because it can minimize the scenery disturbance, avoid the noise problems generated by wind-driven blades, provide high wind speed by low surface roughness and make use of extremely abundant deep water wind resources. In our present study we will give more emphasis on the floating offshore wind turbine structures in deep waters.

1.1.2 Wind power in different countries and current wind project

In the last few years, a number of offshore wind farms have been put into operation in European countries such as Denmark, United Kingdom (UK) and Netherlands. They are all situated in shallow waters, having a water depth of less than 25 meters and are relatively close to shore. For these developments, it proved economical to use either simple concrete gravity structures or steel monopiles as substructures (see Musial and Butterfield, 2006).

A list of the offshore wind projects built in the last few years can be found in Herbert et al. (2007). In terms of installed power, the main projects were the following: in the UK, the Lynn and Inner Dowsing (194 MW), the Kentish Flats project (90 MW) and the Burbo Banks project (90 MW); in the Netherlands, the Q7 project (120 MW); and in Denmark, the Nysted offshore Windfarm (165 MW) and the Horns Rev project (160 MW). The new projects that were being carried out are for deeper water depths. So the cost of the support structure and foundation will be proportionally higher than for turbines in shallow waters. This means that finding an economically feasible design is vital for overall project viability.

Recently, in Portugal a 2 MW prototype offshore wind turbine is being installed in the north of the country placed on the floating device WindFloat developed by Principle

Power. In the next phase an additional 5MW turbine will follow. The project is undertaken by EDP, Portugal and it is proposed to achieve a total capacity of 150 MW.

1.1.3 Wind turbine size and development

In the early and mid 1980s, the typical wind turbine size was less than 100 kW. By the late 1980s and early 1990s, the turbine sizes had increased from 100 to 500 kW. Further, in the mid-1990s, the typical size ranged from 750 to 1000 kW. And by the late 1990s, the turbine size had gone up to 2.5MW. Now turbines are available with capacities above 5MW which is shown in Figure 1.1. (Herbert et al. (2007))

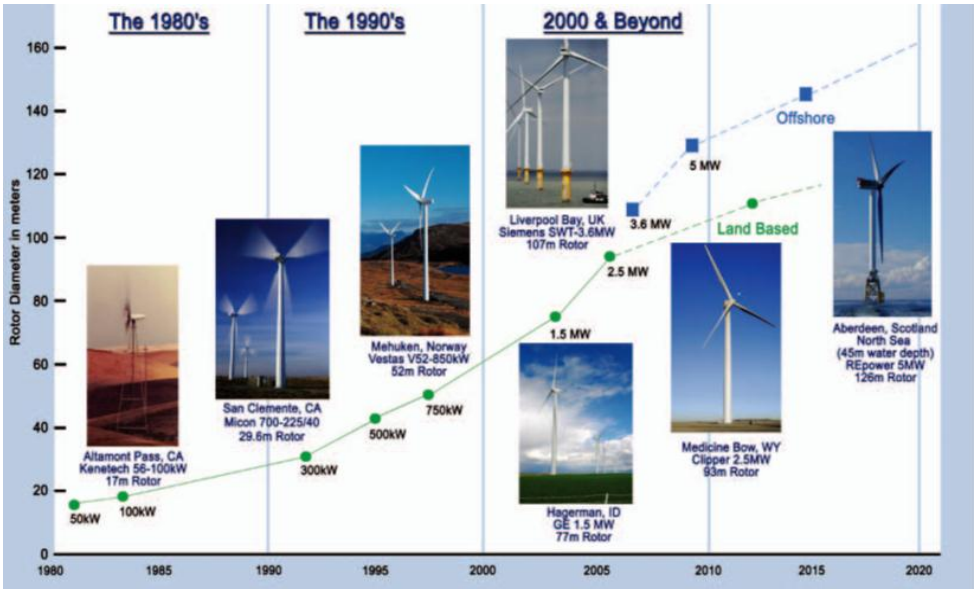

Figure 1.1: Trends of the wind turbine sizes and capacity (US Dept. of Energy)

So, now days, the research is on a full swing to develop floating wind turbines of high power. Thus in recent years, the studies on the performances of the floating wind turbine for various floater concepts are carried out by various researchers to improve the energy capacity of the system.

1.2 Outline of the present thesis

In the present thesis, detailed studies on the dynamic behavior of the floating wind turbine concepts are presented. The thesis consists of seven chapters. The details of the chapters are as follows:

In Chapter 1, the current situation of the wind energy and the developments achieved during the last few years are presented. The simulation tools used to analyze various floaters concepts is also discussed in detail. In Chapter 2, the literature review on various floaters concepts along with the research and development on offshore floating wind turbines carried out by various researchers and it is applications are discussed. The components associated with the wind turbines and the performances of various floating wind turbine models in different water depths are outlined to understand the importance of the water depth for power generation. The working principle of various floater concepts and the conceptual designs for floating platforms used for floating wind turbines are also described.

In Chapter 3, the mathematical formulation used to analyze the floaters and wind turbine concept is presented in brief. In Chapter 4, the influence of the environmental conditions on wind turbine design loads for a NREL 5MW monopile foundation is studied by analyzing the bending moment at the tower base and tower root for various values of water depth, tower height, pile diameter and turbulence model.

In Chapter 5, coupled dynamic analysis is performed on three different types of floating wind turbines for various environmental parameters. The coupled dynamic analysis are focused on NREL 5MW spar-type, NREL 5MW ITI barge-type and 5MW semi-submersible type floating wind turbine for tower base motions and platform rotations. Model to model comparisons is studied according to coupled dynamic simulation results. FAST (Fatigue, Aerodynamics, Structures, and Turbulence) code is used for fully coupled aero-servo-elastic simulations. The hydrodynamic study is carried out using WAMIT for various floaters configuration and is then coupled with FAST code to analyze the dynamic behavior of floating wind turbine.

In Chapter 6, an optimization of mooring system on WindFloat floating wind turbine is performed using 4 lines mooring and 6 lines mooring. The mooring system is observed important for floating concepts especially for pitch motion and it is found to effect directly on electricity generation. So the main focus was to obtain translational and rotational motion with different mooring properties. In Chapter 7, the summary of the whole work is presented in detail.

1.3 Design tools

Three different types of floating wind turbines are performed for same environmental parameters as in the design loads. The FAST (Fatigue, Aerodynamics, Structures, and Turbulence) code is used for simulations which employs a combined modal and multi-body dynamics formulation. The FAST code can model most common wind turbine configurations and control scenarios, including three-bladed turbines with a rigid hub, two-bladed turbines with a rigid or teetering hub, turbines with gear boxes or direct drives, turbines with induction generators or variable-speed controllers, turbines with active blade-pitch regulation or passive stall regulation, turbines with active or passive nacelle-yaw control, and turbines with passive rotor or tail furling. (see Jonkman and Bhul (2004a), Jonkman and Bhul (2004b), Jonkman (2009)). Jonkman and Sclavounos (2006) developed a fully coupled aeroelastic and hydrodynamic models for offshore wind turbines.

1.3.1 FAST Code

The FAST code is developed by National Renewable Energy Laboratory (NREL) and it is a fully coupled dynamic analysis simulator that could be used for floating wind turbine concepts. FAST code uses two different subroutine such as AeroDyn and HydroDyn and they seek wind data and hydro data for the analysis. Thus a hydrodynamic simulator and a wind simulator are required. AeroDyn calculates wind load along blades using blade element theory. TurbSim (Turbulence modeling scaling) generates wind data for FAST code and HydroDyn calculates wave load on floating system. To obtain the hydrodynamic loads on the floaters WAMIT (Wave Analysis at MIT) or similar hydrodynamic simulator are also used for FAST code. The FAST code simulates stochastic time-domain turbine response and computes hydrodynamic loads using Morison's equation. In the present study for the hydrodynamic loading on the floating platform, irregular waves are simulated using a JONSWAP spectrum with FAST code.

A floating wind turbine is splited into two bodies such as floater and wind turbine. Therefore, there is an interactive dynamic relation between floating platform and wind turbine and thus it is called multi-body dynamics. FAST code uses Kane's Method for multi-body problem between floating platform and wind turbine. Multi-body motion has

in total 22 degrees of freedom (DOF) for a two-bladed horizontal axis floating wind turbine model and 24 degrees of freedom (DOF) for a three-bladed horizontal axis floating wind turbine model. FAST code can simulate two or three bladed floating wind turbine.

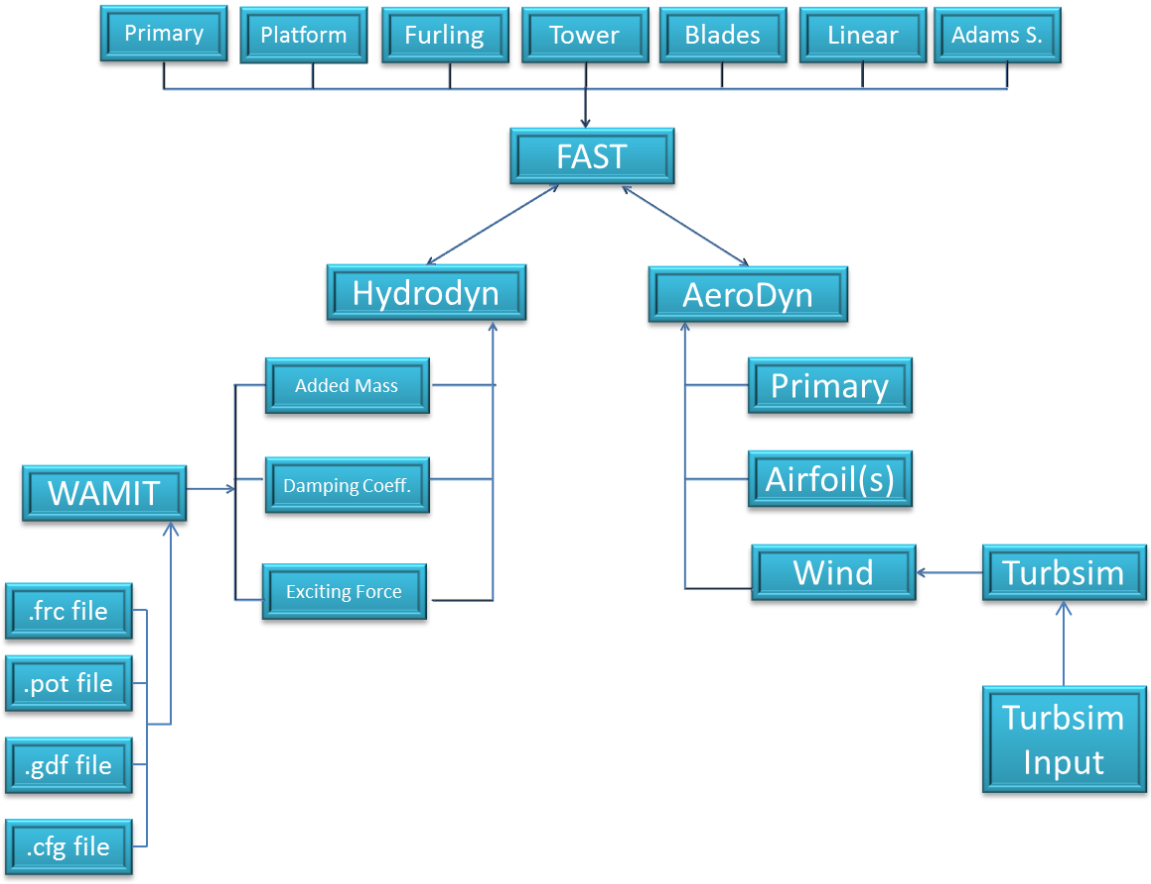

Figure 1.3: Simulation of FAST code

Multi body motions in degrees of freedom are platform translation and rotation (6 DOF), tower flexibility (4 DOF), nacelle yaw (1 DOF), variable generator and rotor speeds (2 DOF), rotor furl (1 DOF), and tail furl (1 DOF) for both bladed kind horizontal axis floating wind turbine. The main difference is blade flexibility (6 DOF) in two bladed turbine and (9 DOF) in three bladed turbine. The blade teetering (1 DOF) in two bladed wind turbine is considered whereas it is ignored in three bladed turbine. The FAST code simulation diagram is shown in Figure 1.3.

1.3.2 TurbSim Code

The TurbSim is a wind simulator for FAST code. TurbSim generates two dimensional vertical rectangular grids on rotor and it numerically simulates time series of three component wind speed vectors at each point in the gird. The gird height and grid width are kept minimum size as compared to rotor diameter and time series is kept same or higher than FAST code.

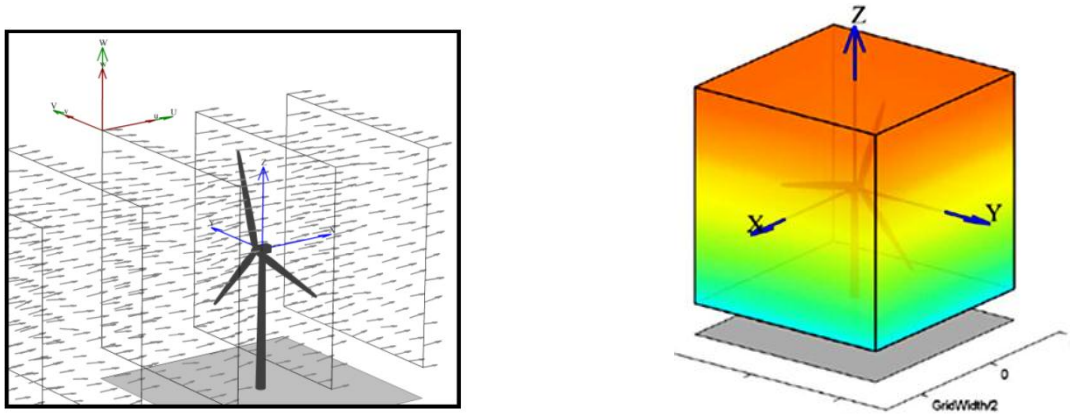

Figure 1.4: Wind speed vectors on each grid

The Risø Smooth-Terrain model (SMOOTH), a Kaimal power spectrum (IECKAI) and a Von Karman power spectrum (IECVKM) are employed to describe the turbulence random field over the rotor plane. The wind speed vectors on each grid are shown in Figure 1.4. Turbsim considers the hub height and mean wind speed for distribution wind speed on each point in grid.

CHAPTER 2

OVERVIEW OF OFFSHORE FLOATING WIND TURBINES

In the present chapter, a detailed literature survey on the research and development of offshore floating wind turbines and it is applications are presented. The performances of various floating wind turbine models in different water depths are outlined to understand the importance of the water depth for power generation. The working principle of various floater concepts, the conceptual designs of floating platforms used for floating wind turbines and also the components of floating wind turbines are described.

2.1 Components of offshore floating wind turbines

The wind turbine has seven major subsystems such as blades, nacelle, controller, generator, rotor, tower, and floating body. The detail description of these components are as follows

- **Blades**:

The generation of power increases with the increase in the number of blades. Most of the wind turbines have three blades, though there are some with two blades. The blades are generally 30m to 50m long, with the most common sizes around 40m. Blade weights vary, depending on the design and materials. A 40m LM Glasfiber blade for a 1.5 MW turbine weighs 5,780 kg (6.4 tons) and one a 2.0 MW turbine weighs 6,290 kg (6.9 tons).

- **Nacelles**:

The nacelle houses the main components of the wind turbine, such as the controller, gearbox, generator, and shafts. This part protects the wind turbine equipment.

- **Controller**:

The controller monitors the condition of the turbine and controls the turbine movement. The control system changes the blade pitch, nacelle yaw, and generator loading of a wind turbine. The control system can also change the pitch of the blades to alter the amount of torque produced by the rotor. The purpose of the control system is to maximize power output.

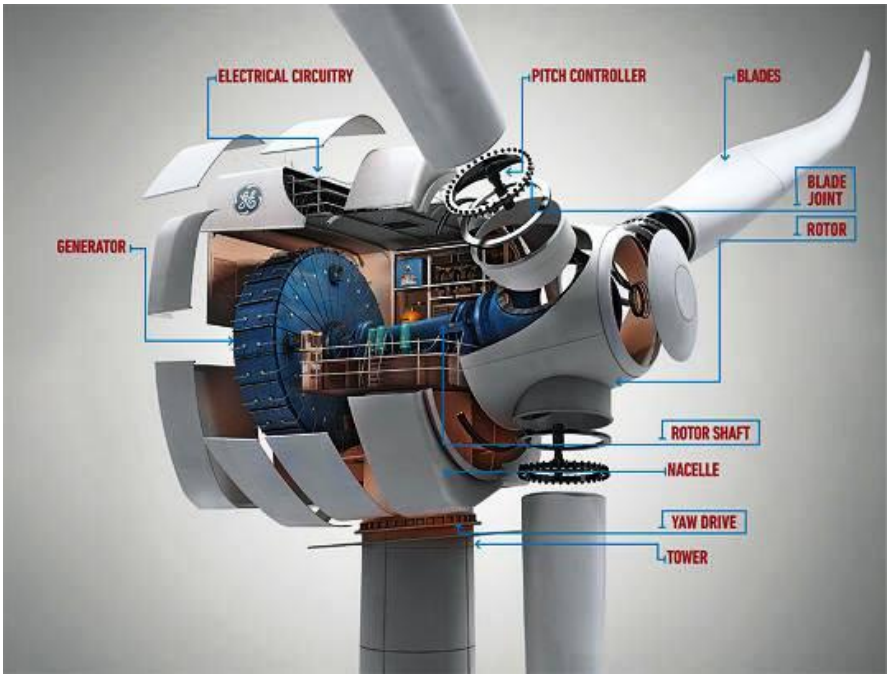

Figure 1.2: Components of wind turbine

- **Gearbox**:

The gearbox present in the turbine helps in increasing the rotational speed of the shaft. A low-speed shaft feeds into the gearbox and a high-speed shaft feeds from the gearbox into the generator. Some turbines use direct drive generators that are capable of producing electricity at a lower rotational speed.

- **Generators**:

Wind turbines typically have a single AC generator that converts the mechanical energy from the wind turbine's rotation into electrical energy. Clipper wind power uses a different design that features four DC generators. Offshore wind turbines typically send power through cables.

- **Rotor**:

The rotor includes both the blades and the hub which consists of normally two or three blades attached to a hub. The system performance of the wind turbine is based on the selection of blade number, shape, and length. The rotor can be either upwind or downwind design. Most wind turbines are three bladed upwind designs.

- **Towers**:

Towers are usually tubular steel towers 60m to 80m high that consist of three sections of varying heights. There are some towers with heights around 100m. The tower supports the wind turbine nacelle and rotor.

- **Floating body**:

The floating body supports all wind turbine elements in the ocean. The floating body is tied up by the mooring systems and has enough buoyancy to support the structure. The placement of wind turbines in harsh offshore environments is an engineering challenge, which requires development of suitable platforms to support the floating turbines therefore floating wind turbine concepts are classified according their floater.

2.2 Offshore wind energy

Currently, there are a number of offshore wind turbine floating foundation concepts in various stages of development. The main concern is to study the floating wind turbine in deep water depth where the generation of power can be improved. The platforms for floating wind turbines in deep water falls into four main categories:

- Spar-type
- Tension Leg Platform (TLP) type
- Pontoon (barge) type
- Semi-submersible type

In general terms, the spar- type have better heave performance than semi-submersibles due to their deep draft and reduced vertical wave exciting forces, but have more pitch and roll motions, since the water plane area contribution to stability is reduced. TLPs have very good heave and angular motions, but the complexity and cost of the mooring

installation, the change in tendon tension due to tidal variations, and the structural frequency coupling between the mast and the mooring system, are three major hurdles for such systems. Semi-submersible concepts with a shallow draft and good stability in operational and transit conditions are significantly cheaper to tow out, install and commission than spar-buoy, due to their draft.

A brief review of offshore wind energy in Europe is presented by Henderson et al. (2003) and a detail study on the ocean, wind and wave energy utilization is discussed in Nielsen et al. (2009). The development of offshore wind energy in United States can be found in Watson et al. (2005) and a brief review of the research on floating wind turbines is presented in Wang et al. (2010). In the next subsection, we will discuss various offshore floating wind turbines in detail.

2.2.1 Spar-type floating wind turbine

The spar-type wind turbine comprises the floating foundation which is referred as the floater, the tower and the rotor-nacelle assembly (RNA). The floater may be towed in the horizontal position to calm waters near the deployment site. It is then upended, stabilized, and the tower and the RNA mounted by a derrick crane barge-type before finally being towed by escort tugs in the vertical position to the deployment site for connection to the mooring system (see Figure 2.1).

Figure 2.1: Spar-type floating wind turbine

The floating foundation consist a steel and/or concrete cylinder filled with a ballast of water and gravels to keep the center of gravity well below the center of buoyancy which ensures the wind turbine floats in the sea and stays upright since it creates a large righting moment arm and high inertial resistance to pitch and roll motions. The floater is ballasted by permanent solid iron ore ballast, concrete or gravel from a chute. Alternatively, the ballast tanks may be injected with grout. It should be remarked that the spar-type is difficult to capsize. The draft of the floating foundation is usually larger than or at least equal to the hub height above the mean sea level for stability and to minimize heave motion. Therefore, it is necessary to have deep water for deployment of this spar-type floating wind turbine as adequate keel to seabed vertical clearance is required for the mooring system to be effective.

The spar-type floating wind turbine is usually kept in position by a taut or a catenary spread mooring system using anchor-chains, steel cables and/or synthetic fiber ropes. Alternatively, it may be moored by a single vertical tendon held at the base by a swivel connection that allows the wind turbine to revolve as the wind changes direction (as proposed by the company SWAY). This free yawing effect is similar to the swinging mechanism found in a Floating Production Storage and Offloading vessel (FPSO) turret mooring in the offshore oil and gas industry. Although favorable because the wind turbine will always face the direction of incoming wind thus optimizing power generation and the single vertical tendon may not provide for a degree of redundancy in the event of failure, resulting in unrestrained drifting of the floater. The first full scale spar-type floating turbine has been deployed off the south-west coast of Karmoy Island, Norway by Statoil in the Hywind demonstration project.

Tong (1998) analyzed the technical and economic aspect of wind farms. The conceptual design for FLOAT which is a spar-type floating wind turbine was presented. Nielson et al. (2006) discussed the integrated dynamic analysis of spar-type floating wind turbines and they developed simulation models for Hywind and compared their numerical results with model scale test results. Skaare et al. (2007) presented the importance of control strategies on fatigue life of floating wind turbines. They considered various environmental conditions and wind turbine control schemes. They showed the importance of the effect of pitch-angle control of blades on the dynamic response of the floating wind

turbine for wind speeds above the rated wind speed. Suzuki and Sato (2007) investigated the load on turbine blade induced by motion of floating platform and design requirement for the platform. Here, the effect of a stabilizing the fin attached at the base of the floating foundation in reducing the pitch motion of the floating spar-type wind turbine was analyzed.

Matsukuma and Utsunomiya (2008) performed a motion analysis of a spar-type floating wind turbine under steady wind considering rotor rotation. The wind loads acting on the rotor blades are calculated using the blade element momentum theory. As a result, the motion of yaw, sway and roll are generated due to the effect of the gyro moment for the rotor-rotation. Utsunomiya et al. (2009) continued the experimental validation for motion of a spar-type floating offshore wind turbine. In this case the motion of a prototype spar-type wind turbine was determined under regular and irregular waves and a steady horizontal force that simulates the steady wind condition was analyzed. Karimirad and Moan (2010) carried out structural dynamic response analyses of a spar-type wind turbine in the extreme survival condition. Numerical simulation for coupled wave and wind induced motion and structural response in harsh conditions for a parked floating wind turbine were undertaken. Recently, a detailed review on offshore floating wind turbine and the dynamic analysis of spar-type floating offshore wind turbine is studied by Bagbanci et al. (2011a,c).

2.2.2 Tension leg platform (TLP) type floating wind turbine

The TLP type comprises a floating platform structure to carry the wind turbine as in Figure 2.2. In the offshore oil and gas industry, the conventional TLP platform comprises a square pontoon with columns on which the topside deck rests. A smaller version of this conventional hull form is the mini-TLP which has been adopted by the TLP-type floating wind turbine. Unlike the spar-type floating wind turbine which needs to be assembled in water, the TLP wind turbine may be assembled and commissioned onshore thereby avoiding the logistic difficulties of offshore assembly. The fully fitted up platform is towed to the deployment site thus precluding the need to charter and mobilize expensive heavy-lift vessels or derrick crane barge-types for offshore construction. The floating platform is held in position by vertical tendons (also called tethers) which are anchored

either by a template foundation, suction caissons or by pile driven anchors. The pre-tensioned tethers provide the righting stability.

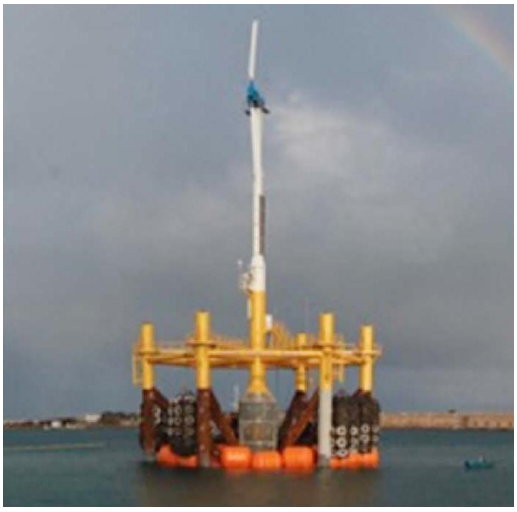

Figure 2.2: TLP floating wind turbine

This type of floating wind turbine has a relatively less dynamic response to waves when compared to the spar-type, the semi-submersible type or the pontoon type. A TLP wind turbine has since been installed off the coast of Puglia, southern Italy by Blue H Technologies. This large scale prototype is used to test the assembly, transportation and installation of the TLP type wind energy converter as well as to serve as a metering platform with sensors to measure site specific data.

Withee and Sclavounos (2004) studied the fully coupled dynamic analysis of a floating wind turbine system. They performed fully coupled time domain simulations of the system responses for a 1.5MW wind turbine mounted on a TLP floater under wind and wave forces. They observed that the two damping mechanisms were comparable in magnitude and that the damping arising from the turbine rotor appears to obey a distinctly linear law. Lee (2004) analyzed the responses of floating wind turbines to wind and wave excitation. He carried out frequency domain response analysis of both TLP and spar-type floating wind turbines in order to compare the performances of the two floater concepts. Suzuki et al. (2009) developed a conceptual design of a TLP-type floating structure for offshore wind farms. The design is based on their past experience in the design and fabrication of TLP which takes into consideration the stability of the structure, mooring forces and ease in maintenance. Weinzettel et al. (2009) performed a life cycle

assessment of a floating offshore wind turbine based on the sway concept TLP type floater. The preliminary life cycle assessment considered the environmental impact of the floating wind turbine and highlighted the importance of the decommissioning scenario whereby materials are recycled to mitigate detrimental effects on the environment.

Bae et al. (2010) performed a rotor-floater-tether coupled dynamic analysis on a mini TLP-type offshore floating wind turbine. The dynamic coupling between the rotating blades, floater and the mooring-floater dynamic coupling was considered and assessed. Nihei and Fujioka (2010) investigated the motion characteristics of a TLP type offshore wind turbine in waves and wind. Their experiments indicated that in the case of applied waves and wind, the wind has the beneficial effect of stabilizing the floater pitch motion and decreasing the vibration of the mooring lines.

2.2.3 Pontoon (Barge) type floating wind turbine

The pontoon type floating wind turbine has a very large pontoon structure to carry a group of wind turbines. The large pontoon structure achieves stability via distributed buoyancy and by taking advantage of the weighted water plane area for righting moment. The pontoon type may be moored by conventional catenary anchor chains. However, the setback of the pontoon-type wind turbine is that it is susceptible to the roll and pitch motions in waves experienced by ocean going ship shaped vessels and may only be sited in calm seas, like in a harbour, sheltered cove or lagoon.

Figure 2.3: Barge-type floating wind turbine

The National Maritime Research Institute (NMRI) in Tokyo has made some studies on such pontoon-type floating wind turbines. It should be remarked that there are clearly hybrid types of floating wind turbines, for example a combination of spar-type floater and tension leg mooring system. Also, there is an interesting concept of a sailing-type floating wind turbine that was studied at the National Institute for Environmental Studies, Japan. The floating wind power plant has no mooring system but navigates with sails and azimuth thrusters. The self-sailing and self-propelled mobility allows the wind farm to move to a location that maximizes the generation of wind power as well as to weather route from storms.

Based on the buoyancy stabilized concept, NREL and MIT collaborated in a pontoon-type (or barge-type) floating wind turbine. The pontoon-type is adopted because of it is simplicity in design, fabrication and installation. Jonkman and Buhl (2007) presented fully coupled aero-hydro-servo-elastic simulation tools for a preliminary loads analysis for a 5MW pontoon-type wind turbine. The analysis aims to characterize the dynamic response and to identify potential loads and instabilities that would be detrimental to such a pontoon-type design. They found that coupling between the turbine response and the pontoon pitch motion produces larger extreme loads in the floating turbine tower and blades. The pontoon was found to be susceptible to excessive pitching in extreme wave conditions. The compliance of the floating pontoon wind turbine however reduces a tower side-to-side instability that occurred in land-based turbines. So some design modifications are suggested to reduce the pontoon motions and to eliminate the instabilities.

Skaare et al. (2006) analyzed integrated dynamic analysis of floating offshore wind turbines. Wayman and Sclavounos (2006) presented the coupled dynamic modeling of floating wind turbine system in frequency domain. The floating wind turbine is kept in place by mooring lines. Iijima et al. (2010) described their numerical procedure for the fully coupled aerodynamic and hydroelastic time-domain analysis of an offshore floating wind turbine system including rotor blade dynamics, dynamic motions and flexible deflections of the structural system. The dynamic coupling between the rotating blades and the structural system under wind and wave loads was taken into account. Recently, a

detailed comparison between the dynamic analysis of spar-type and barge-type floating offshore wind turbine is studied by Bagbanci et al. (2011d).

2.2.4 Semi-submersible type floating wind turbine

The semi-submersible type comprises a few large column tubes connected to each other by tubular members. A wind turbine may sit on one of the column tubes or there could be wind turbines sitting in all the columns. Alternatively, the wind turbine may be positioned at the geometric centre of the column tubes and supported by lateral bracing members. The column tubes provide the ballast and they are partially filled with water. In the float condition, the water-plane area of the columns primarily provides floatation stability. This design is good in providing stability to the wind turbine and it is relatively shallow draft allows for site flexibility.

Figure 2.4: Semi-submersible type floating wind turbine

The semi-submersible floating wind turbine is kept in position by mooring lines. This type of floating wind turbine may be constructed onshore. Until now, there is no semi-submersible floating wind turbine in operation. Principle Power Inc. is promoting the semi-submersible type which consists of three column tubes with patented horizontal

water entrapment heave plates at the bases. The heave plates primarily serve to reduce heave and pitch motion without increasing floating platform size.

Henderson and Patel (1998) presented analytical and numerical design tools for evaluating the performance of semi-submersible floating wind turbines. Zambrano et al. (2006) presented the dynamic modeling of deep water offshore structure fitted with three wind turbines in the Gulf of Mexico storm conditions using Fourier spectrum based model and the WAMIT was used to develop the wave forces on the platform. Shimada et al. (2007) and Ishihara et al. (2007a, 2007b, 2008) studied the dynamic response of a semi-submersible type under resonance condition. In the numerical computations, nonlinear damping effect due to hydrodynamic drag forces and the inertia forces are considered in the equation of motion, where the linear hydrodynamic forces are obtained from the Green's function model. Ishihara et al. (2009) analyzed the influence of heave plate on dynamic response of floating offshore wind turbine in water tank experiment. It is observed that the heave plates help to increase the natural period of heave, thereby resulting in a reduction of heave response at rated and extreme sea states.

Roddier et al. (2009), Cermelli et al. (2009) and Aubault et al. (2009) conducted a feasibility study for the WindFloat technology for a semi-submersible floating wind turbine. Roddier et al. (2009) focused on the design basis for wind turbine floating foundations. The authors pointed out that the design of the hull for a large wind turbine must draw on the synergies with oil and gas offshore platform technology, while accounting for the different design requirements and functionality of the wind turbine. Then, Cermelli et al. (2009) carried out hydrodynamic analysis of the hull of the floating foundation. Aubault et al. (2009) discussed the structural assessment of a column-stabilized floating foundation. They focused on the methodology for estimating the strength and fatigue of the structural components.

2.3 Offshore monopile wind turbine

Most of the offshore wind turbines are installed on fixed bottom substructures mostly in shallow water not more than 20m by driving monopiles into the seabed or by relying on conventional concrete gravity bases. In shallow water region, monopile offshore wind turbines are mostly found to be used for the generation of electricity. So, the detailed

study on the performance of monopile offshore wind turbine is very necessary. A brief study on the modal dynamics of large wind turbine with different support structures can be found in Bir and Jonkman (2008). Agarwal and Manuel (2009) simulated the response for long-term extreme load prediction of offshore wind turbine.

Figure 2.5: (a) Monopile wind turbine and (b) monopile foundation

Recently, many countries are involved in the design and installation of offshore wind turbines in deep waters. A lot of research is going on the performances of offshore floating wind turbines. Bulder et al. (2002) used linear frequency-domain hydrodynamics techniques to find the response amplitude operators (RAOs) and amplitude standard deviations of the six rigid-body modes of motion for the support platform of a tri-floater design for a 5MW wind turbine. Lee (2005) used linear frequency domain hydrodynamics techniques to analyze a TLP design and a taut leg spar-type for a 1.5MW wind turbine. Wayman et al. (2006) and Wayman (2006) also used a similar process to analyze multiple TLP designs and a shallow drafted barge design for a 5MW wind turbine. Most recently, through frequency domain analysis, Vijfhuizen (2006) designed a barge for a 5MW wind turbine, which was also a platform for an oscillating water column (OWC) wave energy device. Klose et al. (2007) analyzed integrated load and strength analysis for offshore wind turbines with jacket structures. Recently, Bagbanci et al. (2011b) studied the effect of environment on design loads on monopile offshore wind turbine.

Since, most of the support platforms that have been proposed for floating wind turbines are more or less axisymmetric, and because there is no hydrodynamic mechanism that

`will induce yaw moments on such floating bodies, one might question whether the support platform yaw rotation degree of freedom is necessary. The wind turbine, however, induces yaw moments that are primarily the result of (i) the aerodynamic loads on the rotor when a yaw error exists between the rotor axis and nominal wind direction; and (ii) the spinning inertia of the rotor combined with pitching motion, which induces a gyroscopic yaw moment.

In both cases of offshore wind turbine concepts for shallow water with fixed foundation and for deep water with floating foundation, the effect of the wind turbine is dominant on the design load for the supporting structure. So an integrated load analyses are carried out with comprehensive simulation tools. For offshore based wind turbine these design codes are labeled as aero-servo-hydro-elastic tools, which mean that they incorporate aerodynamic models (aero), control system (servo) models, hydrodynamic loads (hydro) and structural dynamic (elastic) models in a fully coupled simulation environment. More precisely, these simulation tools incorporate sophisticated models of both turbulent and deterministic wind inflow; aerodynamic, gravitational, and inertial loading of the rotor, nacelle, and tower; elastic effects within and between components and in the foundation; and mechanical actuation and electrical responses of the generator and of the control and protection systems. The analysis of offshore wind turbines must also account for the dynamic coupling between the motions of the support platform and the wind turbine, as well as for the dynamic characterization of the mooring system for compliant floating platforms. A detailed study on the offshore floating wind turbine can also be found in Musial et al. (2004a), Musial and Butterfield (2004b) and Musial et al. (2006).

2.3.1 Structural design of offshore monopile wind turbines

The monopile has historically been the most commonly selected foundation type due to it is lower cost, simplicity, and appropriateness for shallow water (less than 20 m). The monopile generally does not require any preparation of the seabed and is installed by drilling or driving the structure into the ocean floor to depths of up to 40 meters. The monopile is relatively simple to manufacture, keeping it is cost down despite reaching weights of over 500 tons and diameters of up to 5.1 m, which can be heavier than some more complex foundation designs. While the monopile is an appropriate foundation

choice for many projects, it can be unsuitable in some applications. These foundations are not well suited for soil strata with large boulders. Additionally the required size of an acceptable monopile increases disproportionately as turbine size increases and site conditions become more challenging. Therefore, sites with deeper water, harsh waves and currents and larger turbines may require the implementation of more complex and sturdier designs, such as the jacket, the tripod, or the tripile.

2.4 Conclusions

In this Chapter, a brief overview and a detailed literature survey of research and development of offshore floating wind turbine concepts for various floaters configuration is presented. The following conclusions are drawn based on the study carried out in this Chapter:

- The performances of various floating wind turbine models in different water depths are outlined to understand the importance of the water depth for power generation.
- The working principle of various floater concepts, the conceptual designs for floating platforms used for floating wind turbines and also components of floating wind turbines are described.
- The energy production capacity and the importance of offshore floating wind turbines are discussed in detail.
- The studies carried out on monopile offshore wind turbine and its structural properties are presented.

CHAPTER 3

MATHEMATICAL FORMULATION

In the present Chapter, a brief mathematical formulation of floating turbine motions under wave and wind effects are described in detail. The hydrodynamic behavior of the floaters and the potential theory is applied using panel method. The generalized inertia forces and the active forces used for the floating wind turbine along with the hydrodynamic model and the mooring system are studied.

3.1 Mathematical Model

The hydrodynamic study of the floater is combined with and aerodynamic model to obtain a coupled aero-servo-hydro-elastic model. Generalized inertia forces for floating wind turbine concepts are described for tower, nacelle, hub, platform and blades. The generalized active forces are described for aerodynamic forces, hydrodynamic forces, gravity force, drive train force and elastic forces.

3.1.1 Equation of Motion

The complete nonlinear equation of motion for the coupled wind turbine and platform equation is defined by following equation

$$M_{ij}(q,u,t)\ddot{q}_j = f_i\ (q,\dot{q},u,t) \tag{3.1}$$

where, M_{ij} is the (i,j) component of the inertia mass matrix, q is the degrees of freedom, $\dot{q}$ is the first time derivative degrees of freedom, u is the set of control inputs and t is

\time, $\ddot{q}$ is the second time derivative degrees of freedom (Jonkman (2007)). The inertia mass matrix is given by

$$M = \begin{bmatrix} m & 0 & 0 & 0 & mz_{B,g} & -my_{B,g} \\ 0 & m & 0 & -mz_{B,g} & 0 & mx_{B,g} \\ 0 & 0 & m & my_{B,g} & -mx_{B,g} & 0 \\ 0 & -mz_{B,g} & my_{B,g} & (I^{B}_{XX}) & -I^{B}_{YX} & -I^{B}_{ZX} \\ mz_{B,g} & 0 & -mx_{B,g} & -I^{B}_{XY} & (I^{B}_{ZZ}) & -I^{B}_{YZ} \\ -my_{B,g} & mx_{B,g} & 0 & -I^{B}_{XZ} & -I^{B}_{YZ} & (I^{B}_{zz}) \end{bmatrix} \tag{3.2}$$

The FAST code uses Kane's method for deriving the equations of motion. Kane's method is very useful way for deriving equations of motion of complex rigid-body systems also continuous flexible systems. This method is improved from Newton's second law or Lagrange–D'Alembert principle. It is possible to use it for holonomic and non-holonomic systems. Holonomic systems are based on the coordinates and time. A holomonic system can be defined by following equation.

$$F_r + F_r^* = 0 \quad \text{for} \quad r = 1,\ 2,\ 3.....n, \tag{3.3}$$

where n is the number of generalized coordinates which means degree of freedom (DOF). Is defines body of movement. F_r^* is generalized inertia forces and F_r is the generalized active forces. Generalized inertia forces for floating wind turbine concepts described tower, nacelle, hub, platform and blades.

3.1.2 Generalized inertia forces

The generalized inertia forces is written as

$$F_r^* = F_r^*\big|_{Hub} + F_r^*\big|_{Nacelle} + F_r^*\big|_{Tower} + F_r^*\big|_{Platform} + F_r^*\big|_{Blades} \tag{3.4}$$

where the generalized inertia forces for hub, nacelle, tower, platform and blades are describe as

For nacelle:

$$F_r^*\Big|_{Nacelle} = {}^{E}v_r^{D}.(-m_N\,{}^{E}a^{D}) + {}^{E}\omega_r^{N}.(-{}^{E}H^{D}) \tag{3.5}$$

For hub:

$$F_r^*\Big|_{Hub} = {}^E v_r^D.(-m_H\ {}^E a^D) + {}^E\omega_r^H\ .(-{}^E H^D) \tag{3.6}$$

where, D is center of mass of hub or nacelle, ${}^E v_r^D$ is the r[th] partial velocity of the center of mass, m is the mass, ${}^E a^D$ is the acceleration of the center of the mass in inertial frame, ${}^E\omega_r^N$ is the r[th] partial angular velocity and ${}^E H^D$ is the time derivative of angular momentum of center of mass in inertial frame of the abovementioned units.

For Tower:

$$F_r^*\Big|_{Tower} = -\int_0^H \mu_T(h)\,{}^E v_r^T.{}^E a^T dh \tag{3.7}$$

where, $\mu\ (h)$ is the tower distributed lineal density of tower, ${}^E v_r^T$ is the r[th] partial velocity of the point T in the tower and ${}^E a^T$ is the acceleration of same point in the inertial frame.

For blades:

$$F_r^*\Big|_{Blades} = -\int_0^{R-R_H} \mu_B(r_1)\,{}^E v_r^{X_1}\,{}^E a^{X_1} dr_1 - \int_0^{R-R_H} \mu_B(r_2)\,{}^E v_r^{X_2}\,{}^E a^{X_2} dr_2 \tag{3.8}$$

where, μ_B is the distributed lineal density of blade, ${}^E v_r^X$ is the r[th] partial velocity of point X for each different blade, ${}^E a^X$ is the acceleration of same point in the inertial frame for each blade.

3.1.3 Generalized active forces

The generalized active forces for floating wind turbine concepts described aerodynamic forces, hydrodynamic forces, gravity force, drive train force and elastic forces. It is possible to write equation as

$$F_r = F_r\Big|_{Aero} + F_r\Big|_{Hydro} + F_r\Big|_{Gravity} + F_r\Big|_{Elastic} + F_r\Big|_{Drivetrain} + F_r\Big|_{Mooring} \tag{3.9}$$

where $F_r\Big|_{Aero}$ is aerodynamic load and $F_r\Big|_{Hydro}$ is hydrodynamic load which are represent external loads. FAST uses the AeroDyn subroutine package to generate aerodynamic forces along the blade. AeroDyn is based on wind speed and the blades displacement and velocity. $F_r\Big|_{Aero}$ will be presented in the next stage.

3.2 Hydrodynamic Model

The added mass is important to include hydrodynamic loads for computing total external force on platform. The total external force on the platform can be defined by

$$F_r^{Platform} = A_{ij}\ddot{q}_{ij} + F_r^{Hydro} + F_r^{Lines} \tag{3.10}$$

where, A_{ij} is the (i, j) component of the impulsive hydrodynamic added-mass matrix. F_r^{Hydro} is the hydrodynamic loads on platform. F_r^{Lines} is the component of total mooring system. FAST code has another subroutine package HydroDyn, which computes hydrodynamic loads in the time domain. HydroDyn subroutine of FAST code use hydrodynamic added-mass and damping matrices $(A_{ij}$ and $B_{ij})$ and wave-excitation force (X_i) for hydrodynamics loads

The hydrodynamic problem is three separate problems such as radiation, diffraction, and hydrostatic problem. The radiation problem obtains loads on the platform when there is oscillatory motion of the platform in the water. Diffraction problem obtains loads on the platform when the body is not moving and waves are scattered by the platform. The hydrostatic problem is not the critical factor for the overall behavior of the platform. The hydrodynamic problem can be defined by following equation

$$F_r^{Hydro} = F_r^{Waves} + \rho g V_0 \delta_{i3} - c_{ij}^{\ Hydrostatic} q_j - \int_0^t K_{ij}(t-\tau)\dot{q}_j(\tau)d\tau \tag{3.11}$$

In Equation (3.11) the first term F_i^{Waves}, describes diffraction loads, second term $\rho g V_0 \delta_{i3} - c_{ij}^{\ Hydrostatic} q_j$, describes hydrostatic loads, third term $\int_0^t K_{ij}(t-\tau)\dot{q}_j(\tau)d\tau$, describes radiation loads. The hydrostatic matrix is shown as

$$C_{ij}^{Hydrostatic} = \begin{bmatrix} 0 & 0 & 0 & 0 & 0 & 0 \\ 0 & 0 & 0 & 0 & 0 & 0 \\ 0 & 0 & \rho g A^{(0)} & 0 & -\rho g \iint_{A^0} x dA & 0 \\ 0 & 0 & 0 & \rho g \iint_{A^0} y^2 dA + \rho g V_0 z_{COB} & 0 & 0 \\ 0 & 0 & -\rho g \iint_{A^0} x dA & 0 & \rho g \iint_{A^0} x^2 dA + \rho g V_0 z_{COB} & 0 \\ 0 & 0 & 0 & 0 & 0 & 0 \end{bmatrix} \tag{3.12}$$

bending moment maximum value and mean value are higher when pile height is maximum (Fig 4.9(b)).The diffraction loads, F_r^{Waves} is the external load on the platform from incident waves and it is related to the wave elevation. Diffraction problem, the term, is given by

$$F_r^{Waves}(t) = \frac{1}{2\pi}\int_{-\infty}^{\infty} W(\omega)\sqrt{2\pi S_\zeta^{2-Sided}(\omega)}X_i(\omega,\beta)e^{j\omega t}d\omega \tag{3.13}$$

where, $X_i(\omega,\beta)$ is a complex-valued array that represents the wave-excitation force on the support platform normalized per unit wave amplitude, ω is frequency, β is direction of the incident waves, $S_\zeta^{2-Sided}$ is the desired two-sided power spectral density (PSD) of the wave elevation per unit time and $W(\omega)$ is the Fourier transform of a realization of a white Gaussian noise (WGN) time-series process with zero mean and unit variance it is called standard normal distribution (see Jonkman (2007)).

3.2.1 Radiation Problem

The radiation problem and the diffraction problem are independent therefore the wave-radiation loads are not depending on the incident waves. Oscillation of platform and radiation has related each other. Computing of oscillation platform considers hydrodynamic added mass and damping matrices. Equation of radiation problem is defined by

$$F^{Radiation} = \int_0^t K_{ij}(t-\tau)\dot{q}_j(\tau)d\tau \tag{3.14}$$

where, K_{ij} is the (i, j) component of the matrix known as the wave radiation retardation kernel, t is simulation time and, τ is a user variable time. The radiation loads are obtained in the time domain with hydrodynamic added mass and damping matrices. In this study WAMIT is used to calculation of hydrodynamic added mass and damping matrices also excitation forces.

3.2.2 Hydrostatic Problem

The hydrostatic loads can impact laterally or vertically on platform therefore it is related buoyancy forces and moments however it is not very important effect on overall

rotational or translational motion of platform. The equation of hydrostatic equilibrium is defined by

$$F^{Hydrostatic} = \rho g V_0 \delta_{i3} - c_{ij}^{Hydrostatic} \tag{3.15}$$

where, ρ is the water density, g is the gravity, V_0 is the displaced volume of fluid, δ_{i3} is the (*i*,*3*) component of the Kronecker-Delta function and $c_{ij}^{Hydrostatic}$ is the (*i*,*j*) component of the linear hydrostatic-restoring matrix of water plane and center of buoyancy (see Jonkman (2007)).

3.3 Mooring System

The mooring system is very important to keep the floating platform stable under wind, waves, and current effects. Mooring components are the number of cables that are connected to floating platform and the anchor is connected to seabed. Mooring system cables are made from different materials and these could be chain, steel or composites. The tension on the cables is important to keep the platform stable under environment conditions and it is dependent on cable elasticity, location in water, cable weight in the water, extensional stiffness of cable and number of cables. The mooring system is modeled as linear system in the FAST code and it ignores inertia and damping. The FAST code mooring system model is homogenous catenary mooring lines. It computes weight of fluid, elastic stretching, and seabed friction of each line however it ignores the bending stiffness (Jonkman (2007)). The total load on the platform from all mooring lines is defined by

$$F_r^{Lines} = F_r^{Lines,0} - c_{ij}^{Lines} q_j \tag{3.16}$$

where, F_i^{Lines} is the component of total mooring system, $F_i^{Lines,0}$ is the pre-tension of lines from the weight of the cable not resting on the seafloor if the lines are buoyant $F_i^{Lines,0}$ should be zero, c_{ij}^{Lines} is the elastic stiffness of the mooring lines and the effective geometric stiffness by the weight of the cables in water also depends on the layout of the mooring system, q_j is the *j*th DOF.

3.4 Conclusions

In this Chapter, a brief mathematical background of floating wind turbine motions under wave and wind are presented. The following conclusions are drawn based on the study carried out in this Chapter:

- The hydrodynamic behavior of the floaters, the potential theory was applied using panel method and WAMIT is used for the calculation of radiation and diffraction loads.
- HydroDyn subroutine of FAST code uses the hydrodynamic added-mass, damping matrices and wave-excitation force for hydrodynamics loads.
- The hydrodynamic study of the floater is combined with and aerodynamic model to obtain a coupled aero-servo-hydro-elastic model.
- Generalized inertia forces for floating wind turbine concepts are described for tower, nacelle, hub, platform and blades.
- The generalized active forces are described for aerodynamic forces, hydrodynamic forces, gravity force, drive train force and elastic forces.

CHAPTER 4

OFFSHORE FIXED MONOPILE WIND TURBINE

In this chapter, the design loads for a monopile foundation are studied by analyzing the bending moment at the tower base and tower root for various values of water depth, tower height, pile diameter and turbulence model. The FAST code is used to study the bending moment at the tower base and tower root for a 5MW offshore wind turbine.

4.1 Structural design of offshore monopile wind turbine

The monopile has historically been the most commonly selected foundation type due to it is lower cost, simplicity, and appropriateness for shallow water (less than 20 m, see Figure 4.1). The design is a long hollow steel pole that extends from below the seabed to the base of the turbine. The monopile generally does not require any preparation of the seabed and is installed by drilling or driving the structure into the ocean floor to depths of up to 40 meters. The monopile is relatively simple to manufacture, keeping it is cost down despite reaching weights of over 500 tons and diameters of up to 5.1 m, which can be heavier than some more complex foundation designs.

While the monopile is an appropriate foundation choice for many projects, it can be unsuitable in some applications. These foundations are not well suited for soil strata with large boulders. Additionally the required size of an acceptable monopile increases disproportionately as turbine size increases and site conditions become more challenging. Therefore, sites with deeper water, harsh waves and currents, and larger turbines may require the implementation of more complex and sturdier designs, such as the jacket, the tripod, or the triple.

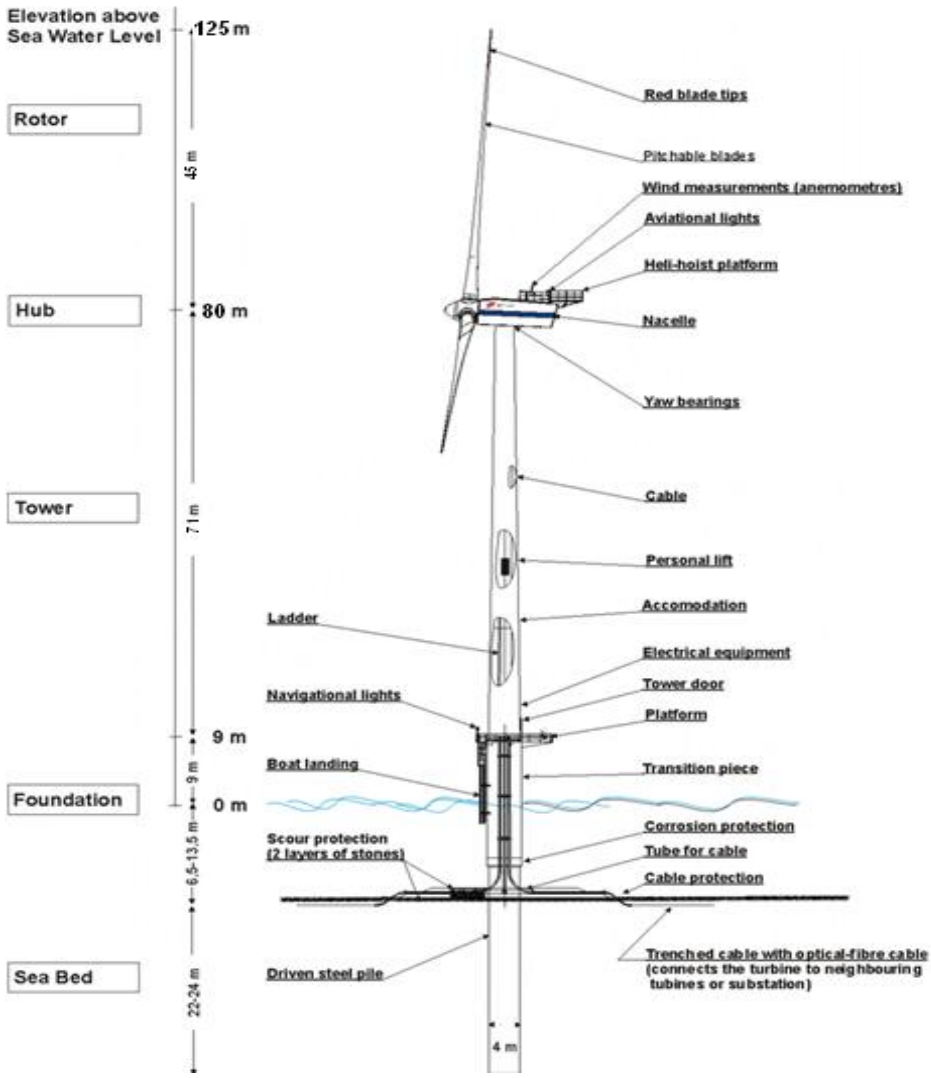

Figure 4.1: Monopile wind turbine

4.2 Loads on monopile foundation

In the present section, various loads on the monopile foundation are described in detail in order to study the effect of the loads on the wind turbine.

4.2.1 Wind loads

The wind load applied on the turbine tower comprises of the effects of the direct wind pressure on the tower and the wind turbine. Therefore in designing the tower, calculations

are made to reflect each characteristic load and suitable safety factor. Loads that occur simultaneously are combined whenever necessary. The wind turbine loads have two components namely stationary and cyclic. The cyclic loads are aerodynamic loads from a uniform, steady wind speed and the stationery loads arise from the centrifugal forces. A stationary but spatially uneven flow field over the swept areas causes cyclic load changes on the turning rotor. Further, the inertia forces that result from the rotating rotor blade masses cause periodic, non-stationery loads.

In addition to the stationary and cyclic loads, the rotor is exposed to non-periodic and random loads caused by wind turbulence. The variables to be considered are direct wind pressure, gust factor and force coefficient. The static lateral wind load along the tower height is calculated by the direct wind pressure on the projected area that varies with the diameter. The wind shear force, the overturning moment along the tower height and the tower deflection along the height are computed using formulae. If site specific wind loads and directions are used, the design of the tower becomes more economical. Also the optimum hub height for the location will result in increased production.

4.2.2 Wave and Current loads

When the waves impinge on structures, their energy is transferred as loads on the structure. The wave forces are calculated for slender structures using simplified linear theory and based on the Morison equation. The wave loads comprise of the inertia component and the drag component and they depend on the wave height, wave periods and water depth at the location. Since the wave loads depend on the water depth the shallow water and deep water structures are influenced by the wave loads. The shape of the structure influences the drag and the inertia coefficients. The wave loads decrease exponentially towards the sea bottom. The loads due to the water current are dependent on the square of the velocity of the current and similar to wind loads and calculated using drag coefficients of members.

4.2.3 Loads from Wind Rotor

The static and dynamic reaction components from the rotor on to the wind tower have to be properly accounted for as they will produce axial force, shear force, overturning moment and twisting moment on the foundation. It is worthwhile to mention here that

special wind rotors that transfer minimum reactions on to the tower have been developed recently.

4.2.4 Dynamic Behavior

A designer is required to study the dynamic characteristics of the tower with the help of simulation or modeling to understand dynamic properties of the tower. It is necessary to understand the extent to which the flexibility in the foundation plays a role as a design parameter in influencing the dynamic behavior of the tower. The dynamic magnification effects can directly influence the fatigue loads to be considered in the tower design. It is necessary for the designer to design the tower frequency such that it avoids excitation of the resonant oscillations that result from rotor thrust fluctuations at the blade passing frequency or at the blade rotational frequency. Larger and heavier turbines will inevitably experience longer periods of natural oscillation. Offshore wind turbines are also bigger than onshore turbines to take advantage of the steadier offshore winds and economies of scale. A typical onshore turbine installed today has a tower height of about 60 m to 80 m, and blades about 30 m to 40 m long; most offshore and onshore wind turbines are at the top end of this range. Offshore turbines installed today are generally between 2 MW and 4 MW, with tower heights greater than 60 m and rotor diameters of 75 m to 105 m.

4.3 Simulation results

In the present study, a 5MW wind turbine model developed at NREL is used in the simulation studies. The turbine design variables are hub height of 90 m above the mean sea level, and a rotor diameter of 126 m. The turbine is a variable-speed and collective pitch-controlled machine, with a maximum rotor speed of 12.1 rpm. The rated wind speed is 11.5 m/s. According to the NREL design variables the turbine is assumed to be placed in 20 m of water depth with a monopile support structure. The FAST code is used to study the bending moment at the tower base and tower root for various values of water depth, tower height, pile diameter and turbulence model. Bending moment at blade root and bending moment at tower base are examined for significant wave heights of 0.5 m, 4.2 m and 9.4 m. The mean wind speed, diameter of pile and turbulence model are fixed respectively at 12.1 m/s, 6 m and smooth, for three different water depth conditions and for same control units significant wave heights of 0.5 m, 4.2 m and 9.4 m is examined

with mean wind speed, diameter of pile and turbulence model are fixed respectively at 12.1 m/s, 6 m and smooth, for three different water depth conditions (10 m, 20 m, 30 m.)

4.3.1 Water depth

It is observed that wave height does not affect the blade root for each water depth as shown in Fig. 4.2 (a). It is shown that the maximum, mean and standard deviations according to 10 minute simulations, there is no difference for each water depth when wave height increases.

The bending moment at the tower base is maximum when water depth is 30m and minimum when water depth is 10m while wave height is increasing as in Fig 4.2 (b). Maximum value increases differently during 10 minutes simulation for 30 m water depth but mean and standard deviation increases differently.

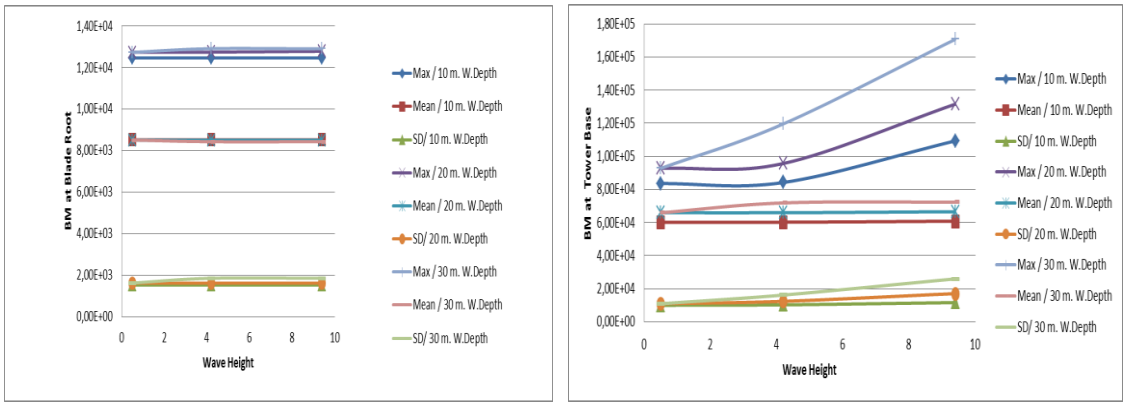

Figure 4.2: BM at (a) blade root , (b) tower base versus wave height

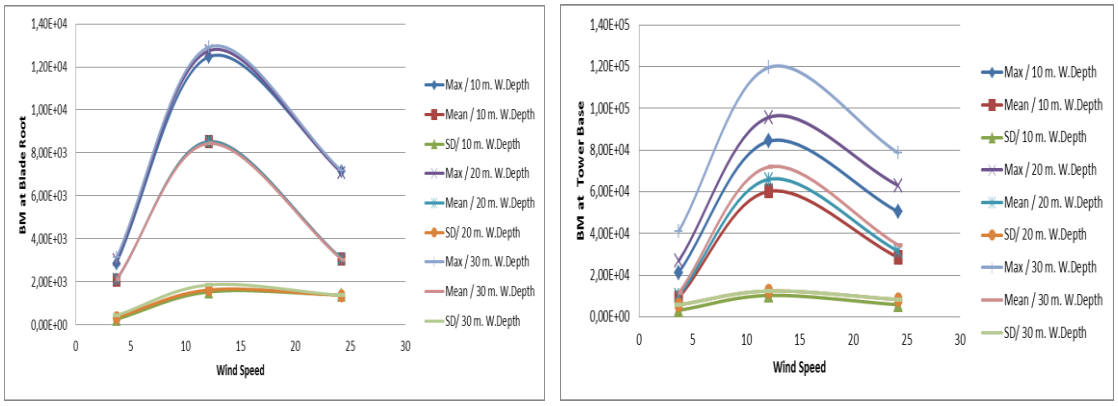

Figure 4.3: BM at (a) blade root, (b) tower base versus wind speed

For each water depth, bending moment at the blade roots is similar. No effect of water depth at the blade root is observed as shown in Fig. 4.3 (a) and there is no difference for each water depth when wind speed increases. Bending moment at tower base is maximum when water depth is maximum while wind speed increases and is minimum when water depth is minimum.

4.3.2 Pile diameter

Bending Moment at tower base and blade root is examined under the same wave height and wind speed conditions for each pile diameter which are 4m, 6m, 8m. The bending moment has maximum value at tower base for pile diameter of 8m and minimum for pile diameter of 4m but mean and standard deviation are almost same as shown in Fig. 4.4 (b). There is no difference for each pile diameter when the wave height increases. After 10 minutes simulation it is observed there is no effect on blade root as shown in Fig. 4.4 (a).

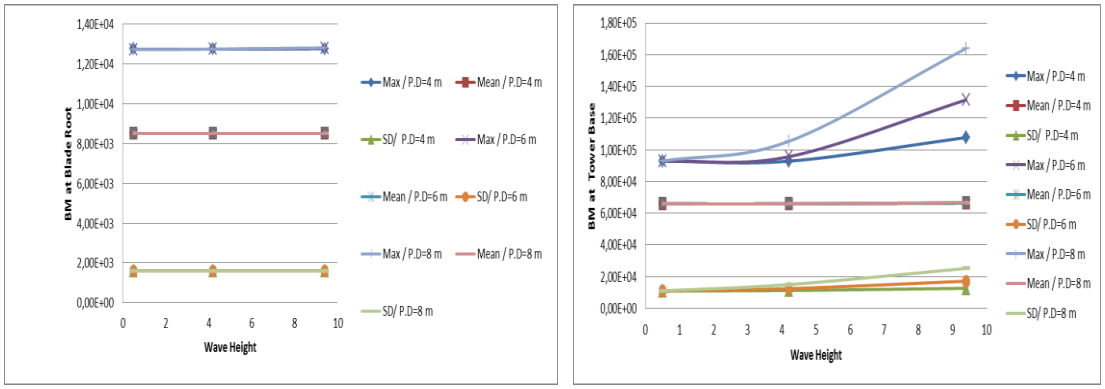

Figure 4.4: BM at (a) blade root, (b) tower base versus wave height

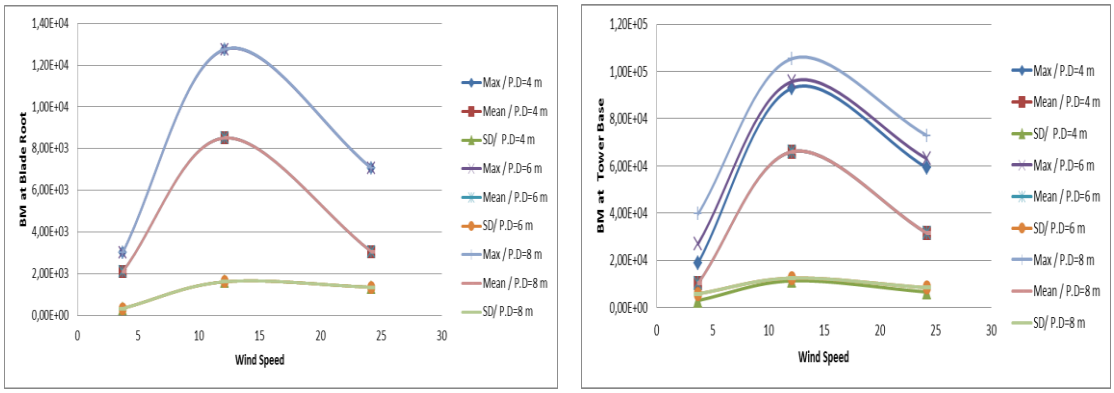

Figure 4.5 : BM at (a) blade root, (b) tower base versus wind speed

Bending moment at blade root is completely similar for each pile diameter while wind speed increases as in Fig. 4.5 (a). Maximum bending moments are different for each pile diameter however mean and standard deviations are same as shown in Fig 4.5 (b). This shows the bending moment at blade root does not change for each pile diameter.

4.3.3 Turbulence model

Bending moment at tower base and blade root is examined for each turbulence model. The Risø Smooth-Terrain model (SMOOTH), a Kaimal power spectrum (IECKAI) and a Von Karman power spectrum (IECVKM) are employed to describe the turbulence random field over the rotor plane

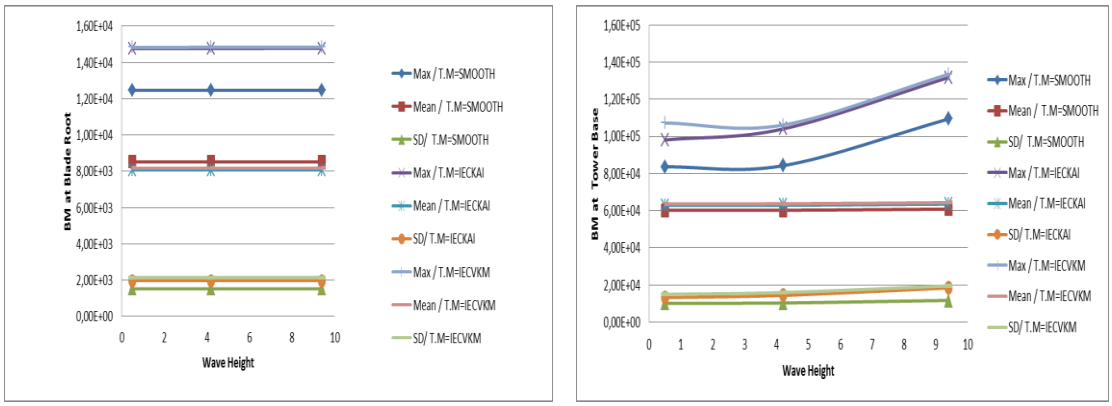

Figure 4.6: BM at (a) blade root, (b) tower base versus wave height

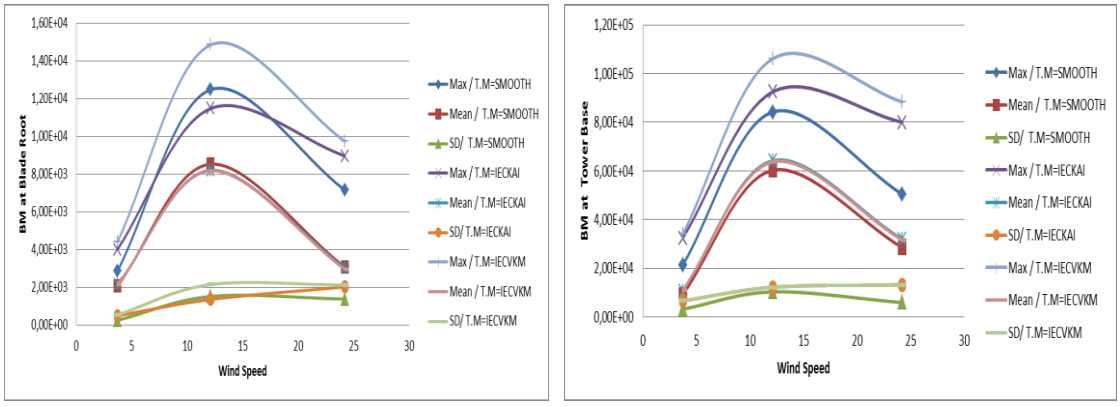

Figure 4.7 : BM at (a) blade root, (b) tower base versus wind speed

The bending moment maximum values are similar for IECKAI and IECVKM models and bigger than SMOOTH turbulence model at the blade root (Fig 4.6 (a, b)) and tower base

(Fig 4.7 (a, b)). However standard deviation and mean values are almost same. The bending moment at tower base does not change due to change in turbulence model according to wind speed and wave height.

4.3.4 Pile height

Bending Moment at tower base and blade root is examined under same wave height and wind speed conditions for each pile height which are 80m, 90m, 100m. It is observed there is no effect on blade root for each pile height while wave height (Fig 4.8 (a)) or wind speed (Fig 4.9 (a)) increases. Difference is seen when pile height is higher, the bending moment at tower base is also higher. Bending moment is bigger for pile heights which are 100m, 90m, 80m when wave height increases (Fig 4.8 (b)). The bending moment maximum value and mean value is observed to be higher when pile height is maximum (Fig 4.9(b)).

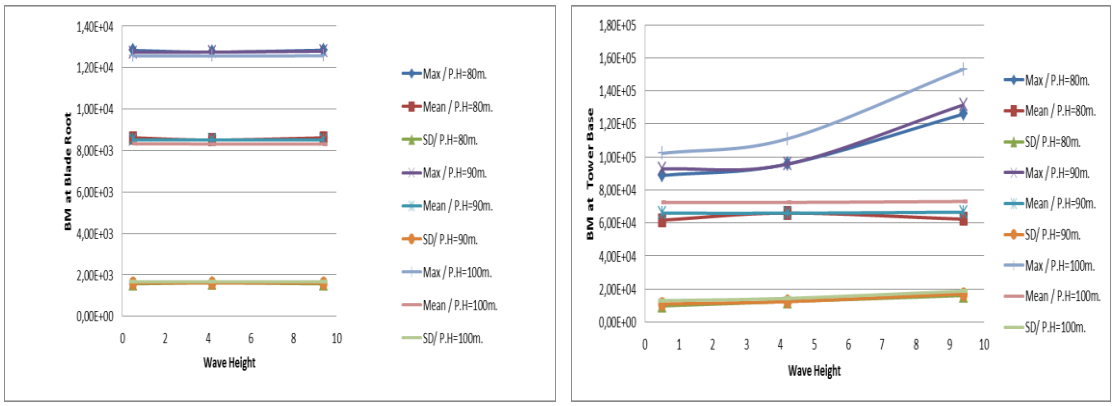

Figure 4.8: BM at (a) blade root, (b) tower base versus wave height

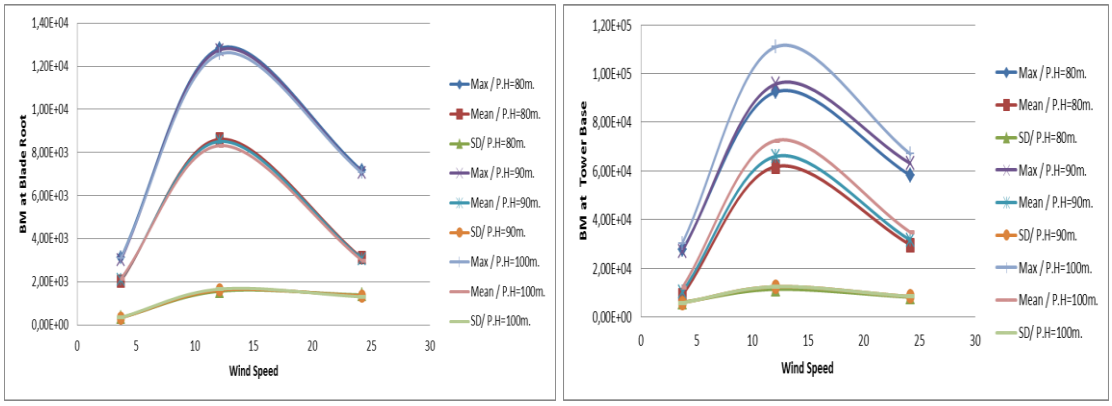

Figure 4.9: BM at (a) blade root, (b) tower base versus wind speed

4.3.5 Wind speed

The bending moment at tower base and blade root is examined for various values of wind speed. It is observed that at the blade root the bending moment is higher for wind speed 12.1m/s as in Fig. 4.10 (a).

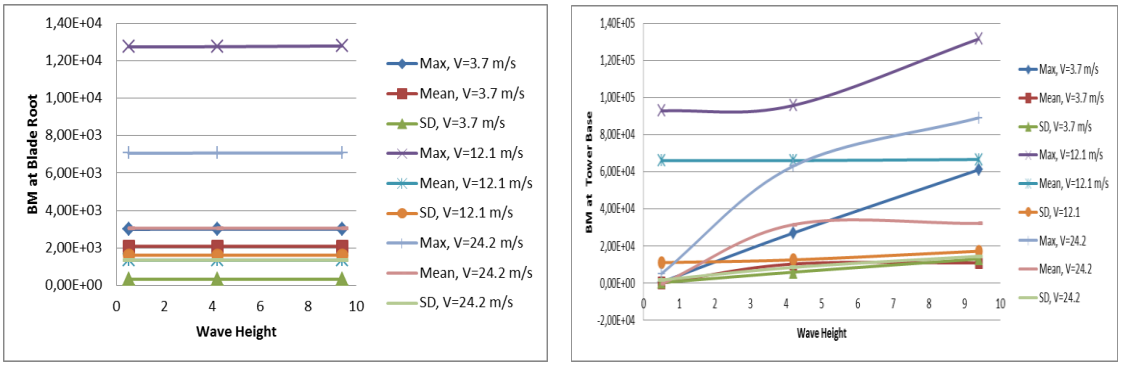

Figure 4.10: BM at (a) blade root, (b) tower base versus wave height

The bending moment remains constant with the change in the wave height. On the other hand, the bending moment in the tower base increases with the increase in wave height whereas the bending moment is higher for wind speed 12.1m/s as in Fig. 4.10 (b).

4.3.6 Wave height

The bending moment at tower base and blade root versus wind speed is obtained for various values of wave height.

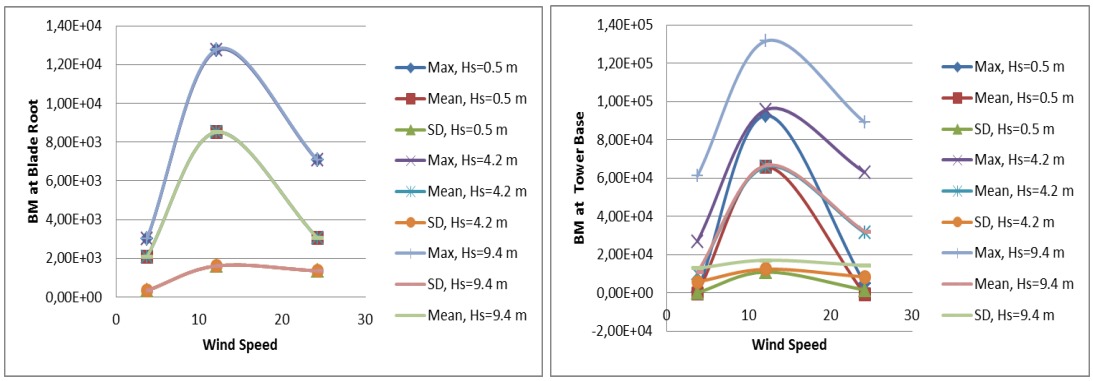

Figure 4.11: BM at (a) blade root, (b) tower base versus wind speed

The bending moment of the blade root is observed to be higher for lower values of wave height as in Fig 4.11(a) but the bending moment at the tower base also changes with change in wave height as in Fig. 4.11 (b). The bending moment at the tower base is observed to be higher for lower values of the wave height. This suggests that with the increase in the wave height the bending moment at the blade root and the tower base decreases. It may also be noted that with the increase in the wind speed the bending moment at the blade root and the tower base initially increases but after certain values of wind speed the bending moment decreases

4.4 Conclusions

In this Chapter, the design loads for a monopile foundation is studied by analyzing the bending moment at the blade root and tower base for various values of water depth, tower height, pile diameter and turbulence model. The following conclusions are drawn based on the study carried out in this Chapter:

- The FAST code is used to study the bending moment at the tower base and tower root for a 5MW offshore wind turbine.
- The maximum blade bending moment increases with wind speed, up to the rated wind speed of 11.5m/s, and then decreases, as is expected due to blade-pitch control actions.
- For each water depth the bending moment at the tower base is maximum when water depth is 30m and minimum when water depth is 10m.
- The change in the wave height and the wind speed effects the bending moments of blade roots and tower base of the offshore monopole floating wind turbine.

CHAPTER 5

OFFSHORE FLOATING WIND TURBINES

In the present chapter, the coupled dynamic analyses of floating wind turbine are performed for three different types of floater concepts NREL 5MW spar-type, NREL ITI barge-type and 5MW WindFloat semi-submersible type floaters are used in the simulation studies. Typically the turbine design variables for three concepts are hub height of 90 m above the mean sea level and a rotor diameter of 126 m. The turbine is a variable-speed and collective pitch-controlled machine with a maximum rotor speed of 12.1 rpm. The 5MW spar-type, ITI barge-type and 5MW WindFloat semi-submersible floating wind turbines are examined for various values of mean wave height and wave heading angle with three different wind speed conditions. The FAST code is used for aero-hydro-servo-elastic simulation.

5.1 NREL 5MW Spar-type Floating Turbine

A coupled dynamic analysis of 5MW spar-type floating wind turbine is analyzed in detail. The hydrodynamic study of the floater is done using WAMIT and is combined with FAST code to obtain an aero-servo-hydro-elastic model. The tower base motions and platform motions are obtained for various values of wind speed with 4m wave height and 0^o and 30^o wave heading angle.

5.1.1 Model Description

In the present study, the NREL 5MW spar-type floating wind turbine is considered for the analysis. The wind turbine properties, platform properties and mooring system properties are kept same as described in OC3 Hywind (see Jonkman (2010)). The wind

turbine properties, platform properties and mooring system properties for the spar-type floating wind turbine is presented in Table 5.1(a,b,c).

Table 5.1(a) Spar-type wind turbine properties

Hub Height	90 m
Center of Mass Location (From Sea Level)	43.4 m
Rotor Diameter	126 m
Number of Blades	3
Initial Rotational Speed	12.1 rpm
Blades Mass	53,220 kg
Nacelle Mass	240,000 kg
Hub Mass	56,780 kg
Tower Mass	249,000 kg
Power Output	5 MW
Cut-In, Rated, Cut-Out Wind Speed	3 m/s, 11.4 m/s, 25 m/s

Table 5.1(b) Spar-type platform properties

Total Draft	120 m
Depth to Top of Taper Below Sea Water Level	4 m
Depth to Bottom of Taper Below Sea Water Level	12 m
Platform Diameter Above Taper	6.5 m
Platform Diameter Below Taper	9.4 m
Platform Mass, Including Ballast	7,466,330 kg
Center of Mass Location Below Sea Level Along Platform Centerline	89.9155 m
Platform Roll Inertia (I_{xx})	4,229,230,000 kg.m^2
Platform Pitch Inertia (I_{yy})	4,229,230,000 kg.m^2
Platform Yaw Inertia (I_{zz})	164,230,000 kg.m^2

Table 5.1(c) Spar-type mooring system properties

Number of Mooring Lines	3
Angle Between Lines	120º
Depth of Anchors From Sea Level	320 m
Depth to Fairleads Below Sea Level	70.0 m
Radius to Anchors from Platform Centerline	853.87 m
Radius to Fairleads from Platform Centerline	5.2 m
Unstretched Mooring Line Length	902.2 m
Mooring Line Diameter	0.09 m
Equivalent Mooring Line Mass Density	77.7066 kg/m
Equivalent Mooring Line Weight in Water	698.094 N/m
Equivalent Mooring Line Extensional Stiffness	384,243,000 N
Additional Yaw Spring Stiffness	98,340,000 Nm/rad

5.1.2 Hull Geometry

The spar-type floater is modeled with two geometric planes of symmetry with 1,900 rectangular panels within a quarter of the body for WAMIT. The spar-type floating wind turbine and the geometry of the spar-type floater is shown in Figure 5.1(a,b).

(a) 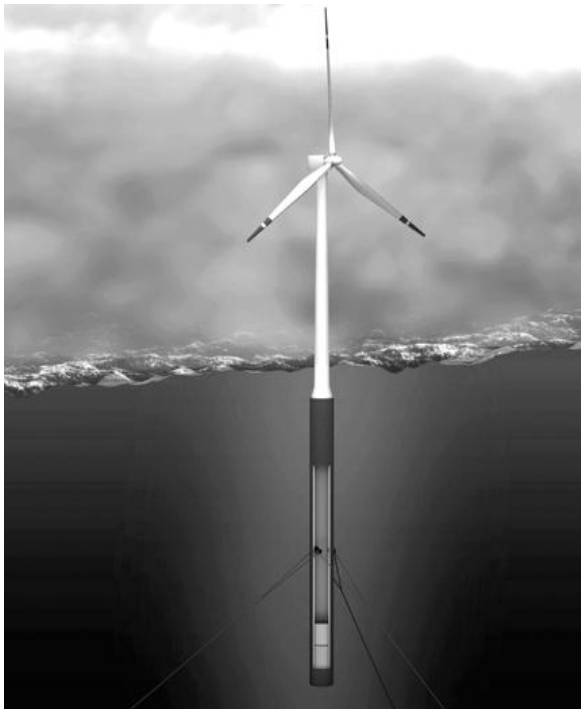 (b) 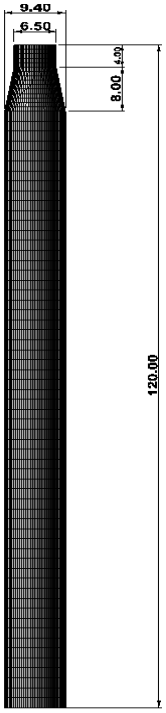

Figure 5.1: (a) Spar-type floating wind turbine (b) Hull geometry for spar-type floater

The FAST code seeks for damping coefficient, added mass and exciting force for aero-hydro-servo-elastic simulation. Thus damping coefficient, added mass and exciting force for the spar-type floater are obtained using WAMIT.

5.1.3 Added Mass and Damping Coefficient

The analysis is carried out using WAMIT in frequency domain. The mesh size of 1900 panels for a quarter body is simulated in frequency domain from 0.05 rad/s to 3 rad/s. Added mass, damping coefficient, hydrostatic matrices and exciting force are generated using WAMIT, which depends on the shape of the floater. In Figure 5.2(a), the added mass for force-translation modes are obtained and in Figure 5.2(b), the added mass for

the moment-rotational modes are obtained using the geometry of the spar-type floating wind turbine. It is observed that the surge-surge element of the frequency dependent added mass for force-translation mode is identical to the sway-sway element. On the other hand, the roll-roll element for the moment-rotational mode is identical to the pitch-pitch element. This is due to the symmetry in the spar's body.

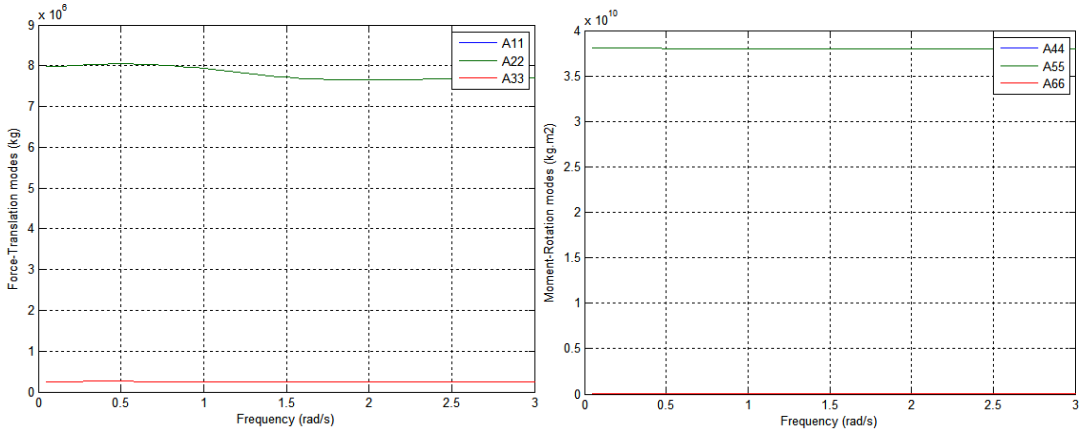

Figure 5.2: (a) Hydrodynamic added mass for (a) force-translation modes, (b) moment-rotation modes.

In Figure 5.3(a), the damping coefficients for the force-translation modes are plotted, whereas, in Figure 5.3(b), the damping coefficients for the moment-rotational modes are plotted. In this case also the surge-surge element for force-translation mode is identical to the sway-sway element and the roll-roll element for the moment-rotational modes is identical to the pitch-pitch element. The comparison of the present result with OC3-Hywind results shows that both the force-translation modes and the moment-rotational modes are almost same.

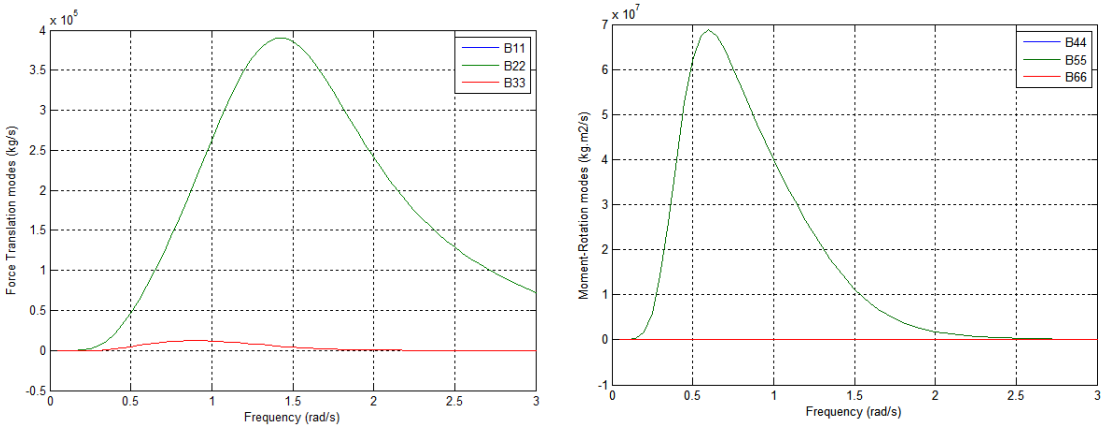

Figure 5.3: (a) Damping coefficient for (a) force-translation modes, (b) moment-rotation modes

In the next section, the results obtained for damping coefficient, added mass and exciting force using WAMIT for spar-type floater are used in the FAST code for fully coupled aero-hydro-servo-elastic simulation.

5.1.4 Fully Coupled Aero-Hydro-Servo-Elastic Simulation

The coupled aero-hydro-servo-elastic simulations are performed using the FAST code for 0º and 30º wave heading angle. The simulation is performed for 15 min time series of tower base motions such as surge, heave, sway and platform rotations such as pitch, roll, yaw motions.

5.1.4.1 Platform motions for 0º wave heading angle

The mean wave height is fixed at 4 m with 0º wave heading angle for three different wind speed conditions of 3.7 m/s, 12 m/s and 24 m/s. Tower base motions and platform rotations results are shown for each different wind speed respectively Figure 5.4 (a), Figure 5.4 (b) and Figure 5.4 (c).

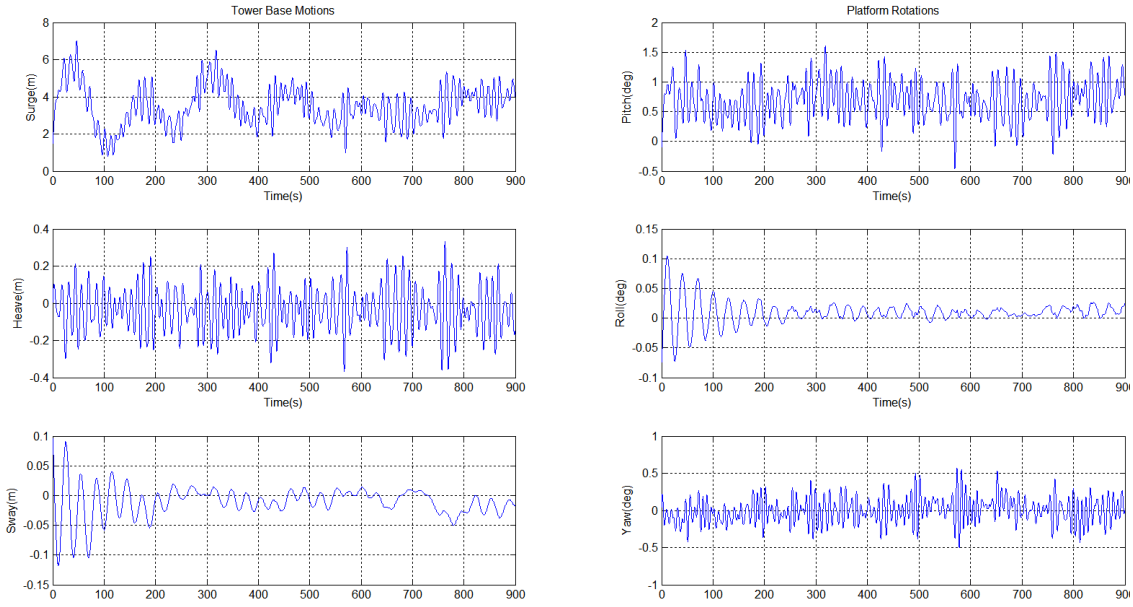

Figure 5.4 (a): Tower base motions and platform rotations for 4m wave height and 0º wave heading angle with 3.7 m/s wind speed

Stability is an important case of wind generation for floating wind turbines. In Figure 5.4(a), fully coupled sample time series for tower base motions: surge, heave, sway and platform rotations; pitch, roll yaw for fifteen minutes are obtained. It is observed that

within first 400 s, the surge motion is between 1 m-7 m but after 700 s, the surge motion decreases to 3 m-5 m. Heave motion is in between approximately +/- 0.1 m. Sway motion is observed to be decreasing after 200 s, and is in between approximately +/- 0.01 m. Pitch oscillation is approximately within 1º-0.5º. The roll motion approaches to zero after 200s, and yaw oscillation is very close to 0º.

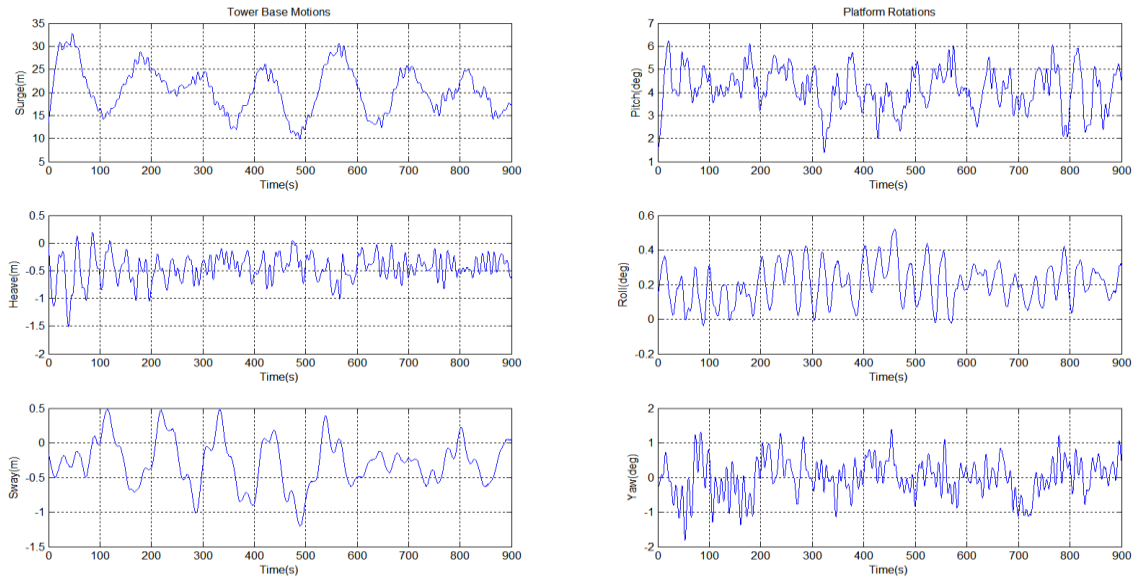

Figure 5.4 (b): Tower base motions and platform wind speed rotations for 4m wave height and 0º wave heading angle with 12 m/s

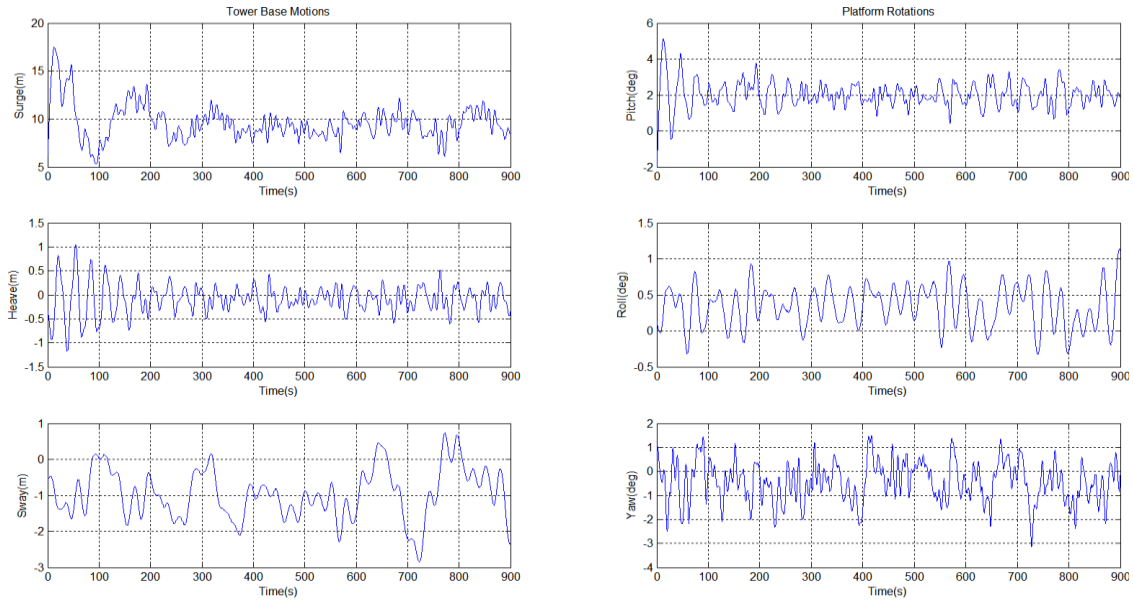

Figure 5.4 (c): Tower base motions and platform rotations for 4m wave height and 0º wave heading angle with 24 m/s wind speed

In Figure 5.4(b), the wind speed is increased to 12 m/s in the simulation run for 15 min. The surge motion is observed to be increased as compared to figure 5.4(a). The heave motion is decreased from +/-2 to around 0.5m with the increase in wind speed. Pitch angle oscillation obtained around between 3º-5º and Yaw oscillation is obtained within +/-1º. In Figure 5.4 (c), with the increase in wind speed to about 24 m/s the surge motion decreased to 10m and pitch angle oscillation obtained around between 1º-3º. There is no big difference for heave, sway, yaw, roll when the wind speed increases.

5.1.4.2 Platform motions for 30º wave heading angle

The mean wave height is fixed at 4m with 30º wave heading, for three different wind speed conditions of 3.7 m/s, 12 m/s and 24 m/s. The tower base motions and platform rotations results are shown in Figure 5.5 (a), Figure 5.4 (b) and Figure 5.4 (c).

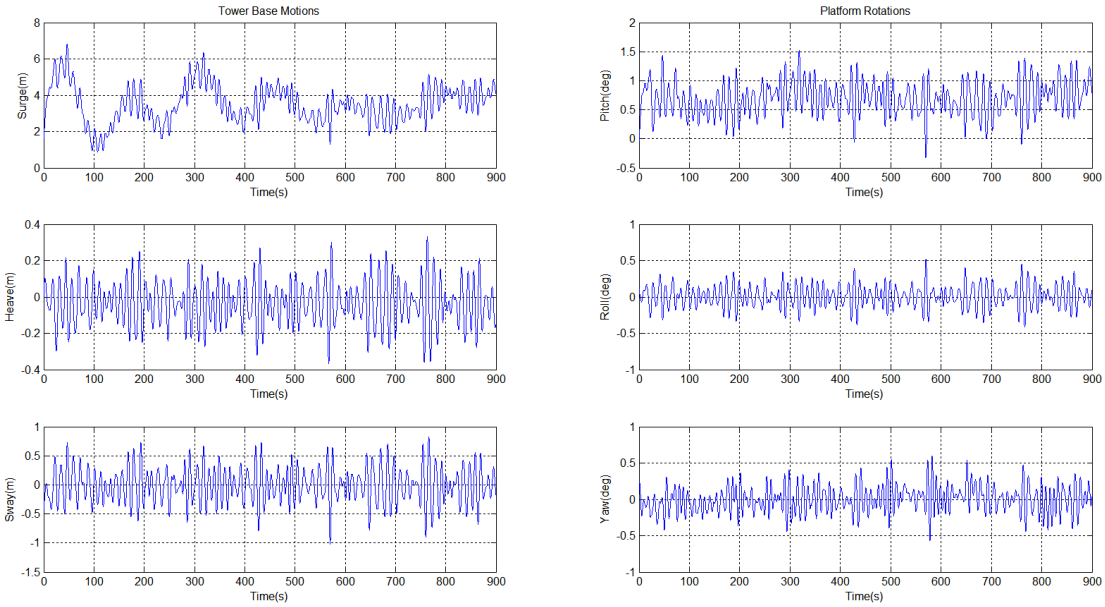

Figure 5.5 (a): Tower base motions and platform rotations for 4m wave height and 30º wave heading angle with 3.7 m/s wind speed

In Figure 5.5 (a), sample time series results are obtained for 30º wave heading angle. The turbine is for kept similar motion characteristics. The difference is observed for sway and roll motion compared to 0º wave heading angle, 3.7 m/s wind speed and 4m wave height. The sway motion is observed increased to -/+0.5m from 0 m, roll oscillation increased approximately -/+0.25º from 0º. In Figure 5.5 (b), it is observed that the surge motion is almost same as observed for 0º wave heading angle. The surge motion is between 15 m to

25 m. The heave motion is the same and it is around 0.5m with the increase in wave heading angle. Pitch angle oscillation obtained within 3º to 5º and Yaw oscillation is obtained within +/-1º.

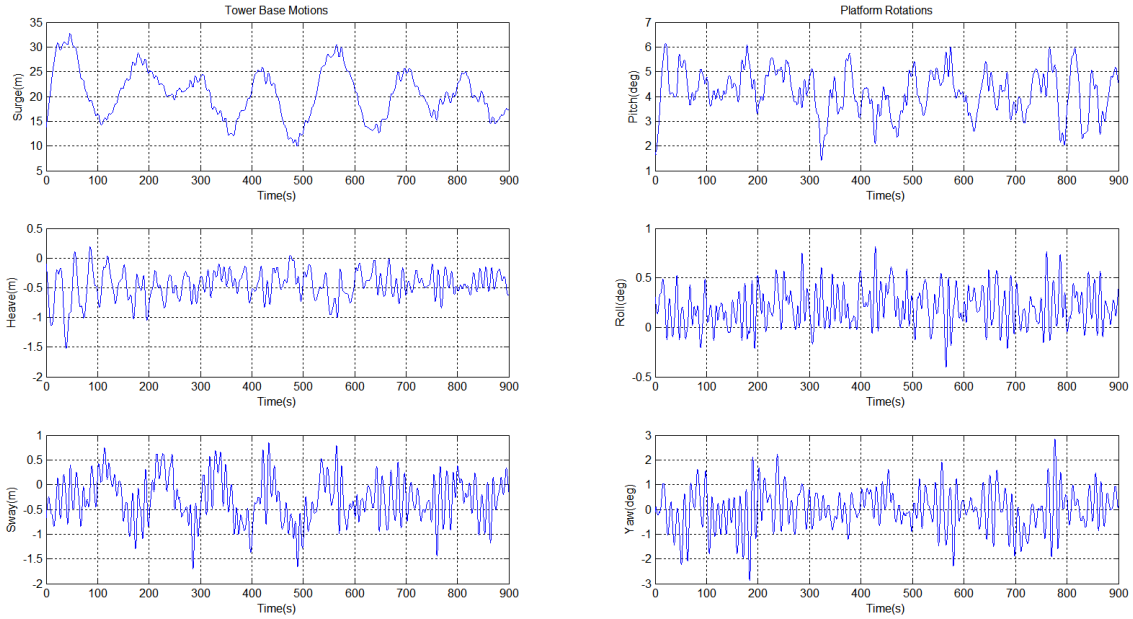

Figure 5.5 (b): Tower base motions and platform rotations for 4m wave height and 30º wave heading angle with 12 m/s wind speed

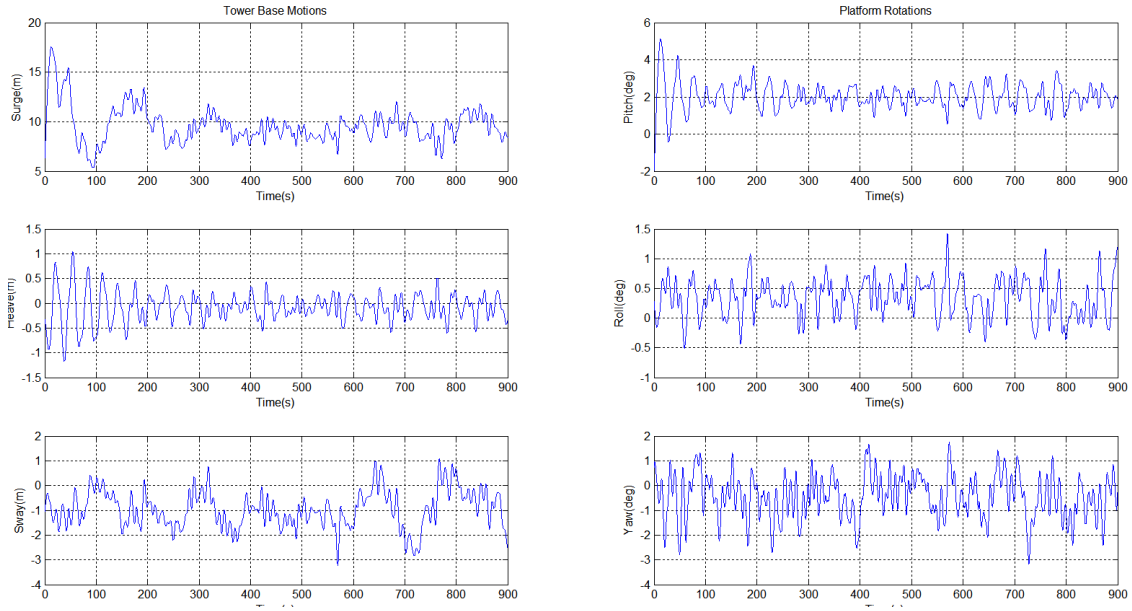

Figure 5.5 (c): Tower base motions and platform rotations for 4m wave height and 30º wave heading angle with 24 m/s wind speed

In Figure 5.4 (c), with the increase in wave heading to about 30º the surge motion is within 10m and pitch angle oscillation obtained around 1ºto 3º. There is no big difference for heave, sway, yaw and roll motions when wave heading angle is 30º with 12 m/s and 24 m/s wind speed for 4m wave height.

5.2 NREL 5MW barge-type floating turbine

A coupled dynamic analysis of 5MW barge-type floating wind turbine is analyzed in detail. The hydrodynamic study of the floater is done using WAMIT and is combined with FAST code to obtain an aero-servo-hydro-elastic model. The hydrodynamic added mass and damping coefficient are obtained using WAMIT. The tower base motions and platform motions are obtained for various values of wind speed with 4m wave height and 0º and 30 º wave heading angle.

5.2.1 Model Description

The hydrodynamic analysis of the barge-type floating wind turbine is carried out and the detail descriptions for the study are as follows. The wind turbine properties, platform properties and mooring system properties are kept same as described in Jonkman and Bhul (2007) and Jonkman (2007). In general, the studies are carried out for 5MW floating wind turbine with hub height of 90m and the rotor diameter is considered to be of 126m. The wind turbine is also considered to be of 3 bladed having the initial rotational speed of 12.1 rpm. The wind turbine properties, platform properties and the mooring system properties are shown in Table 5.2 (a,b,c).

Table 5.2(a) Barge-type wind turbine properties

Hub Height	90 m
Center of Mass Location (From Sea Level)	38.234 m
Rotor Diameter	126 m
Number of Blades	3
Initial Rotational Speed	12.1 rpm
Blades Mass	53,220 kg
Nacelle Mass	240,000 kg
Hub Mass	56,780 kg
Tower Mass	347,460 kg
Power Output	5 MW
Cut-In, Rated, Cut-Out Wind Speed	3 m/s, 11.4 m/s, 25 m/s

Table 5.2(b) Barge-type platform properties

Size (Width×Lenght×Height)	40 m × 40 m × 10 m
Moon pool (Width×Lenght×Height)	10 m × 10 m × 10 m
Operating Draft, Freeboard	4 m, 6 m
Water Displacement	6,000 m3
Mass, Including Ballast	5,452,000 kg
Center Of Mass Location Below Sea Level	0.281768 m
Roll Inertia about CM (I_{xx})	726,900,000 kg.m2
Pitch Inertia about CM (I_{yy})	726,900,000 kg.m2
Yaw Inertia about CM (I_{zz})	1,453,900,000 kg.m2

Table 5.2(c) Barge-type mooring system properties

Number of Mooring Lines	8 (4 x 2)
Angle Between Lines	90º
Depth of Anchors from Sea Level	150 m
Depth to Fairleads Below Sea Level	4.0 m
Radius to Anchors from Platform Centerline	423.422
Radius to Fairleads from Platform Centerline	28.2843
Unstretched Mooring Line Length	473.3 m
Mooring Line Diameter	0.0809 m
Equivalent Mooring Line Mass Density	130.4 kg/m
Neutral Line Length Resting on Seabed	250 m
Separation between Opposing Anchors	773.8 m

5.2.2 Hull Geometry

The barge-type floater is modeled with two geometric planes of symmetry with 2,600 rectangular panels within a quarter of the body for WAMIT. The barge-type floating wind turbine and the floater for WAMIT is shown in Figure 5.6(a,b).

(a)

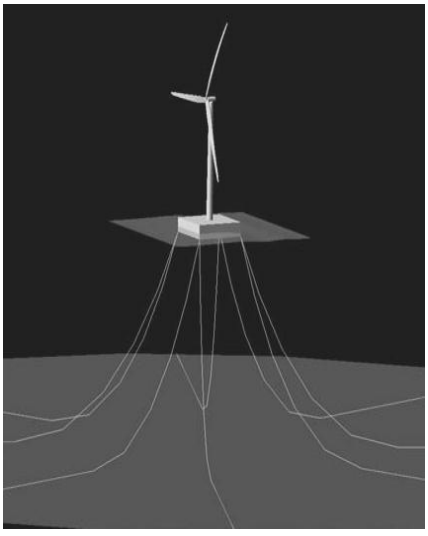

(b)

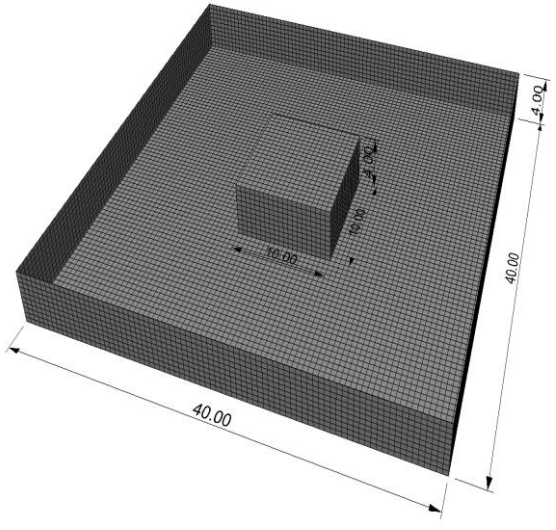

Figure 5.6: (a) Barge-type floating wind turbine (b) Hull geometry for barge-type floater

In the next subsection, the added mass, damping coefficient and exciting force are obtained by WAMIT for the barge-type floating wind turbine.

5.2.3 Added Mass and Damping Coefficient

In Figure 5.7(a), the added mass for force-translation modes are obtained and in Figure 5.7(b), the added mass for the moment-rotational modes are obtained using the geometry of the barge type floating wind turbine. It is observed that the surge-surge element for force translation mode is identical to the sway-sway element and the roll-roll element for the moment-rotational mode is identical to the pitch-pitch element. It is observed that the added mass using the proposed geometry are same as compared to the result obtained for ITI barge-type (see Jonkman (2007)).

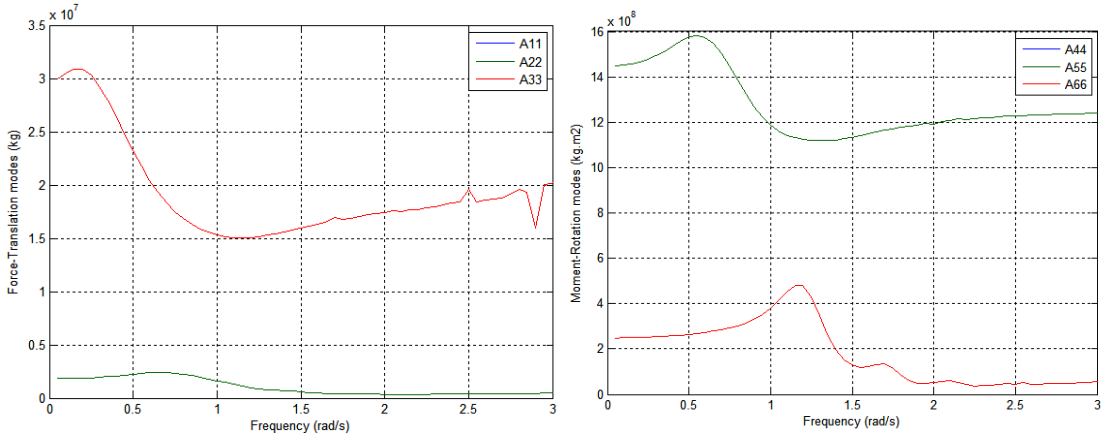

Figure 5.7: (a) Hydrodynamic added mass for (a) force-translation modes, (b) moment-rotation modes.

In Figure 5.8(a), the damping coefficients for the force-translation modes are plotted whereas in Figure 5.8(b), the damping coefficient for the moment-rotational modes is plotted. In this case also it is observed that the surge-surge element for force translation mode is identical to the sway-sway element and the roll-roll element for the moment-rotational mode is identical to the pitch-pitch element. The comparison with ITI barge-type results shows that the force-translation mode and the moment-rotational modes are almost same. The results obtained for the added mass and damping coefficients are observed to similar with result of obtained for ITI-Barge (see Jonkman (2007)).

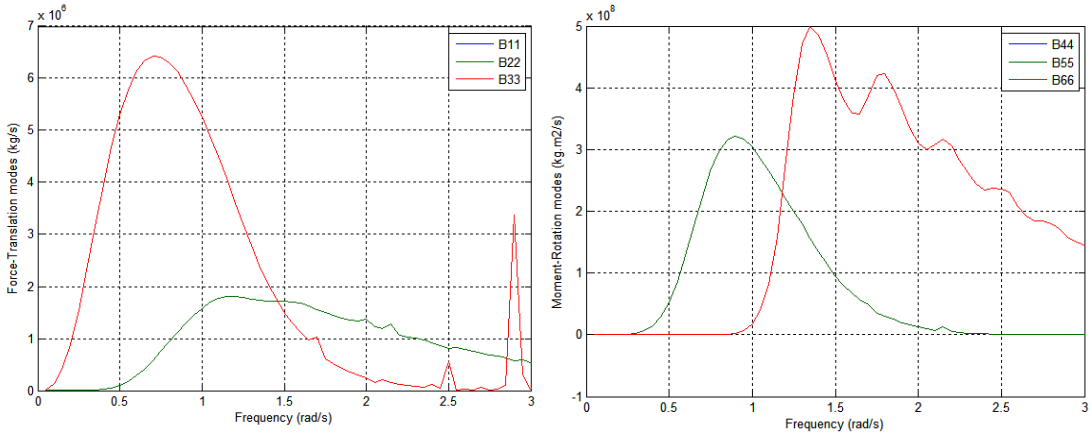

Figure 5.8: (a) Damping coefficient for (a) force-translation modes, (b) moment-rotation modes.

In the next section, the results obtained for damping coefficient, added mass and exciting force using WAMIT for barge-type floating wind turbine are used in the FAST code for fully coupled aero-hydro-servo-elastic simulation.

5.2.4 Fully Coupled Aero-Hydro-Servo-Elastic Simulation

The coupled aero-hydro-servo-elastic simulations are performed using the FAST code for 0º and 30º wave heading angle. The simulation is performed for 15 min time series of tower base motions such as surge, heave, sway and platform rotations such as pitch, roll, yaw motions.

5.2.4.1 Platform motions for 0º wave heading angle

The mean wave height is fixed at 4 m with 0º wave heading angle for three different values of wind speed conditions 3.7 m/s, 12 m/s and 24 m/s. Tower base motions and platform rotations results are shown for each different wind speed respectively in Figure 5.9 (a), Figure 5.9 (b) and Figure 5.9 (c). In Figure 5.9(a), the surge motion is obtained between 4m-10m. The heave motion is within +/-2m and sway motion in first 200s is 0m but after 200s it is approximately between +/-0.5m. The pitch oscillation is observed to be approximately in between +/-4º in first 700s whereas after 700s it is increased to +/-8º. The roll motion is observed to be within 0º for the first 400s whereas after 400s it increases to +/-0.5º and yaw motion is in between -/+0.5º.

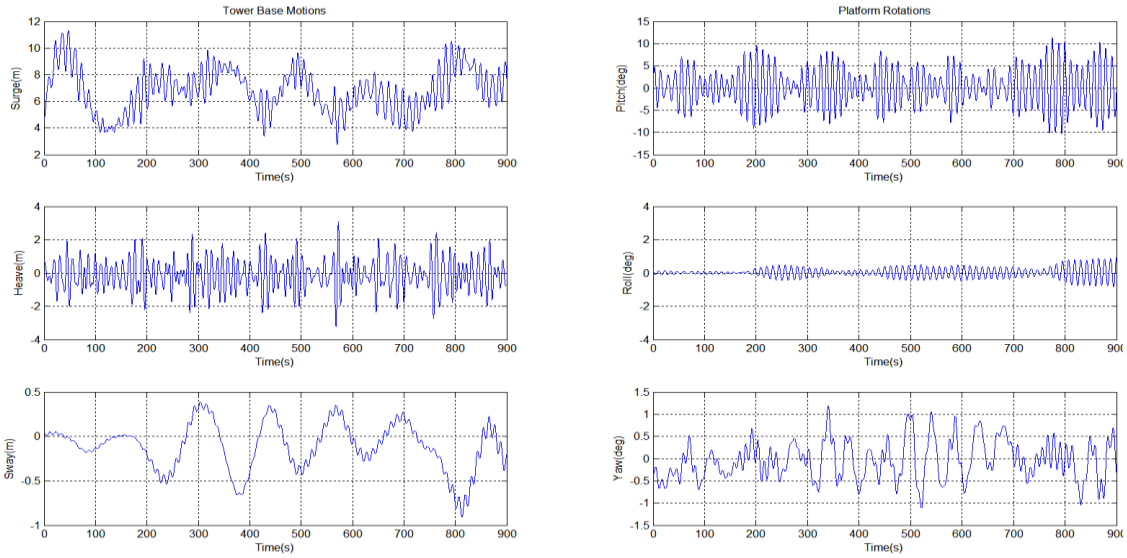

Figure 5.9 (a): Tower base motions and platform rotations for 4m wave height and 0º wave heading angle with 3.7 m/s wind speed

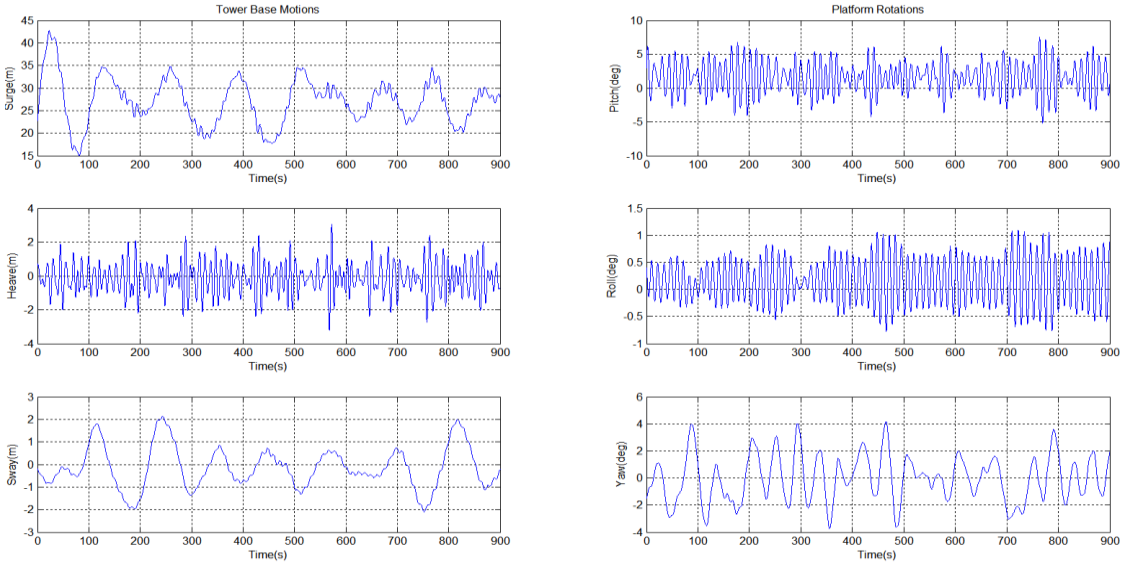

Figure 5.9 (b): Tower base motions and platform rotations for 4m wave height and 0º wave heading angle with 12 m/s wind speed

In Figure 5.9(b) with the increase in wind speed the surge motion is increased to 20m-35m. There is no difference found for heave motion, which is obtained within +/-2m. Pitch angle oscillation is obtained around between 0º-5º and yaw oscillation is obtained within +/-2º. Sway motion is +/-2m in first 300s whereas after 300s it is decreased to -/+1m. Roll motion oscillation is obtained within -/+0.5º.

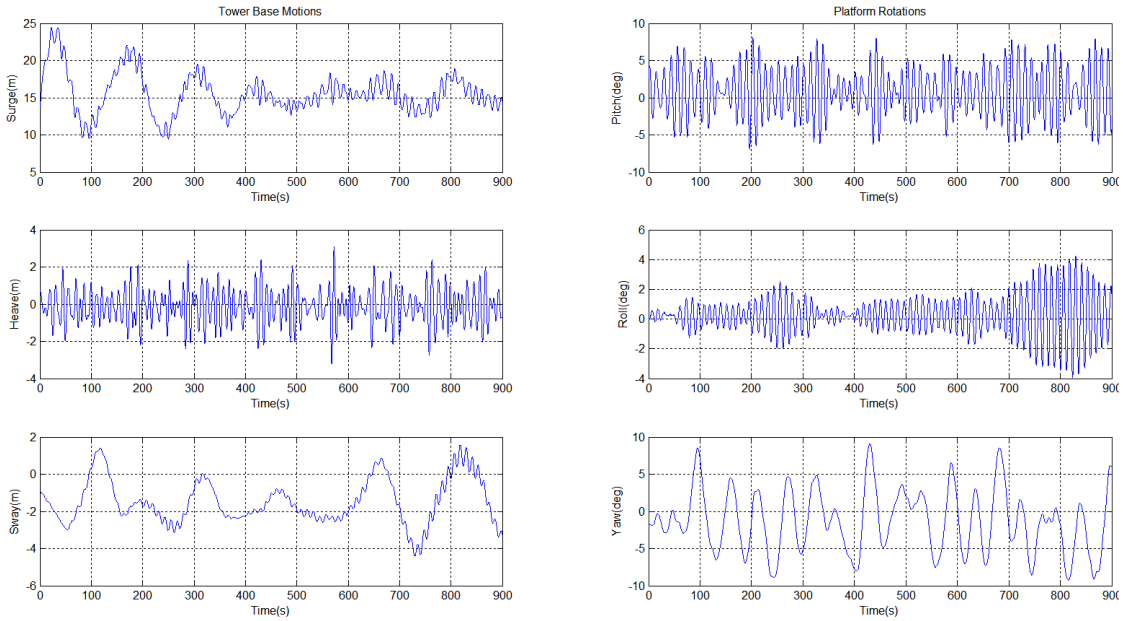

Figure 5.9 (c): Tower base motions and platform rotations for 4m wave height and 0º wave heading angle with 24 m/s wind speed

In Figure 5.9 (c), the surge motion is increased to 10m-25m in first 400s of simulation. After 400s of simulation surge motion observed around 15m. There is no difference obtained for heave motion. The heave motion is observed to be around +/-2m. Pitch angle oscillation obtained around between +/-5º and yaw oscillation is obtained between 4º and -6º. Sway motion is observed between 0m and -2m in the first 600s but after first 600s it is increased and is observed within 1m and -4m. The roll motion oscillation obtained within +/-1º.

5.2.4.2 Platform motions for 30º wave heading angle

The mean wave height is fixed at 4m with 30º wave heading, for three different wind speed conditions of 3.7 m/s, 12 m/s and 24 m/s. The tower base motions and platform rotations results are shown in Figure 5.10 (a), Figure 5.10 (b) and Figure 5.10 (c). In Figure 5.10(a), there is very small difference observed for surge motion, heave motion and pitch motion when wave heading angle increased from 0º to 30º. Sway motion is observed increased from +/-0.5 to +/- 1m. Roll motion is around 0º and Yaw motion is +/-0.5º with 0º wave heading angle. Roll motion increased to +/-5º and yaw motion increased within +/-5º with wave heading angle 30º.

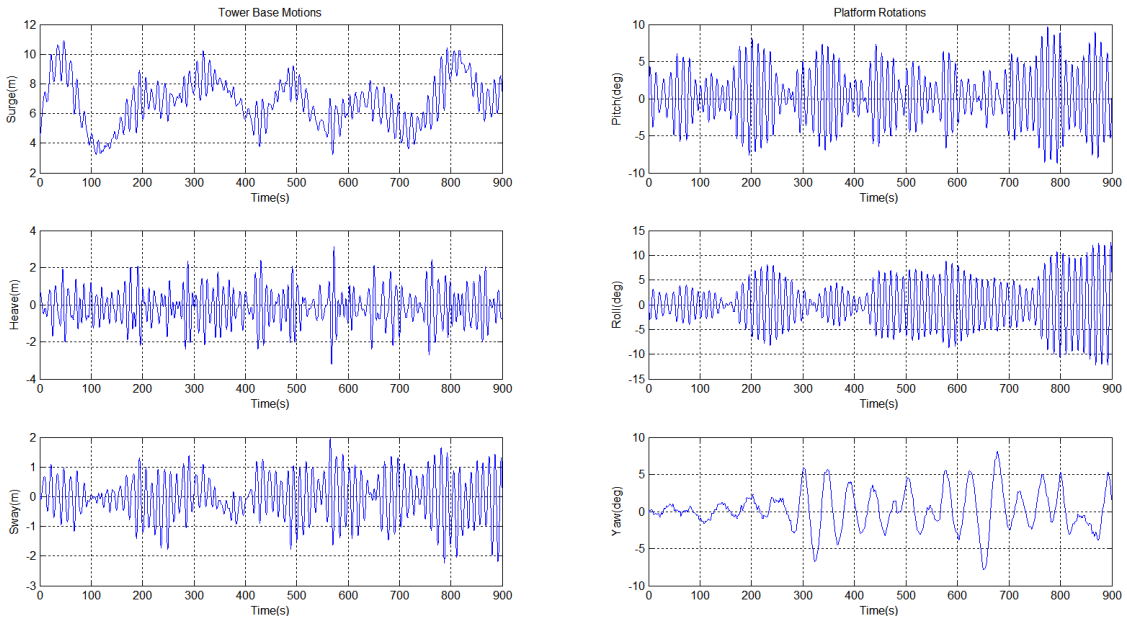

Figure 5.10 (a): Tower base Motions and platform rotations for 4m wave height and 30º wave heading angle with 3.7 m/s wind speed.

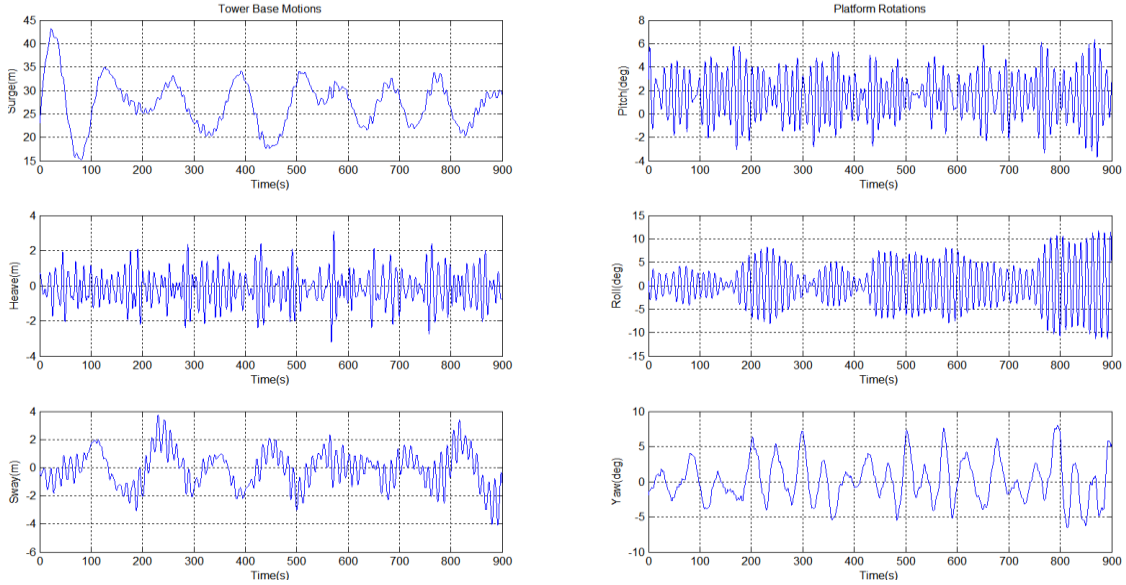

Figure 5.10 (b): Tower base Motions and platform rotations for 4m wave height and 30º wave heading angle with 12 m/s wind speed.

In Figure 5.10(b), no difference is observed when the wave heading angle increase to 30º for the surge motion. The surge motion is observed to be within 20m to 35m. The heave motion is obtained within +/-2m. The pitch angle oscillation is obtained around between 0º to 4º. The yaw oscillation is obtained within +/-2º and the sway motion is +/-2m

however motion periods are more frequent with 30º wave heading angle. Only difference is obtained for roll motion oscillation which is increased to -/+2.5º from -/+0.5º.

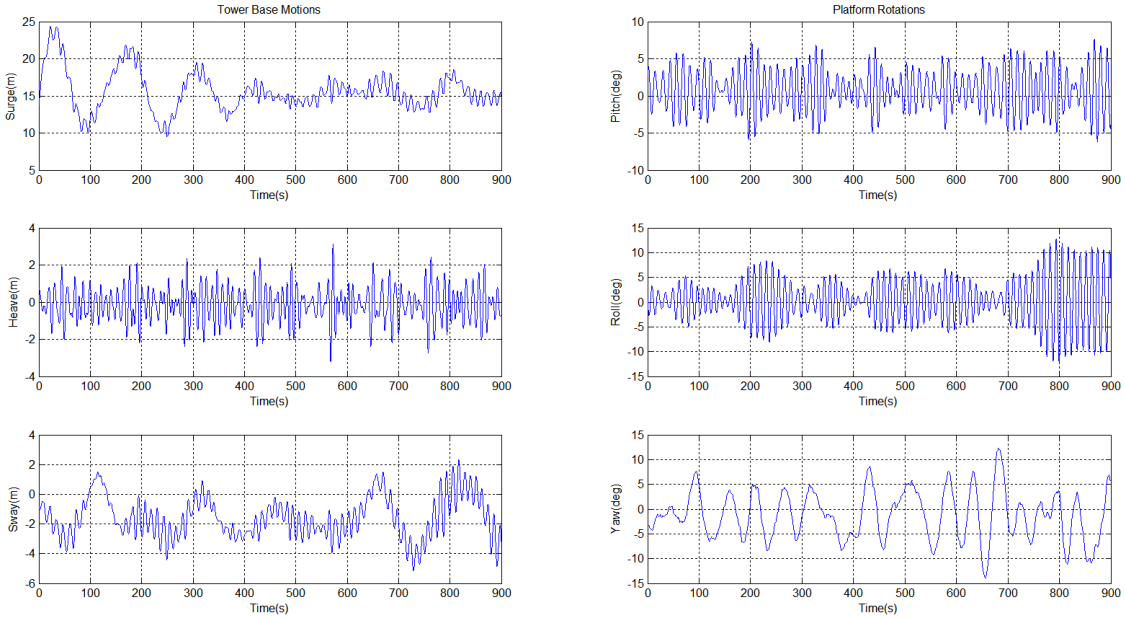

Figure 5.10 (c): Tower base Motions and platform rotations for 4m wave height and 30º wave heading angle with 24 m/s wind speed.

In Figure 5.10(c), the same difference is observed for 24 m/s wind speed with 30º wave heading angle and the motion periods are more frequent with 30º wave heading angle. The tower base motions and rotations are observed to be same except roll motion. Roll motion is increased to -/+2.5º from +/-1º.

5.3 5MW WindFloat semi-submersible type floating turbine

A coupled dynamic analysis of 5MW semi-submersible type floating wind turbine is analyzed in detail. The hydrodynamic study of the floater is done using WAMIT and is combined with FAST code to obtain an aero-servo-hydro-elastic model. The tower base motions and platform motions are obtained for various values of wind speed with 4 m wave height and 0º and 30 º wave heading angle.

5.3.1 Model Description

The semi-submersible type floater components consist of columns, water entrapments, main beams, bracing beams and asymmetric mooring system. The water entrapment is located in each column. The columns are interconnected with main beams, the bracings

connecting main beams to columns or other main beams. Semi-submersible type floater is WindFloat as shown on Figure 5.11.

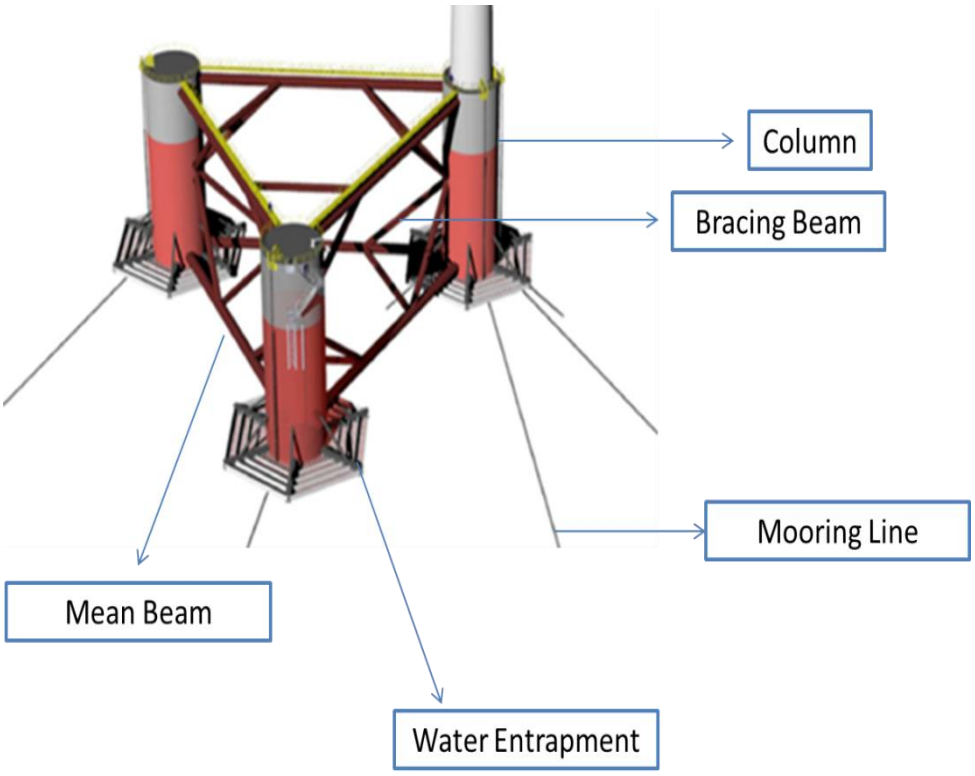

Figure 5.11: Components of WindFloat floater

The hydrodynamic analysis of the semi-submersible type floating wind turbine is also carried out and the detail descriptions for the study are as follows. The wind turbine properties, platform properties and mooring system properties are shown in Table 5.3 (a,b,c). The top view of WindFloat is shown in Figure 5.12.

Table 5.3(a) WindFloat wind turbine properties

Hub Height	90 m
Center of Mass Location (From Sea Level)	38.234 m
Rotor Diameter	126 m
Number of Blades	3
Initial Rotational Speed	12.1 rpm
Blades Mass	53,220 kg
Nacelle Mass	240,000 kg
Hub Mass	56,780 kg
Tower Mass	347,460 kg
Power Output	5 MW
Cut-In, Rated, Cut-Out Wind Speed	3 m/s, 11.4 m/s, 25 m/s

Table 5.3(b) WindFloat platform properties

Operating Draft	17 m
Length of Entrapment Plate Edge	15 m
Length of Column to Center	46 m
Main Beam Diameter	2.1 m
Bracing Diameter	1.5 m
Column Diameter	10 m
Mass, Including Balast	4,640,000 kg
Center of Mass Location Above Sea Water Level	3.728 m
Platform Roll Inertia (I_{xx})	5,720,000,000 kg.m^2
Platform Pitch Inertia (I_{yy})	5,650,000,000 kg.m^2
Platform Yaw Inertia (I_{zz})	3,260,000,000 kg.m^2

Table 5.3(c) WindFloat mooring system properties

Number of Mooring Lines	4
Depth to Anchors Below SWL (Water Depth)	320 m
Depth to Fairleads Below SWL	17.0 m
Radius to Anchors from Platform Centerline 1 Radius to Anchors from Platform Centerline 2	870.273 m 876.890 m
Radius to Fairleads from Platform Centerline 1 Radius to Fairleads from Platform Centerline 2	32.759 m 30.087 m
Unstretched Mooring Line Length 1 Unstretched Mooring Line Length 2	890.556 m 900.007 m
Mooring Line Diameter	0.0809 m
Equivalent Mooring Line Mass Density	127.0 kg/m
Neutral Line Length Resting on Seabed	320 m
Equivalent Mooring Line Extensional Stiffness	586,450,000 N

The length of entrapment plate edge, length of column to center, main beam diameter, bracing diameter and radius of three angles are shown in Figure 5.12.

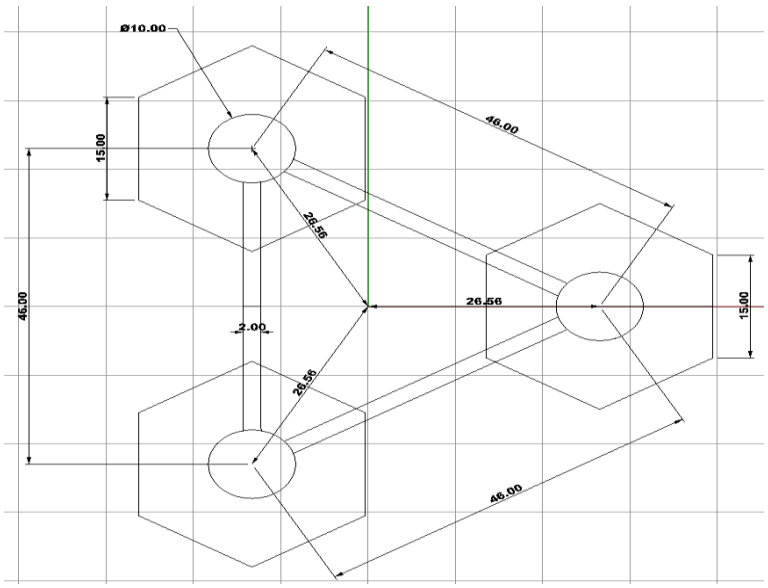

Figure 5.12: Top view of WindFloat (m)

5.3.2 Hull Geometry

The semi-submersible type floater column has one water-entrapment plate. The water-entrapment plate is helpful to provide additional hydrodynamic inertia to the structure.

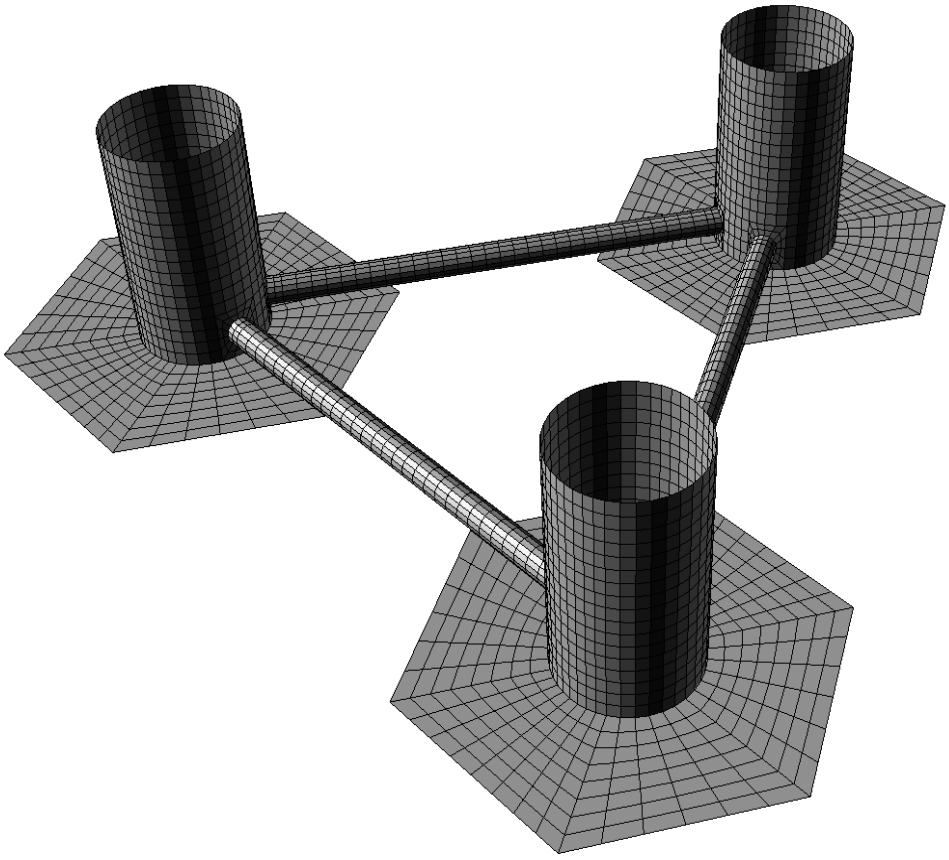

Figure 5.13: Hull geometry for semi-submersible type floater

The platform motions decreases if additional hydrodynamic inertia to structure increases and in addition, plates generate large damping forces to decrease platform motion. In the WAMIT model, these plates are included to the geometry of the structure. The semi-submersible type floater is modeled totally with 5,328 rectangular panels for a full body. Same blades, tower, nacelle, hub properties of 5MW ITI barge-type floating wind turbine are applied for WindFloat semi-submersible type in FAST code. WAMIT is used from 0.05 rad/s to 3 rad/s to obtain added mass, damping, hydrostatic matrices and exciting force. The semi-submersible type floater hull geometry used for the WAMIT calculations is shown in Figure 5.13. In the next subsection, the added mass, damping coefficient and exciting force for semi-submersible floater is obtained using WAMIT.

5.3.3 Added Mass and Damping Coefficient

In Figure 5.14(a), the added mass for force-translation modes are obtained and in Figure 5.14(b), the added mass for the moment-rotational modes are obtained using the geometry of the semi-submersible type floating wind turbine.

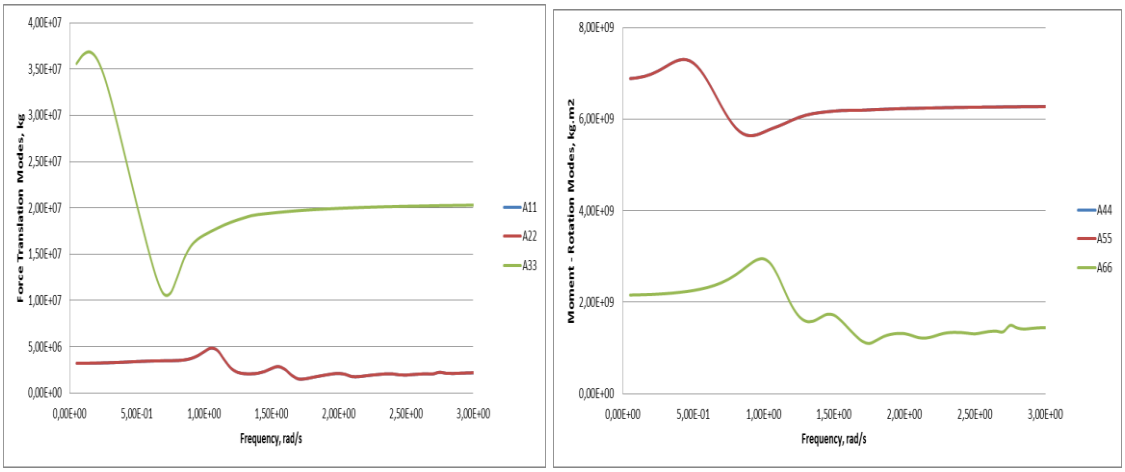

Figure 5.14: Hydrodynamic added mass for (a) force-translation modes, (b) moment-rotation modes

It is observed that the surge-surge element for force-translation mode is identical to the sway-sway element and the roll-roll element for the moment-rotational modes is identical to the pitch-pitch element. In Figure 5.15(a), the damping coefficients for the force-translation modes are plotted whereas in Figure 5.15(b), the damping coefficients for the moment-rotational modes are plotted. In this case also it is observed that the surge-surge element for force -translation mode is identical to the sway-sway element and the roll-roll element for the moment-rotational mode is identical to the pitch-pitch element.

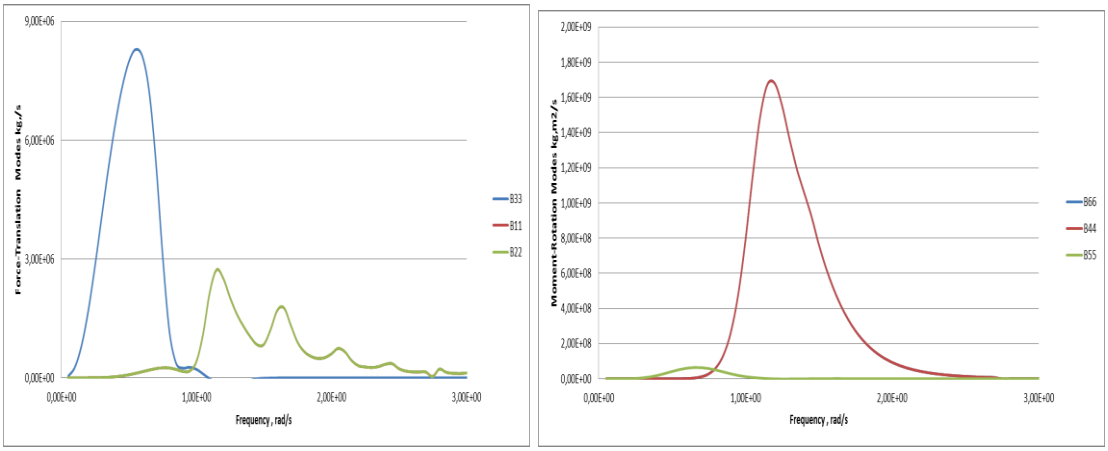

Figure 5.15: Damping coefficient for (a) force-translation modes, (b) moment-rotation modes.

In the next section, the results obtained for damping coefficient, added mass and exciting force using WAMIT for semi-submersible type are used in the FAST code for fully coupled aero-hydro-servo-elastic simulation.

5.3.4 Fully Coupled Aero-Hydro-Servo-Elastic Simulation

The coupled aero-hydro-servo-elastic simulations are performed for semi-submersible type floater using the FAST code in the case of 0º and 30º wave heading angle. The simulation is performed for 15 min time series of tower base motions such as surge, heave, sway and platform rotations such as pitch, roll, yaw motions.

5.3.4.1 Platform motions for 0º wave heading angle

The mean wave height is fixed at 4 m with 0º wave heading angle for three different wind speed conditions of 3.7 m/s, 12 m/s and 24 m/s. Tower base motions and platform rotations results are shown for each different wind speed respectively Figure 5.16 (a), Figure 5.16 (b) and Figure 5.16 (c).

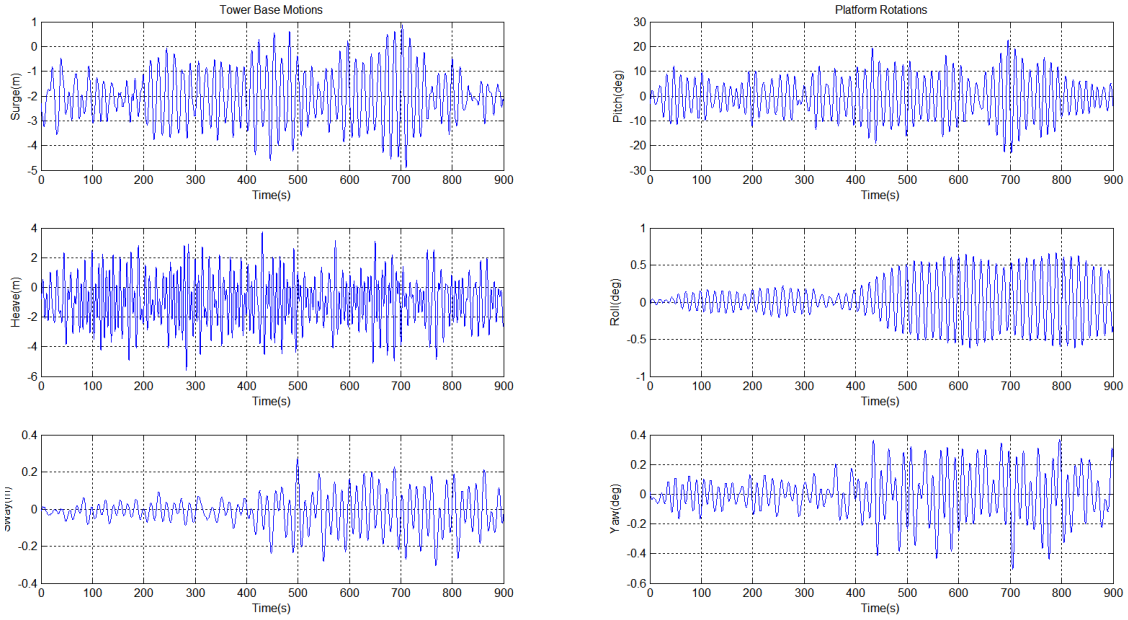

Figure 5.16 (a): Tower base motions and platform rotations for 4m wave height and 0º wave heading with 3.7 m/s wind speed

In Figure 5.16 (a), sample time series shows tower base motions and platform rotations for 15min for WindFloat wind turbine. It is observed surge motion is within -1m to -3m. Heave motion is in between approximately +1.5/ - 2.5m. Sway motion is observed to be

increasing after 500s and is around 0.2m. Pitch oscillation is approximately within 6º to -6º until 400s. The roll motion approaches to zero before 400s and yaw oscillation is very close to 0º until 400s then it is increasing approximately within 0.2º.

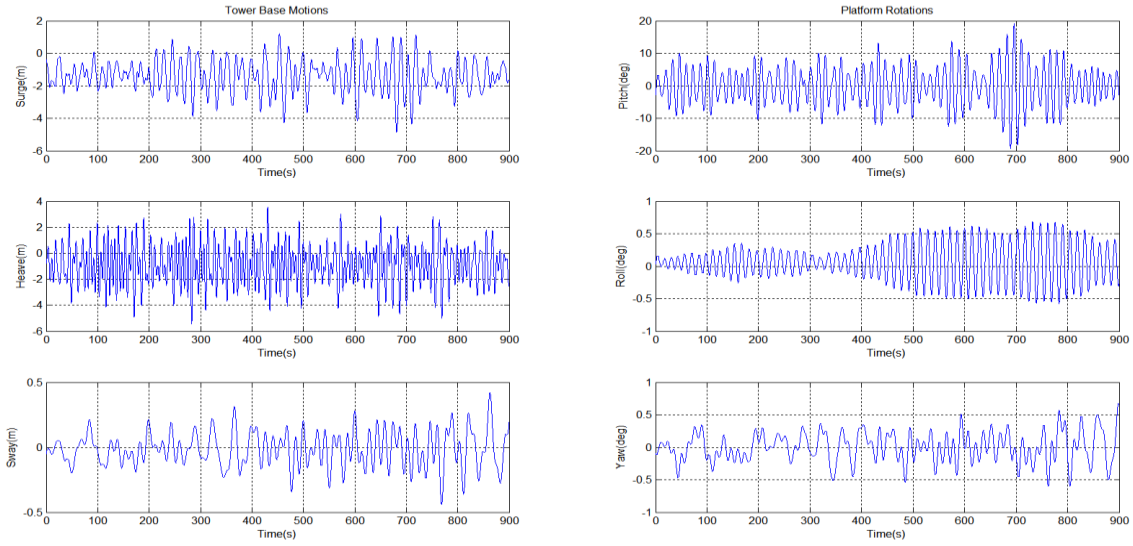

Figure 5.16 (b): Tower base motions and platform rotations for 4m wave height and 0º wave heading with 12 m/s wind speed

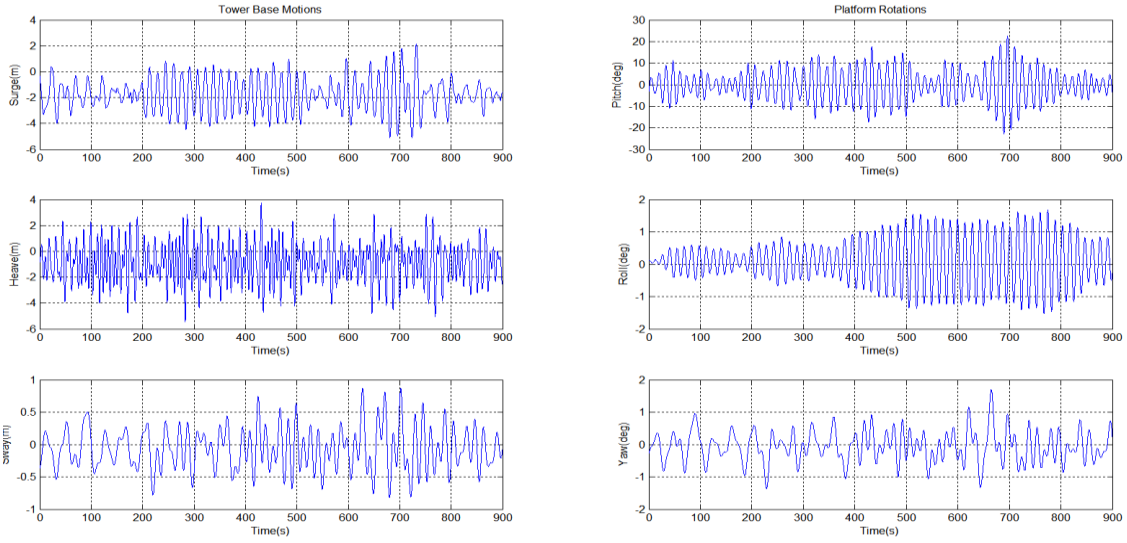

Figure 5.16 (c): Tower base motions and platform rotations for 4m wave height and 0º wave heading with 24 m/s wind speed

In Figure 5.16 (b) it is observed that the surge motion is within 0m to -2m. Sway motion is in between approximately +/- 0.2m. Pitch oscillation is approximately within 8º to -8º

until 600s. The roll motion approaches to zero before 400s and yaw motion is in between approximately 0.2º to -0.2º. In Figure 5.16 (c), it is observed surge motion is within 0m to -4m. Sway motion is in between approximately +/-0.5m. Pitch oscillation is approximately within 8º to -8º until 700 second. The roll motion approaches to 0.5º to -0.5º before 400s and yaw motion is in between approximately within 1º to -1º. Heave motion is observed to be within +1.5/ - 2.5m for all wind speeds with 0º wave heading angle.

5.3.4.2 Platform motions for 30º wave heading angle

The mean wave height is fixed at 4m with 30º wave heading, for three different wind speed conditions of 3.7 m/s, 12 m/s and 24 m/s. The tower base motions and platform rotations results are shown in Figure 5.17 (a), Figure 5.17 (b) and Figure 5.17 (c).

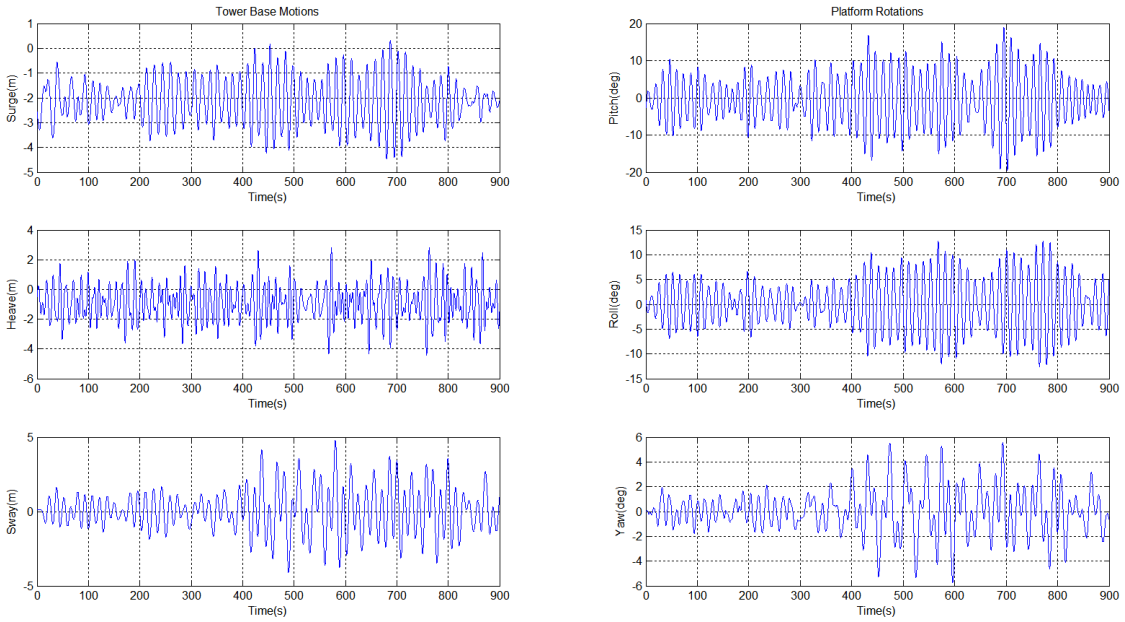

Figure 5.17 (a): Tower base motions and platform rotations for 4m wave height and 30º wave heading with 3.7 m/s wind speed.

In Figure 5.17 (a) sample time series results are plotted for wave heading angle 30º. Surge motion is observed to be within -1m to -3m. Sway motion is in between +/-1m until 400 second of simulation and then increases and is within 4m to -4m. Pitch oscillation is approximately within 6º to -6º until 700s. The roll motion approaches from 5º to -5º and yaw motion is in between 2º to -1º before 400s of simulation.

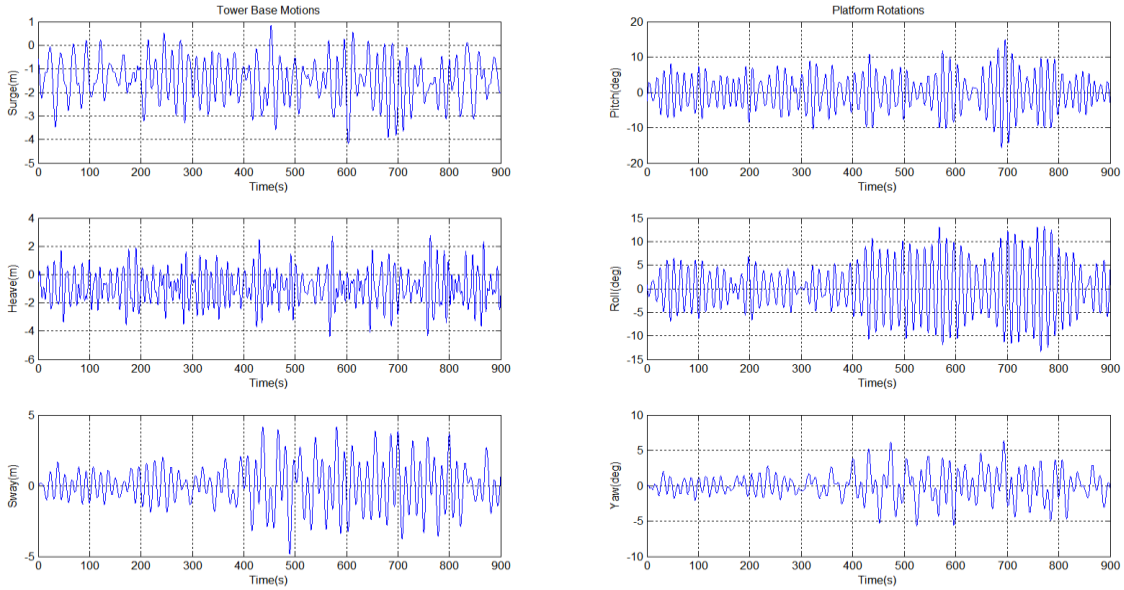

Figure 5.17 (b): Tower base motions and platform rotations for 4m wave height and 30º wave heading with 12 m/s wind speed.

In Figure 5.17 (b), it is observed that the surge motion is in between 0m to -2.5m. Sway motion is in between approximately +/-1.5m. Pitch oscillation is approximately within 8º to -8º until 700 second. The roll motion approaches from 5º to -5º and yaw motion is in between 2º to -2º before 400s of simulation.

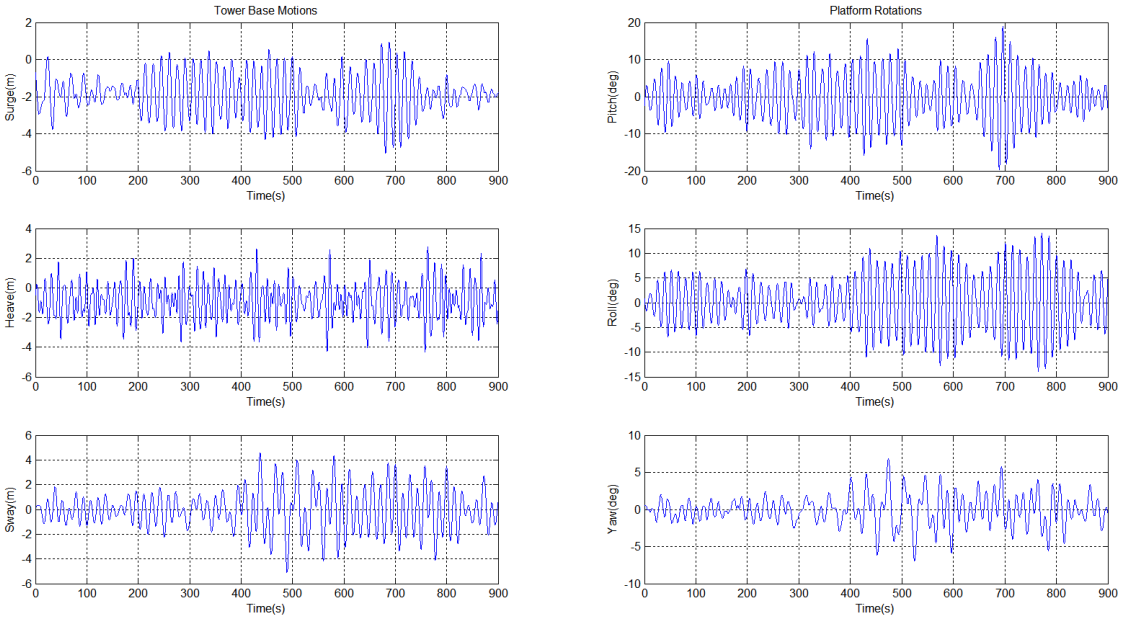

Figure 5.17(c) Tower base motions and platform rotations for 4m wave height and 30º wave heading with 24 m/s wind speed.

In Figure 5.17(c), it is observed that the surge motion is within 0m to -3m. Sway motion is in between approximately +/-2m until 400 second. Pitch oscillation is approximately within 8º to -8º. The roll motion is within 5º to -5º and yaw motion is in between 2º to -2º before 400s of simulation. Heave motion is observed to be within 1.5m to -2.5m for all wind speeds with 30º wave heading angle.

5.4 Conclusions

In this Chapter, a comparative study on the dynamic analysis of 5MW spar-type, barge-type and semi-submersible type floating wind turbine are performed using an aero-servo-hydro-elastic model. The aero-servo-hydro-elastic model is obtained by combining hydrodynamic characteristics of the floater obtained using WAMIT with aero-servo-elastic model of FAST code. The hydrodynamic behaviour of the spar type and barge type floater concepts is studied using WAMIT along with the added mass and damping coefficients are analyzed for both the floater concepts. The following conclusions are drawn based on the study carried out in this chapter:

- The hydrodynamic added mass for the force-translation modes and moment rotation is observed to be same as compared to OC3-Hywind and ITI barge-type (Jonkman (2007, 2010)).

- Due to the symmetry in the body, the surge-surge element for force-translation mode is observed identical to the sway-sway element and the roll-roll element for the moment-rotational mode is observed identical to the pitch-pitch element.

- The simulation results obtained using aero-servo-hydro-elastic model shows that the OC3-Hywind floating wind turbine is more stable in pitch, heave, sway and yaw motions. The results obtained for roll and surge motions are observed lower for ITI barge-type whereas in the case of OC3-Hywind the roll and surge motions are higher than ITI barge-type.

- In the study of spar-type floating wind turbine, the floater is considered connected with three mooring lines whereas in the case of barge-type floating wind turbine, the

floater is connected with eight mooring lines where each two lines is located at each corner of the floater.

- The moorings attached with the floaters helps in the stability of the floaters and it is observed that the pitch motion of the floaters decreases with the increase in the mooring lines. The two concepts were simulated in deep water; i.e the spar-type is examined at 320m water depth and barge-type at 150m water depth.

- The spar-type floating wind turbine is observed better in heave motion than barge type floating wind turbine. It was expected that the barge-type floater could be better in heave than spar-type floater due to large platform area but the spar-type floaters shows better performance.

- The simulation results for tower base motions and platform motions for various values of wind speed are obtained keeping the wave height and wave heading angle same. It is observed that with the increase in wind speed the pitch motion of the spar type floating wind turbine increases whereas the pitch motion decreases for the barge type floating wind turbine.

- In the study of WindFloat floating wind turbine, the floater is considered connected with four mooring lines and it is simulated in deep water of 320m water depth.

- The simulation result for WindFloat shows that the heave is within 1.5m to -2.5m, pitch oscillation is approximately within +/- 6º for 3.7 m/s wind speed and +/- 8º 12 m/s and 24 m/s wind speeds with all wave heading angle.

- The barge-type floater and WindFloat floater have similar heave motion but the spar-type floaters shows better performance than barge-type and WinFloat floaters.

- The WindFloat floater shows that the roll and yaw motion is within 0º for 0º wave heading angle but as wave heading increases to 30º the roll motion is increased approximately within +/- 5º and yaw motion increased to +/- 2º.

CHAPTER 6

MOORING ANALYSIS OF WINDFLOAT WIND TURBINE

In the present chapter, the moorings attached to the WindFloat floating wind turbine is studied in detail for various mooring lines attached to the system. The analysis for the platform motions are carried out for different values of the wave heading angle and wind speeds. The comparison between the 4 mooring lines and 6 mooring lines attached to the floaters are analysed.

6.1 WindFloat mooring line system

The FAST code is used for analysis of the moorings attached to the floaters. The FAST code uses linear and homogenous catenary mooring system model. Inertia and damping are ignored in linear mooring system. It considers mainly the line weight in the fluid, line diameter, elastic stretching, and seabed friction. The structure has four mooring lines and it is examined in chapter 5. The results for the platform rotations and motions in 0º and 30º wave heading angle with 4 m wave height for 3.7 m/s, 12 m/s, and 24 m/s wind speed are presented. In this chapter WindFloat semi-submersible floating wind turbine mooring system will be examined for six mooring lines and platform rotations and motions results will be compared with four mooring lines in 0º and 30º wave heading angle with 4 m wave height for 3.7 m/s, 12 m/s, and 24 m/s wind speed.

6.1.1 WindFloat 4 Lines Mooring System

The WindFloat floater structure consisting of four mooring lines has two lines connected to column which carries turbine and one line connected on each other columns. The detail fairlead and the anchor locations for each of the mooring lines are shown in Table 6.1.

Table 6.1 WindFloat 4 Lines mooring system fairlead and anchor locations

	X (m)	Y (m)	Z (m)
Fairlead 1	29.578	-5.51	-16.8
Fairlead 2	29.578	5.51	-16.8
Fairlead 3	-16.379	28.37	-16.8
Fairlead 4	-16.379	-28.37	-16.8
Anchor 1	600	-600	-319.9
Anchor 2	600	600	-319.9
Anchor 3	-600	600	-319.9
Anchor 4	-600	-600	-319.9

6.1.2 WindFloat 6 Lines Mooring System

Six mooring lines are connected to the floater structure. Four lines are connected to column which carries turbine and one line connected on each other columns. Fairlead and anchor locations are shown in Table 6.2

Table 6.2 WindFloat 6 Lines mooring system fairlead and anchor locations

	X (m)	Y (m)	Z (m)
Fairlead 1	29.578	-5.51	-16.8
Fairlead 2	29.578	5.51	-16.8
Fairlead 3	-16.379	28.37	-16.8
Fairlead 4	-16.379	-2837	-16.8
Fairlead 5	26.558	-5.510	-16.8
Fairlead 6	26.558	5.51	-16.8
Anchor 1	600	-600	-319.9
Anchor 2	600	600	-319.9
Anchor 3	-600	600	-319.9
Anchor 4	-600	-600	-319.9
Anchor 5	26.558	-830	-319.9
Anchor 6	26.558	830	-319.9

In the 4 lines and 6 lines system, cable diameter is 0.09 m, mass per unit length is 127 kg/m and extensional stiffness is 586.450 kN.

6.2 Comparison between 4 and 6 mooring lines

In the present subsection, a detail comparison of the 4 mooring lines and 6 mooring lines connected to the WindFloat floaters are analyzed for various values of wind speeds and wave heading angles.

6.2.1 Platform motions for 0º wave heading angle

The time series simulation for 4 mooring lines and 6 mooring lines present in the WindFloat are analyzed for 0º heading angle for various values of wind speeds. In Figure 6.1 (a), the sample time series for platform rotations are plotted for fifteen minutes in the case of WindFloat wind turbine with six lines and four lines mooring system. Pitch oscillation is observed approximately within 6º to -6º, the roll. The yaw motion approaches to zero and it keeps on increasing after 400s and is observed around +/-0.5º.

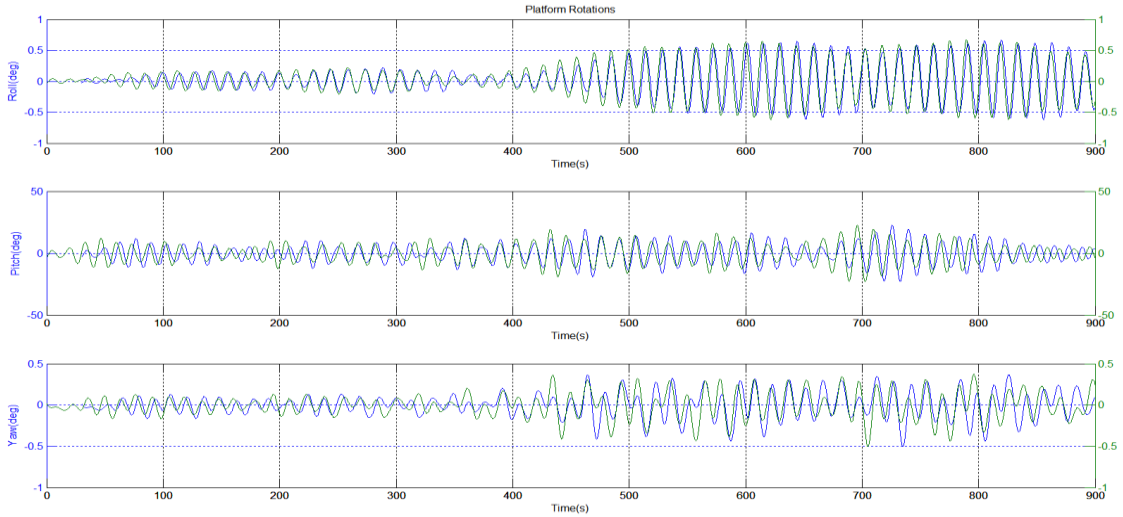

Figure 6.1 (a): Platform rotations with 0º wave heading angle and 3.7 m/s wind speed.

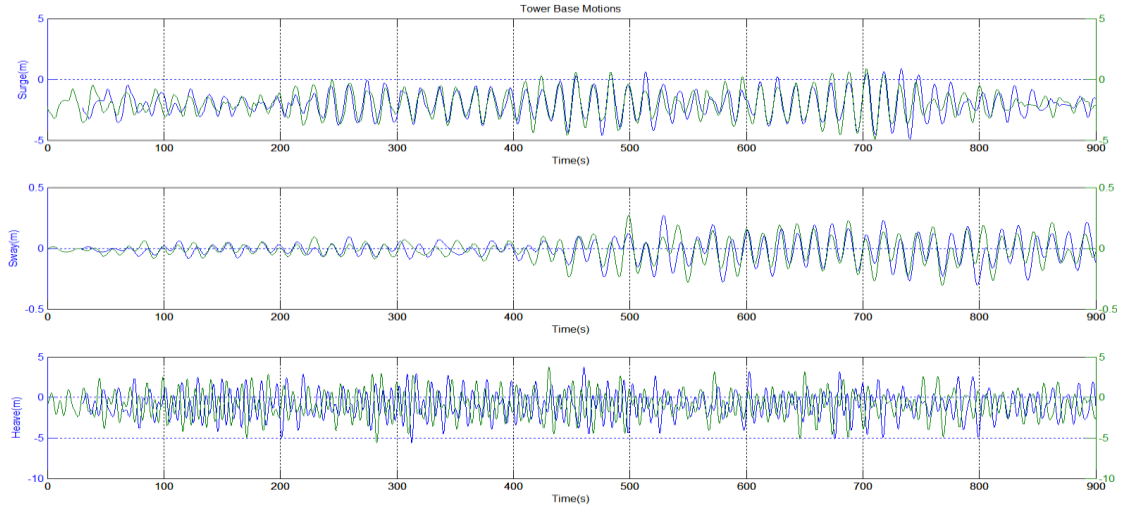

Figure 6.1 (b): Tower base motions for 0º wave heading angle and 3.7 m/s wind speed.

In Figure 6.1 (b), the tower base motions are plotted for 0º wave heading angle and 3.7m/s wind speed. It is observed that the surge motion is within -1m to -3m. Heave

motion is in between approximately +1.5m/-2.5m. Sway motion is observed to be increasing after 500s and is around 0.2m for six lines and for four lines mooring system. There is no difference obtained when wave heading angle is 0º with wind speed of 3.7 m/s.

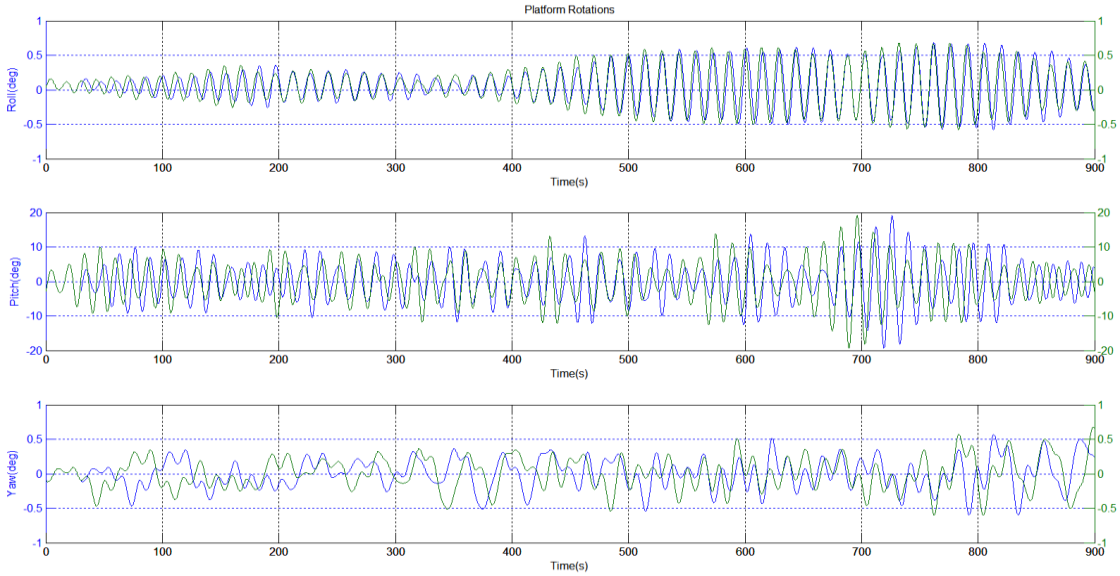

Figure 6.2 (a): Platform rotations for 0º wave heading angle and 12 m/s wind speed.

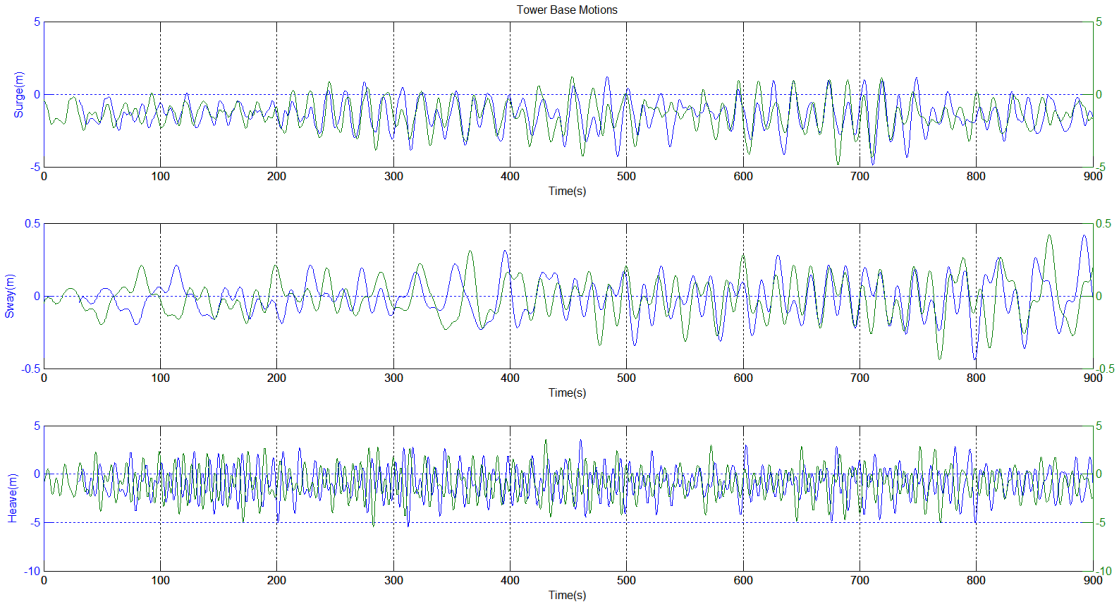

Figure 6.2 (b): Tower base motions for 0º wave heading angle with 12 m/s wind speed

In Figure 6.2 (a), the sample time series shows platform rotations and Figure 6.2 (b) shows tower base motions for fifteen minutes in the case of WindFloat wind turbine with

six and four lines mooing system for 0º wave heading angle with 12 m/s wind speed. It is observed that the surge motion is within 0m to -2m. Sway motion is in between approximately +/- 0.2m. Pitch oscillation is approximately within 8º to -8º until 700 second. The roll motion approaches to zero before 400s and yaw motion is in between approximately within 0.2º to -0.2º until 700 second. The roll motion approaches to 0.5º to -0.5º before 400s and yaw motion is in between approximately 1º to -1º. Heave motion is observed within 1.5m to -2.5m for 12m/s wind speed.

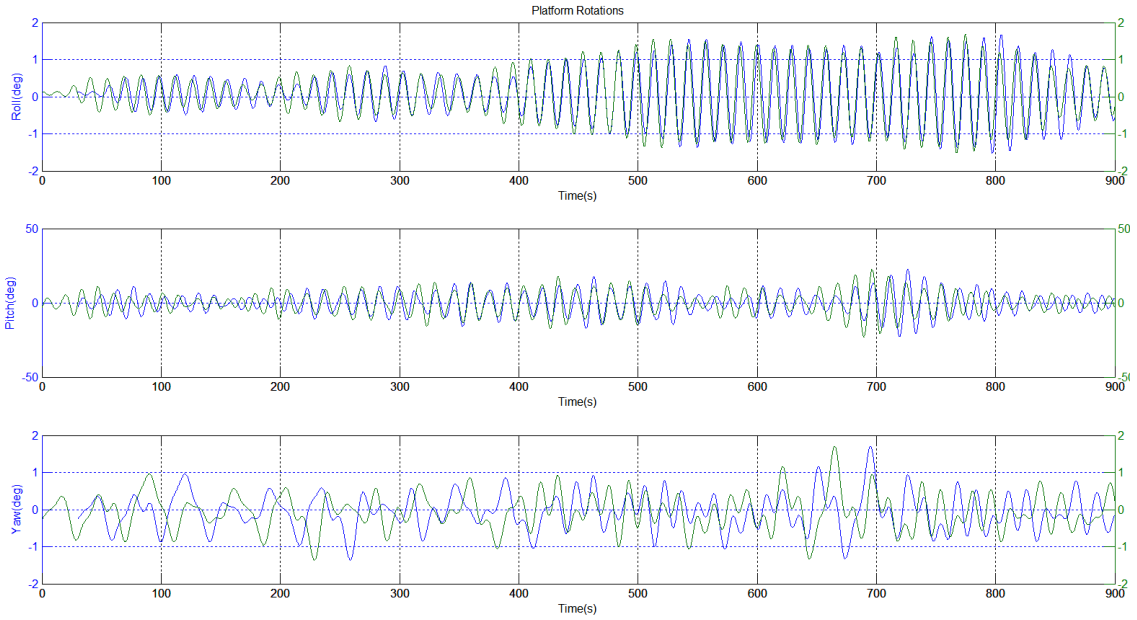

Figure 6.3 (a): Platform rotations for 0º wave heading angle and 24 m/s wind speed

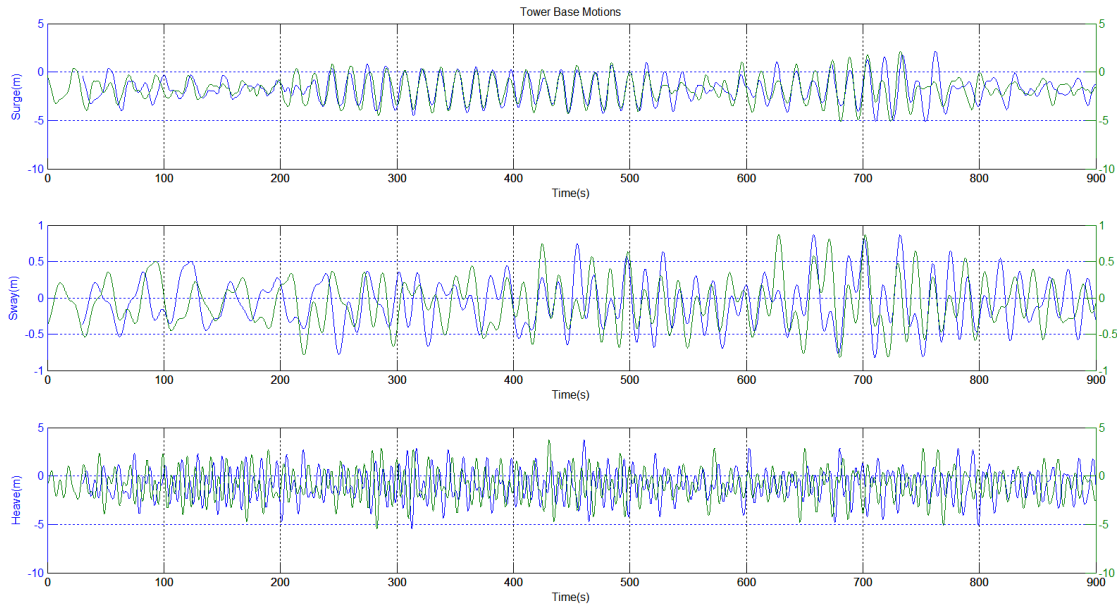

Figure 6.3 (b): Tower base motions for 0º wave heading angle and24 m/s wind speed

In Figure 6.3 (a), the sample time series for platform rotations are plotted for fifteen minutes in the case of WindFloat wind turbine with six lines and four lines mooring system. The pitch oscillation is observed approximately within 8º to -8º until 700 second. The roll motion approaches from 0.5º to -0.5º before 400s and yaw motion is in between 1º to -1º. In Figure 6.3 (b), the sample time series for tower base motions are plotted for WindFloat wind turbine with six lines and four lines mooring system. The surge motion is observed to be within 0m to -4m. Sway motion is in between approximately +/- 0.5m and heave motion is observed to be within 1.5m to -2.5m for 24 m/s wind speed.

6.2.2 Platform motions for 30º wave heading angle

In this subsection, the time series simulation for 4 mooring lines and 6 mooring lines present in the WindFloat are analyzed for 30º heading angle for various values of wind speeds.

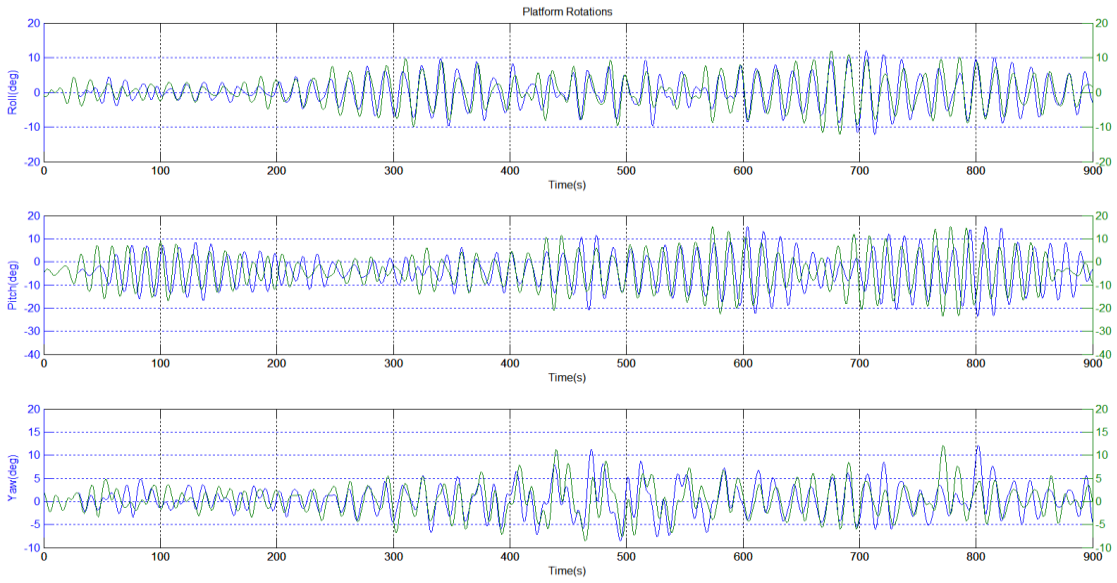

Figure 6.4 (a): Platform rotations for 30º wave heading angle and 3.7 m/s wind speed

In Figure 6.4 (a), the sample time series for platform rotations for 30º wave heading angle are plotted for WindFloat wind turbine with six lines and four lines mooring system. The pitch oscillation is observed approximately within 6º to -6º until 700 second. The roll motion is within 5º to -5º and yaw motion is in between 2º to -1º before 400s of simulation. In Figure 6.4 (b), the sample time series for tower base motions are plotted for WindFloat wind turbine with six lines and four lines mooring system. The surge

motion is observed to be within -1m to -3m. Sway motion is in between approximately +/- 1m until 400 second of simulation and then it is increased within 4m to -4m. The heave motion is observed to be within 1.5m to -2.5m for 3.7 m/s wind speed.

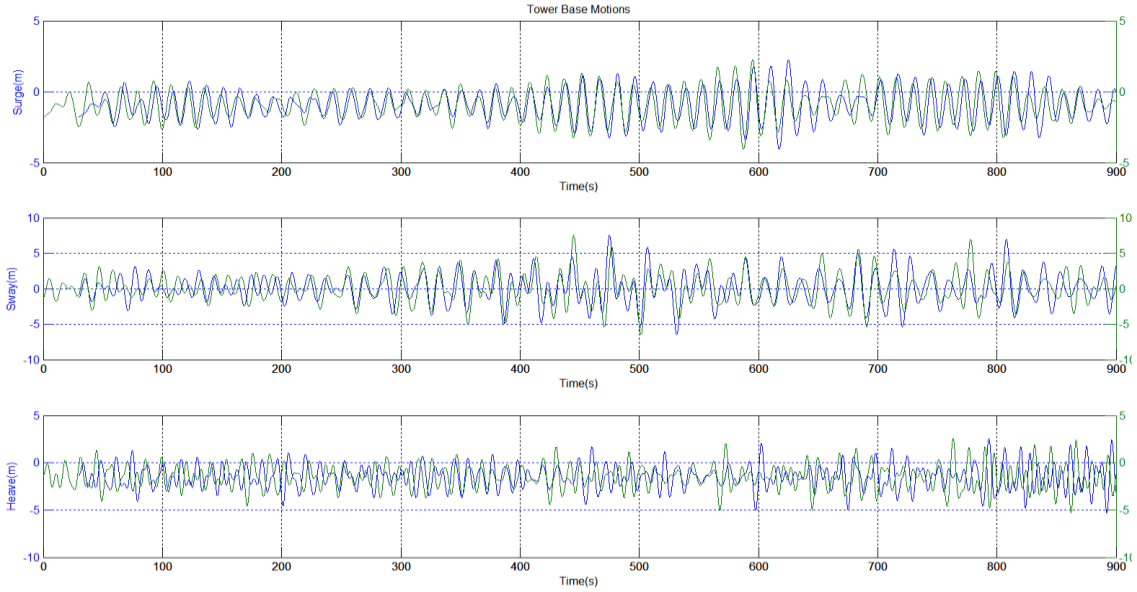

Figure 6.4 (b): Tower base motions for 30º wave heading angle and 3.7 m/s wind speed

In Figure 6.5 (a) the sample time series for platform rotations for 30º wave heading angle are plotted for WindFloat wind turbine with six lines and four lines mooring system. It is observed that the pitch oscillation is approximately within 8º to -8º until 700s. The roll motion is within +/-5º and yaw motion is in between 2º to -2º before 400s of simulation.

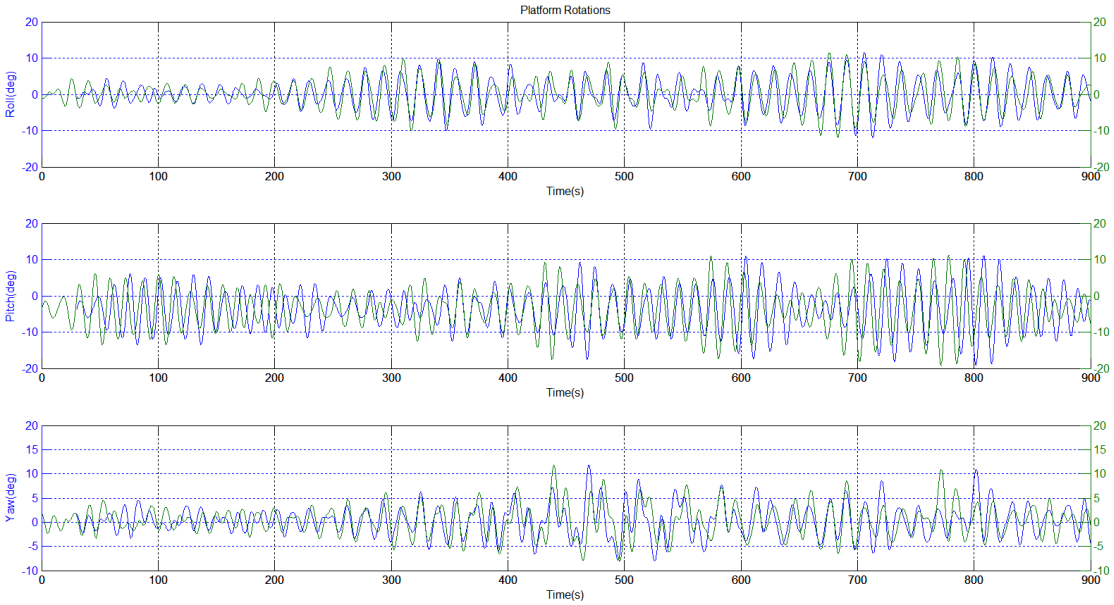

Figure 6.5 (a): Platform rotations for 30º wave heading angle and 12 m/s wind speed

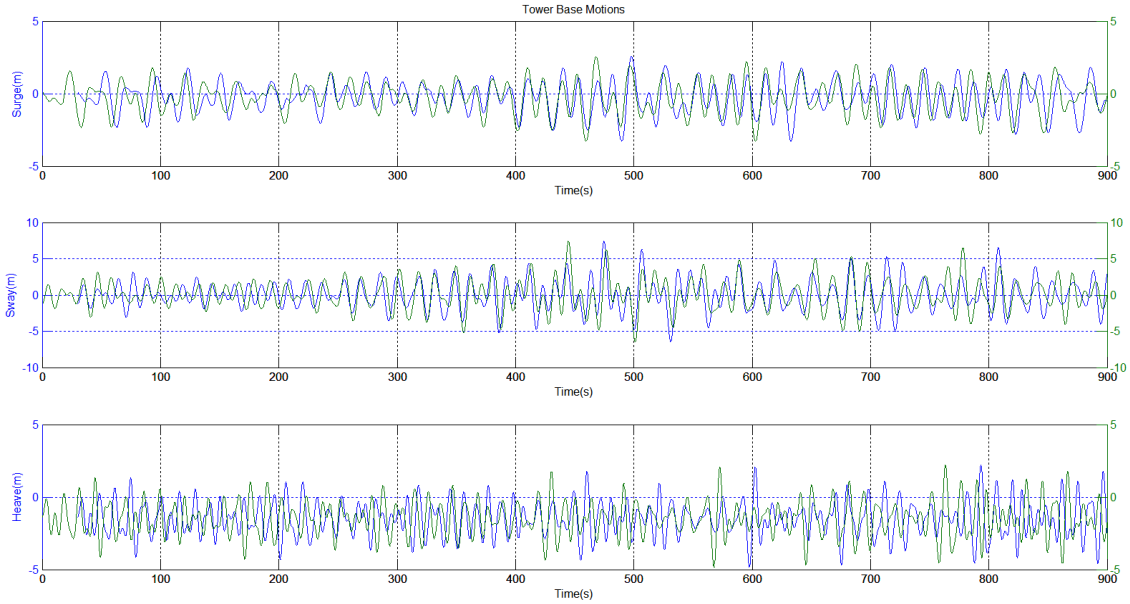

Figure 6.5 (b): Platform motions for 30º wave heading angle and 12 m/s wind speed

In Figure 6.5 (b), the sample time series for tower base motions are plotted for WindFloat wind turbine with six lines and four lines mooring system. It is observed that the surge motion is within 0m to -2.5m. Sway motion is in between approximately +/-1.5m. The heave motion is observed to be within 1.5m to -2.5m for 12 m/s wind speed.

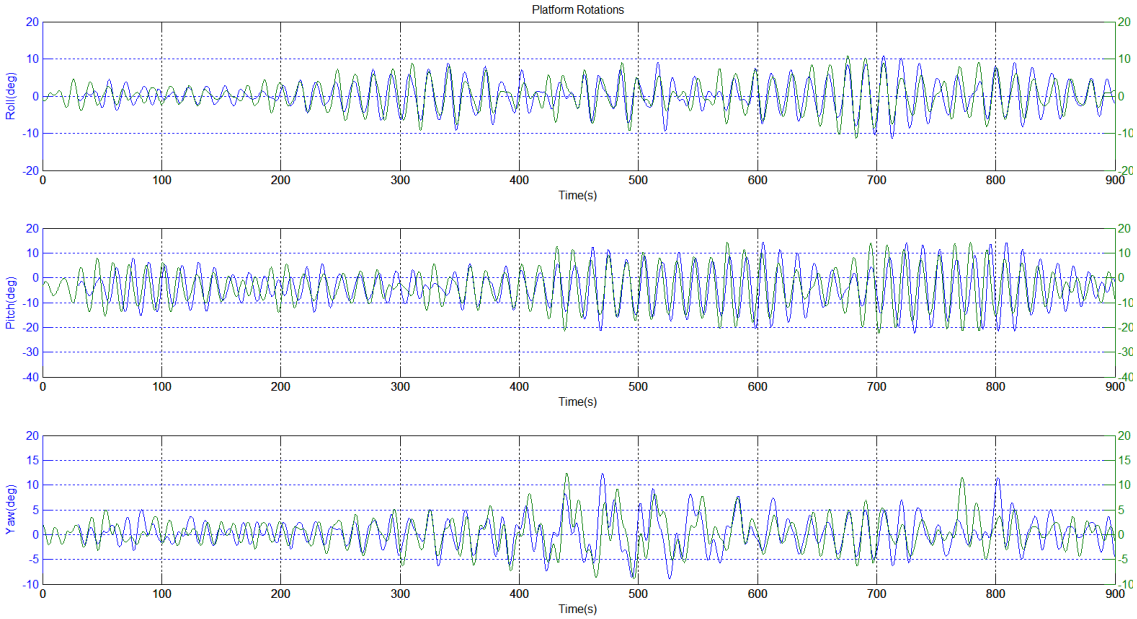

Figure 6.6 (a): Platform rotations for 30º wave heading angle and 24 m/s wind speed

In Figure 6.6 (a) the sample time series for platform rotations for 30º wave heading angle are plotted for WindFloat wind turbine with six lines and four lines mooring system. The

pitch oscillation is approximately within 8º to-8º. The roll motion is within 5º to-5º and yaw motion is in between 2º to -2º before 400s of simulation.

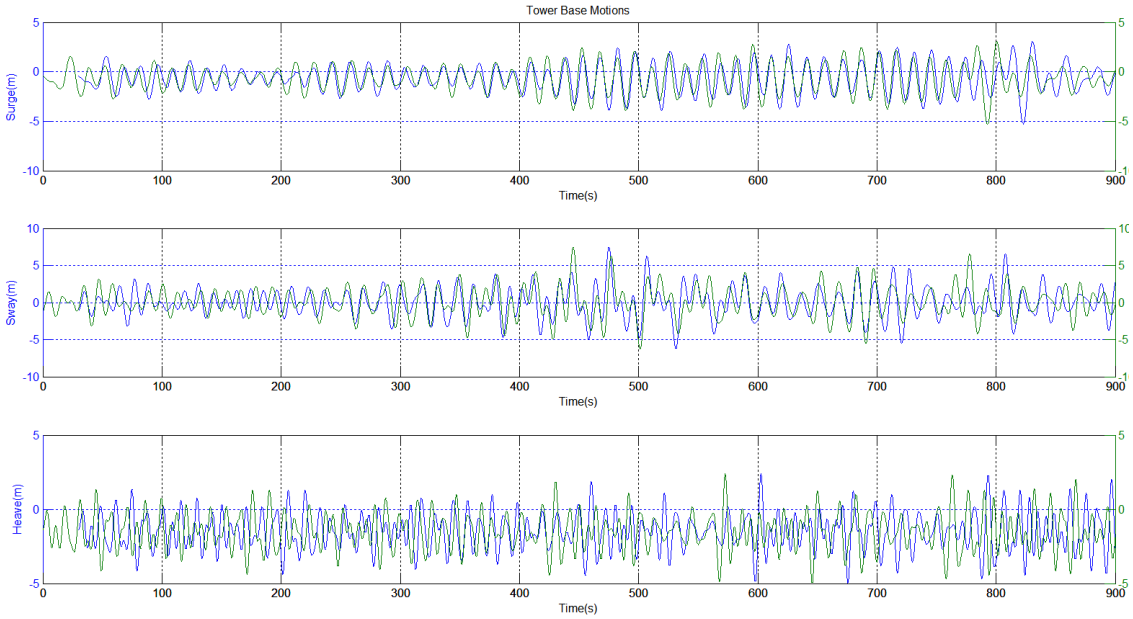

Figure 6.6 (b): Tower base motions for 30º wave heading angle and 24 m/s wind speed

In Figure 6.6 (b), the sample time series for tower base motions are plotted for WindFloat wind turbine with six lines and four lines mooring system. It is observed that the surge motion is within 0m to -3m. Sway motion is in between approximately +/-2m until 400 second. The heave motion is observed to be within 1.5m to -2.5m for all wind speed with 30º wave heading angle.

6.3 Conclusions

In this Chapter, the 5MW WindFloat semi-submersible type floating wind turbine is examined with mean wave height 4m with 0º and 30º wave heading angle with three different wind speed conditions for four lines and six lines mooring system. The following conclusions are drawn based on the study carried out in this chapter:

- In the case of 4 lines mooring system two moorings are attached in the column carrying the turbine tower and in the other two columns one mooring is attached. On the other hand for 6 lines mooring system four moorings are attached in the column carrying the turbine tower and in the other two columns one mooring is attached.

- The 4 lines and 6 lines mooring system tower base motions and platform rotations results are plotted for 0º and 30º wave heading angle.

- The rotational and linear motions for both 4 lines mooring and 6 lines mooring are almost same for 0º and 30º wave heading angle and for different wind speeds.

- The analysis suggest that 4 lines mooring would be better than 6 lines mooring as the results observed are almost same and it will save the construction cost of WindFloat semi-submersible type floating wind turbine.

CHAPTER 7

CONCLUSIONS

In the present thesis, a detailed study on offshore floating wind turbines with the working principle of various floater concepts and the conceptual designs for floating platforms used for floating wind turbines is presented. The main conclusions of the research work pursued are given below:

- The studies carried out for monopile wind turbine shows that the maximum blade bending moment increases with wind speed, up to the rated wind speed of 11.5m/s, and then decreases, as is expected due to blade-pitch control actions. For each water depth the bending moment at the tower base is maximum when water depth is 30m and minimum when water depth is 10m.

- The dynamic analysis of NREL 5MW spar-type, barge-type and WindFloat type floating wind turbines are performed using the FAST code. The hydrodynamic behaviour of the spar-type, barge-type and WindFloat floater concepts are studied using WAMIT. The hydrodynamic added mass and damping coefficient for the force translation modes and moment-rotational modes are observed to be same as compared to OC3-Hywind and ITI-Barge.

- The surge-surge element for force-translation mode is observed to be identical to the sway-sway element and the roll-roll element for the moment-rotational modes is observed identical to the pitch-pitch element due to the symmetry in the body. The aero-servo-hydro-elastic model for FAST code is obtained by combining

hydrodynamic characteristics of the floater obtained using WAMIT with aero-servo-elastic model of FAST code.

- In the study of spar-type floating wind turbine, the floater is considered connected with three mooring lines whereas in the case of barge-type floating wind turbine, the floater is connected with eight mooring lines where each two lines is located at each corner of the floater and WindFloat floating wind turbine floater is connected with four mooring lines. The moorings attached with the floaters help in the stability of the floaters and it is observed that the pitch motion of the floaters decreases with the increase in the mooring lines. The three concepts were simulated in deep water; i.e the spar-type and WindFloat are examined at 320m water depth and barge-type at 150m water depth.

- The simulation result obtained for pitch, heave, sway and yaw motions in the case of spar-type floating wind turbine is more stable than barge-type floating wind turbine. However in the case of roll and surge motions, the results obtained in both the cases agrees well.

- Surge motion in the case of WindFloat-type floating wind turbine is more stable than barge-type and spar-type floating wind turbine. However in the case of pitch and heave motion spar-type floating wind turbine is more stable than barge-type and semi-submersible type floaters. The pitch motion for WindFloat wind turbine is obtained higher than barge-type however in the case of sway, roll, yaw and surge motions the results obtained are lower than barge-type.

- The simulation results for tower base motions and platform motions for various values of wind speed are obtained keeping the wave height and wave heading angle same. It is observed that with the increase of wind speed the pitch and surge motion increases until 12 m/s and decreases for 24 m/s. It is an expected result due turbines has blade pitch controller. The simulation results for tower base motions and platform motions for various values of wind speed are obtained keeping wave heading angle 30º and it is observed roll and yaw motion is increased for three concepts.

REFERENCES

Agarwal, P. and Manuel, L. (2009). Simulation of offshore wind turbine response for long-term extreme load prediction, *J. of Eng. Struct*. 31, pp. 2236-2246.

Aubault, A., Cermelli, C., and Roddier, D., (2009). WIND FLOAT: a floating foundation for offshore wind turbines Part III: structural analysis. *Proc. 28th Intl Conf. on Ocean, Offshore and Arctic Eng., Honolulu, Hawaii, USA, OMAE-79232*.

Bae, Y.H., Kim, M.H., and Shin, Y.S., (2010). Rotor-floater mooring coupled dynamic analysis of mini TLP-type offshore floating wind turbines. *Proc. 29th Intl. Conf. on Ocean, Offshore and Arctic Eng., OMAE-20555*.

Bagbanci, H., Karmakar, D., Knappmann, A., Guedes Soares, C. (2011a). Review of offshore floating wind turbines concepts. *Proc. Intl. Conf. Maritime Tech. and Eng., MARTECH 2011, Lisboa, Portugal*.

Bagbanci, H., Karmakar, D., Guedes Soares, C. (2011b). Effect of the environment on the design loads on monopile offshore wind turbine. *Proc. Intl. Conf. Maritime Tech. and Eng., MARTECH 2011, Lisboa, Portugal.*

Bagbanci, H., Karmakar, D., Guedes Soares, C. (2011c). Dynamic analysis of spar-type floating offshore wind turbine. *Proc. Intl Conf. 2nd Coastal and Maritime Mediterranean, 2011, Tangier, Morocco.*

Bagbanci, H., Karmakar, D., Guedes Soares, C. (2011d). Comparative study on the coupled dynamic analysis of spar-type and barge-type floating wind turbine *Proc. Intl Symposium on Naval Architecture and Maritime, Istanbul, Turkey.*

Bir, G. and Jonkman, J. (2008). Modal Dynamics of Large Wind Turbines with Different Support Structures, *Proceedings of the ASME 27th International Conferences on Offshore Mechanics and Arctic Engineering, Portugal, OMAE2008-57446*.

Bulder, B. H., et al. (2002). Study to Feasibility of and Boundary Conditions for Floating Offshore Wind Turbines, *Novem 2002-CMC-R43, ECN, MARIN, Lagerway the Windmaster, TNO, TUD, MSC*.

Cermelli, C., Roddier, D., and Aubault, A., (2009). WindFloat: a floating foundation for offshore wind turbines Part II: Hydrodynamics analysis. *Proc. 28th Intl Conf. on Ocean, Offshore and Arctic Eng., Honolulu, Hawaii, USA, OMAE-79231.*

Herbert G.M.J. Joselin Herbert, Iniyan, S., Sreevalsan,E., Rajapandian, S. (2007). A review of wind energy Technologies, *Renewable and Sustainable Energy Reviews*, 11, 1117–1145.

Henderson, A.R. and Patel, M.H., (1998). Floating offshore wind energy. *Proc. of 17th Intl Conf. on Ocean, Offshore and Arctic Eng., Lisbon, Portugal, July 5–9, 1998.*

Henderson, A. R., Morgan, C. S., Smith, B., Sørensen, H. C., Barthelmie, R. J., and Boesmans, B. (2003). Offshore Wind Energy in Europe, A Review of the State-of-the-Art, *Wind Energy*, Vol. 6, No. 1, pp. 35–52.

Iijima, K., Kim, J., and Fujikubo, M., (2010). Coupled aerodynamic and hydroelastic analysis of an offshore floating wind turbine system under wind and wave loads. *Proc. 29th Intl. Conf. on Ocean, Offshore and Arctic Eng., OMAE-20772.*

Ishihara, T., Phuc, P.V., and Sukegawa, H., (2007a). Numerical study on the dynamic response of a floating offshore wind turbine system due to resonance and nonlinear wave. *Proc. 2nd EOW, Berlin, Germany.*

Ishihara, T., Phuc, P.V., and Sukegawa, H., (2007b). A study on the dynamic response of a semi-submersible floating offshore wind turbine system Part 1: a water tank test. *Proc. 12th Intl. Conf. on Wind Engineering, Cairns, Australia.*

Ishihara, T., Waris, M.B., and Sukegawa, H., (2009). A study on influence of heave plate on dynamic response of floating offshore wind turbine system. *Proc. 3rd European Offshore Wind Conference and Exhibition, Stockholm, Sweden.*

Jonkman, J. M. and Buhl, M. L., Jr. (2004a). New Developments for the NWTC's FAST Aeroelastic HAWT Simulator, *ASME Wind Energy Symposium, 42nd AIAA Aerospace Sciences Meeting and Exhibit, Reno Nevada, USA, New York.*

Jonkman, J. M. and Buhl, M. L., Jr. (2004b). FAST User's Guide, *NREL/EL-500-29798, Golden, CO: National Renewable Energy Laboratory.*

Jonkman, J. M. and Sclavounos, P. D. (2006). Development of Fully Coupled Aeroelastic and Hydrodynamic Models for Offshore Wind Turbines, *44th AIAA Aerospace Sciences Meeting and Exhibit, 9–12 January 2006, Reno, NV.*

Jonkman, J.M. and Buhl, M.L. Jr, (2007). Loads analysis of a floating offshore wind turbine using fully coupled simulation. *Proc. of Wind Power 2007 Conference and Exhibition, Los Angeles, California.*

Jonkman, J. M. (2009). Dynamics of offshore floating wind turbine – model development and verification, *Wind Energy*, 12, 459-492.

Jonkman, J.M. (2010). Defination of the floating system for phase IV of OC3, *NREL technical report,* 1-25.

Karimirad, M. and Moan, T., (2010). Extreme structural response of a spar-type wind turbine. *Proc. 29th Intl. Conf. on Ocean, Offshore and Arctic Engineering, OMAE-20044.*

Klose, M., Dalhoff, P. and Argyriadis, K. (2007). Integrated load and strength analysis for offshore wind turbines with jacket structures. *Proc. 17th Intl. Offshore and Polar Engineering Conf., Lisbon, Portugal.*

Lee, K.H., (2004). Responses of floating wind turbines to wind and wave excitation. Thesis (MSc). *Massachusetts Institute of Technology.*

Matsukuma, H. and Utsunomiya, T., (2008). Motion analysis of a floating offshore wind turbine considering rotor rotation *The IES Journal Part A: Civil and Structural Eng.,* 1 (4), 268–279.

Musial, W., Butterfield, S. and Boone, A. (2004a). Feasibility of Floating Platform Systems for Wind Turbines, *ASME Wind Energy Symposium, 5–7 January 2004, Reno Nevada, USA, New York.*

Musial, W. and Butterfield, S. (2004b). Future for Offshore Wind Energy in the United States, *Energy Ocean Proceedings, Palm Beach Florida, USA, NREL/CP-500-36313, National Renewable Energy Laboratory*.

Musial, W., Butterfield, S. and Ram, B. (2006). Energy from Offshore Wind, *Offshore Technology Conference, 1–4 May 2006, Houston, TX.*

Nielson, F.G., Hanson, T.D., and Skaare, B. (2006). Integrated dynamic analysis of floating offshore wind turbines. Proc. *25th Intl. Conf. Offshore Mechanics and Arctic Eng. Hamburg, Germany, OMAE-92291.*

Nielsen, F.G., Argyriadis, K., Fonseca, N., Le Boulluec, M., Liu, P., Suzuki, H., Sirkar, J., Tarp-Johansen, N.J., Turnock, S.R., Waegter, J. and Zong, Z. (2009). Ocean, Wind and wave energy utilization. *17th Intl. Ship and Offshore Structures Congress, Seoul, Korea, 201-257.*

Nihei, Y. and Fujioka, H., (2010). Motion characteristics of a TLP type offshore wind turbine in waves and wind. *Proc. 29th Intl. Conf. on Ocean, Offshore and Arctic Eng., OMAE-21126.*

Roddier, D., Cermelli, C., and Weinstein, A., (2009). WindFloat: a floating foundation for offshore wind turbines Part I: Design basis and qualification process. *Proc. 28th Intl. Conf. on Ocean, Offshore and Arctic Eng., Honolulu, Hawaii, USA, OMAE-79229.*

Shimada, K., Ohyama, T., Miyakawa, M., Ishihara, T., Phuc, P.V. and Sukegawa, H. (2007). A study on a semi-submersible floating offshore wind energy conversion system. *Proc. 17th Intl. Offshore and Polar Eng. Conf., Lisbon, Portugal, 384–354.*

Skaare, B., Hanson, T., Nielsen, F.G. (2006). Integrated Dynamic Analysis of Floating Offshore Wind Turbines. *Proc. European Wind Energy Conf. and Exhibition, Athens, Greece.*

Skaare, B., Hanson, T., Nielsen, F.G. (2007). Importance of control strategies on fatigue life of floating wind turbines. *Proc. 26th Intl. Conf. on Offshore Mechanics and Arctic Eng.. OMAE-29277.*

Suzuki, H. and Sato, A., (2007). Load on turbine blade induced by motion of floating platform and design requirement for the platform. *Proc. 26th Intl. Conf. on Offshore Mechanics and Arctic Eng., OMAE-29500.*

Suzuki, H., Kurimoto, M., Kitahara, Y. and Yukinari Fukumoto, Y. (2009). Progressive drifting of floating wind turbines in a wind farm. *Proc. 28th Intl. Conf. on Ocean, Offshore and Arctic Eng., Honolulu, Hawaii, OMAE-79634.*

Tong, K.C., (1998). Technical and economic aspects of a floating offshore wind farm. *J. of Wind Eng. and Industrial Aerodynamics,* 74–76, 399–410.

Utsunomiya, T., Sato, T., Matsukuma, H. and Yago, K. (2009). Experimental validation for motion of a spar-type floating offshore wind turbine using 1/22.5 scale model. *Proc. 28th Intl. Conf. on Ocean, Offshore and Arctic Eng., Honolulu, Hawaii, USA, OMAE-79695.*

Vijfhuizen, W. J. M. J. (2006). Design of a Wind and Wave Power Barge, *M.S. Dissertation, Department of Naval Architecture and Mechanical Engineering, Universities of Glasgow and Strathclyde, Glasgow, Scotland*.

Wang, C.M., Utsunomiya, T., Wee, S.C. and Choo, Y.S. (2010). Research on floating wind turbines: a literature survey. The *IES Journal Part A: Civil and Structural Engineering*, Vol. 3(4), 267-277.

Watson, G., et al, (2005). A Framework for Offshore Wind Energy Development in the United States, *Massachusetts Technology Collaborative (MTC).*

Wayman, E. 2006. Coupled Dynamics and Economic Analysis of Floating Wind Turbine Systems, *M.S. Dissertation, Department of Mechanical Engineering, Massachusetts Institute of Technology, Cambridge, MA, USA.*

Wayman, E.N., Sclavounos, P. D., Butterfield, S., Jason, J., Musial, W. (2006). Coupled dynamic modeling of floating wind turbine systems. *Proc. Offshore Technology Conference, Houston, Texas.*

Weinzettel, J., Reenaas, M., Solli, C. and Hertwich, E.G. (2009). Life cycle assessment of a floating offshore wind turbine. *Renewable Energy*, 34 (3), 742–747.

Withee, J.E. and Sclavounos, P.D. (2004). Fully coupled dynamic analysis of a floating wind turbine system. *Proc. 8th World Renewable Energy Congress, Denver, Colorado, USA.*

Zambrano, T., MacCready, T., Kiceniuk, T. Jr.., Roddier, D.G. and Cermelli, C., (2006). Dynamic modeling of deepwater offshore wind turbine structures in Gulf of Mexico storm conditions. *Proc. 25th Intl. Con. on Offshore Mechanics and Arctic Eng., Hamburg, Germany, OMAE-92029.*